

**A COMPREHENSIVE STUDY OF CORRELATION
COEFFICIENT ESTIMATION METHODS FOR
CLOSELY SPACED MIMO ANTENNA SYSTEMS**

BY

ABDELMONIEM HASSAN

A Thesis Presented to the
DEANSHIP OF GRADUATE STUDIES

KING FAHD UNIVERSITY OF PETROLEUM & MINERALS

DHAHRAN, SAUDI ARABIA

In Partial Fulfillment of the
Requirements for the Degree of

MASTER OF SCIENCE

In

ELECTRICAL ENGINEERING

MAY 2016

KING FAHD UNIVERSITY OF PETROLEUM & MINERALS

DHAHRAN- 31261, SAUDI ARABIA

DEANSHIP OF GRADUATE STUDIES

This thesis, written by **ABDELMONIEM HASSAN** under the direction his thesis advisor and approved by his thesis committee, has been presented and accepted by the Dean of Graduate Studies, in partial fulfillment of the requirements for the degree of **MASTER OF SCIENCE IN ELECTRICAL ENGINEERING**.



Dr. Mohammad S. Sharawi
(Advisor)



Dr. Ali Ahmad Al-Shaikhi
Department Chairman

H. Masoudi 17-5-2016

Dr. Husain M. Masoudi
(Member)



Dr. Salam A. Zummo
Dean of Graduate Studies



Sheikh Sharif 17-5-16

Dr. Sheikh Sharif Iqbal
(Member)

26/5/16

Date

© ABDELMONIEM HASSAN

2016

*To my parents, to my sisters, to my friends
To my country.*

ACKNOWLEDGMENTS

In the name of God, Most Gracious, Most Merciful. Allah said ‘’and my success (in my task) can only come from Allah. In Him have I put my trust, and to Him do I always turn.’’ The Holy Qura'an Hud chapter (88).

Besides, I would like to express my deep gratitude to my supervisor Dr. Mohammad S. Sharawi for his ultimate support and dedication through the time of my project, to anyone who guided me, gave me even a hint which helped me to accomplish my work.

Also, I would also like to thank my thesis committee members, Dr. Husain M. Masoudi and Dr. Sheikh Sharif Iqbal.

Of course all that could not be accomplished without my parents prayers and wishing me successful life. Also, to my lovely twin for her moral support and encouragement to achieve my goals.

TABLE OF CONTENTS

ACKNOWLEDGMENTS	IV
TABLE OF CONTENTS	V
LIST OF TABLES	IX
LIST OF FIGURES	X
LIST OF ABBREVIATIONS	XIV
ABSTRACT.....	XV
ABSTRACT (ARABIC)	XVI
CHAPTER 1 INTRODUCTION.....	1
1.1 Single input single output (SISO) systems	1
1.2 Multiple input single output (MISO) and Single input multiple output (SIMO).....	2
1.3 Multiple input multiple output (MIMO).....	2
1.4 Work Motivation	4
1.5 Thesis Objectives	5

CHAPTER 2 BACKGROUND.....	7
2.1 MIMO Parameters and Performance Metrics	7
2.1.1 The Correlation Coefficient.....	8
2.1.2 Total Active Reflection Coefficient (TARC).....	8
2.1.3 Mean Effective Gain (MEG)	9
2.1.4 Diversity Gain (DG)	12
2.1.5 Branch Power Ratio	12
2.1.6 System Capacity	13
2.1.7 Multiplexing efficiency.....	13
2.2 Some Field Based de-correlation techniques	14
2.2.1 Spatial de-correlation.....	14
2.2.2 Polarization De-correlation	15
2.3 Summary	16
CHAPTER 3 LITERATURE REVIEW.....	17
3.1 Correlation coefficient calculations	17
3.1.1 Correlation coefficient calculation using 3D far fields (method-I).....	18

3.1.2	Correlation coefficient calculation using the S-parameters (method-II)	19
3.1.3	Correlation coefficient calculation using scattering S-parameters and Radiation Efficiencies (method- III)	20
3.1.4	Correlation coefficient calculation based on the equivalent circuit in lossy MIMO antenna (method- IV).....	21
3.1.5	Correlation coefficient calculation for Lossy Compact Monopole Arrays with Decoupling Networks (method-V)	31
3.2	Related Works	33
3.3	Summary	37
CHAPTER 4 ANALYTICAL EXTENSION OF METHOD- III AND IV TO COVER N-PORTS.....		40
4.1	Generalization of method- III to N-Port MIMO Systems	40
4.2	Generalization of Parallel R-L-C equivalent circuit for method- IV to N- Ports MIMO.....	45
CHAPTER 5 RESULTS & DISCUSSION.....		50
5.1	Correlation Coefficient for two elements	50
5.1.1	Two printed dipole elements	50
5.1.2	Two folded monopole elements	55

5.1.3	Two patch elements	58
5.2	Correlation Coefficient Calculation for Four element MIMO antennas	62
5.2.1	Four dipole elements	63
5.2.2	Half Circle Shape 4-Elements monopole elements	64
5.2.3	Annular Slot Based Printed MIMO Antenna System Design	71
5.2.4	Four PIFA Elements	74
5.2.5	The Four Patch Elements	80
5.2.6	The Four Patch Elements with high radiation efficiency	84
5.3	Summary	88
CHAPTER 6 THESIS CONCLUSIONS		89
6.1	Conclusions	89
6.2	Future work	90
APPENDIX – SOFTWARE TOOL		91
REFERENCES.....		92
VITAE.....		97

LIST OF TABLES

Table 5-1 The correlation coefficient of the four dipole array, [17].....	64
Table 5-2 correlation coefficients of four-dipole array.....	64
Table 5-3 correlation coefficients of four curved array with fr4 and reflector at 2.4GHz	71
Table 5-4 correlation coefficients of the four annular slot with FR4 at 2.4 GHz	74
Table 5-5 correlation coefficients of the four PIFA with FR4 at 1.8 GHz	79
Table 5-6 correlation coefficients of four patch array with FR-4 at 2.4 GHz ...	83
Table 5-7 correlation coefficients of high radiation efficiency four patch array with FR-4 at 5.35 GHz	87

LIST OF FIGURES

Figure 1.1 Capacity vs number of antennas for MIMO system, SIMO system, MISO system and SISO system. [1]	4
Figure 2.1 Two antenna elements when vertically and horizontally spaced correlation . [1].....	15
Figure 3.1 Equivalent lossy circuit module of two lossy elements [10].....	22
Figure 3.2 Equivalent circuit model for lossy dual antenna as a Series RLC [10].	24
Figure 3.3 Series equivalent circuits model with lossy lumped components [17]	26
Figure 3.4 parallel equivalent circuits model for lossy dual antenna array [10].	28
Figure 3.5 Classification based on the number of elements.	38
Figure 3.6 Classification based on the method used.....	39
Figure 3.7 Classification based on the frequency.	39
Figure 4.1 Representation of N- antenna elements.....	41
Figure 4.2 equivalent circuit diagram for 4-antenna elements	45
Figure 5.1 Geometries of the dual-dipole array [10]	50
Figure 5.2 S-parameters and magnitude of correlation coefficients for different antenna	51
Figure 5.3 The correlation coefficients $\eta_{\text{(rad,)}}=88\%$	52
Figure 5.4 The correlation coefficients $\eta_{\text{(rad,)}}=79.9\%$	52
Figure 5.5 The correlation coefficient $\eta_{\text{(rad,)}}=73.2\%$	53
Figure 5.6 The power losses $\eta_{\text{(rad,)}}=88\%$	54
Figure 5.7 The power losses $\eta_{\text{(rad,)}}=79.9\%$	54

Figure 5.8 The power losses $\eta_{\text{(rad,)}}=73.2\%$	55
Figure 5.9 Geometries of the folded monopole antennas 2x2 [17].....	56
Figure 5.10 S-parameters and magnitude of correlation coefficients. [14]	56
Figure 5.11 The correlation coefficients [14]	56
Figure 5.12 The correlation coefficients for the 2-elements folded monopole MIMO antenna.....	57
Figure 5.13 The power losses for the folded monopole.....	57
Figure 5.14 <i>Geometries of the dual patch antenna system</i> [11]	58
Figure 5.15 The correlation coefficient $\eta_{\text{(rad,)}}=94.2\%$	58
Figure 5.16 The power losses for the two patch antenna $\eta_{\text{(rad,)}}=94.2\%$	59
Figure 5.17 The correlation coefficients $\eta_{\text{(rad,)}}=81.2\%$	59
Figure 5.18 The power losses for the two patch antenna $\eta_{\text{(rad,)}}=81.2\%$	60
Figure 5.19 The correlation coefficients $\eta_{\text{(rad,)}}=69.7\%$	60
Figure 5.20 The power losses for the two patch antenna $\eta_{\text{(rad,)}}=69.7\%$	61
Figure 5.21 The correlation coefficients $\eta_{\text{(rad,)}}=54.9\%$	61
Figure 5.22 The power losses for the two patch antenna $\eta_{\text{(rad,)}}=54.9\%$	62
Figure 5.23 Geometries of the four dipole array [17].....	63
Figure 5.24 Geometry of the proposed antenna. (a) Top side, (b) Bottom side. (All dimensions are in mm)	65
Figure 5.25 Geometry of the Fabricated antenna. (a) bottom side, (b) top side .	66
Figure 5.26 Four monopole elements S-parameter with FR4.....	66

Figure 5.27 Simulated and measured isolation	67
Figure 5.28 Element 1 realized gain	67
Figure 5.29 Element 2 realized gain	68
Figure 5.30 Element 3 realized gain	68
Figure 5.31 Element 4 realized gain	69
Figure 5.32 Measurement setup in a Satimo star-Lab	70
Figure 5.33 The measured and simulated of E_{Total} for each element at $\theta = 90^\circ$ Along XY axis and $\phi = 0^\circ$ along YZ	70
Figure 5.34 Annular Slot Based Printed MIMO Antenna	72
Figure 5.35 The four annular slot S-parameter with FR4.....	72
Figure 5.36 3D radiation patterns the four annular slot	73
Figure 5.37 PIFA MIMO Antenna geometry. (All dimension are in mm).....	75
Figure 5.38 Geometry of the Fabricated antenna bottom side and top side	75
Figure 5.39 PIFA Simulated and measured S-parameter with FR4.....	76
Figure 5.40 PIFA Simulated and measured isolation	76
Figure 5.41 PIFA Simulated and measured S-parameter with the dielectric constant of 4	77
Figure 5.42 Element 1-3D radiation patterns.....	77
Figure 5.43Element 2-3D radiation patterns.....	78
Figure 5.44 Element 3-3D radiation patterns.....	78
Figure 5.45 Element 4-3D radiation patterns.....	79

Figure 5.46 Four patch geometric (All dimensions are in mm).....	80
Figure 5.47 Four patch elements S-parameter with FR4	81
Figure 5.48 Element 1 realized gain	81
Figure 5.49 Element 2 realized gain	82
Figure 5.50 Element 3 realized gain	82
Figure 5.51 Element 4 realized gain	83
Figure 5.52 Four patch geometric (All dimensions are in mm).....	84
Figure 5.53 Four patch elements S-parameter with FR4	85
Figure 5.54 Element 1 realized gain	85
Figure 5.55 Element 2 realized gain	86
Figure 5.56 Element 3 realized gain	86
Figure 5.57 Element 4 realized gain	87

LIST OF ABBREVIATIONS

MIMO	:	Multiple Input Multiple Output
WLAN	:	Wireless Local Area Network
PIFA	:	Planner Inverted F antenna
DG	:	Diversity Gain
SIMO	:	Single Input Multiple Output
MISO	:	Multiple Input Single Output
SISO	:	Single Input Single Output
XPR	:	Cross Polarization Ratio
RF	:	Radio Frequency
BPR	:	Branch Power Ratio
DG	:	Diversity Gain
TDMA	:	Time Division Multiple Access
FDMA	:	Frequency Division Multiple Access
CDMA	:	Code Division Multiple Access

ABSTRACT

Full Name : ABDELMONIEM TAJELSIR MAHMOUD HASSAN
Thesis Title : A comprehensive study of correlation coefficient estimation methods for closely spaced MIMO antenna systems
Major Field : Master of Science in electrical engineering department
Date of Degree : May 2016

Multiple-Input-Multiple-Output (MIMO) systems have been utilized in 4G wireless communication devices and will be an enabling technology in the upcoming 5G wireless communication standard due to the need for high data rate and reliable communications. Thus, the number of antenna elements within each MIMO system will increase from one element in conventional terminals to at least 4 in 5G handsets. A major performance metric that is used to characterize the behavior of MIMO antenna systems is the correlation coefficient. This metric gives an indication on the isolation of the various channels and thus directly impacts the final communication system channel capacity. Several methods have been discussed in the literature to evaluate the correlation coefficient of MIMO antenna systems. Each method has its advantages and disadvantages. In this work a detailed comparison between these methods is presented, and investigates their performance on various antenna types and across various bands. In addition, some of these equations are extended to cover N-ports rather than only two ports. Moreover, the design of four antenna elements for MIMO antenna systems rather than two elements in current 4G handsets is implemented. The design of monopole based, and patch based MIMO antennas operating at 2.4GHz are performed, in addition to PIFA (planner inverted F antenna) based antennas covering 1.8GHz. Two new MIMO design antenna systems are designed and fabricated with dimensions $110 \times 60 \times 0.8 \text{ mm}^3$ and the correlation coefficient is evaluated using all methods, investigated and compared.

ملخص الرسالة

الاسم الكامل: عبدالمنعم تاج السر محمود حسن

عنوان الرسالة: دراسته معامل الارتباط للهوائيات المستخدمة في الانظمة متعددة المداخل والمتعددة المخارج

التخصص: الهندسه الكهربائيه

تاريخ الدرجة العلمية: مايو 2016

الانظمة متعددة المداخل والمتعددة المخارج استخدمت في الجيل الرابع من اجهزه الاتصال اللاسلكيه وهي التي سوف يتم استخدامها ايضا في الجيل الخامس من نفس الاجهزه وذلك للحوجه الي نظم اتصالات تدعم معدل نقل بيانات عالي بالاضافه الي اجهزه يمكن الاعتماد عليها. لذلك عدد الهوائيات التي سوف تستخدم في الاجهزه اللاسلكيه سيزداد من جهاز واحد فقط في الاجهزه القديمه الي اكثر من اربعة في الاجهزه التي تدعم الجيل الخامس. من اهم المعايير التي تحدد فعاليه الانظمة متعددة المداخل والمتعددة المخارج هو معيار معامل الارتباط وهو معامل يعبر عن مدي الترابط بين قنوات الاتصال ويحدد مدي استغلاليه هذه القنوات عن بعضها البعض وهو معامل مهم حيث يعكس اثره علي سعه قناة الاتصال في الانظمة متعددة المداخل والمتعددة المخارج.

هنالك عدده طرق لتقييم هذا المعامل تمت مناقشتها في المراجع والمنشورات العلميه حيث كل طريقه لها مميزات وعيوب. في هذا العمل تم تقديم دراسته دقيقه ومفصله بين هذه الطرق وتم فحص فعاليتها علي انواع مختلفه من الهوائيات المستخدمه في الانظمة متعددة المداخل والمتعددة المخارج في نطاق ترددي مختلف.

بالاضافه الي ان بعض هذه الطرق صالحه في الانظمة متعددة المداخل والمتعددة المخارج التي تحتوي اثنين من الهوائيات وتم تعديلها لتدعم اي عدد من الهوائيات. كما انه تم تقديم نظامين من الانظمة متعددة المداخل والمتعددة المخارج التي تعمل باربعه هوائيات والتي يمكن استخدامها في اجهزه الجيل الرابع لتعمل في النطاق الترددي 2.4 جيجا هيرتز والنطاق الترددي 1.8 جيجا هيرتز كما انه تمت تصنيعها علي ركيزه ذات ابعاد $0.8 \times 60 \times 110$ ملم مكعب وتم تطبيق مختلف الطرق لحساب معامل الارتباط والمقارنه بين هذه الطرق.

CHAPTER 1

INTRODUCTION

In the past, in order to place a telephone call or to connect to the internet it was a hassle because of the low quality of the coverage and the low data rates provided. Also device sizes of mobile terminals were big. These limitations have been overcome in modern days, since communication technologies especially wireless technologies have grown exponentially to meet people demands. New systems that can comply with the modern requirements which are represented in high performance, high data rate and reduction in size became mandatory for engineers to develop. Radio frequency (RF) engineers play a major role in enhancing antenna designs and front-ends in term of size as well as capability to handle high data rates through the incorporation of modern enabling technologies such as multiple-input-multiple-output (MIMO).

1.1 Single input single output (SISO) systems

SISO systems have been used in conventional communication systems such that the signal is transmitted from a single antenna and received by a single antenna. For instance, the conventional cellular phone contains one antenna that is used to communicate with the base station. In the radio environment there is more than one user and all of them may need to access cellular services at the same time then the signals from all users can be separated in time as time division multiple access (TDMA), in frequency as frequency division multiple

access (FDMA), or code as code division multiple access (CDMA) to guarantee access for all users [1].

1.2 Multiple input single output (MISO) and Single input multiple output (SIMO)

In SISO systems, the communication link between the transmitting and the receiving antennas depend on the environment of the radio channel. For example, in case of a bad environment (fading environment) the communication link may be unreliable and leads to unacceptable quality or dropped calls. Because of this single point of failure, MISO/SIMO systems were developed. These systems depend on diversity techniques where multiple copies of the same signal can be transmitted then the receiver either combines or select from these copies thus enhancing the link quality [1].

Diversity techniques can be done by generating multiple copies of the transmitted signal in multiple time slots (time diversity) or the copies of the transmitted signal can be generated at different frequency bands (frequency diversity). Besides, the multiple copies can be generated from deferent antennas and received by a single antenna (space diversity). So MISO/SIMO depends on the front end of the communication system which supports multiple antennas either at the receiver or transmitter.

1.3 Multiple input multiple output (MIMO)

In SIMO/MISO the problem of single point of failure has been addressed, but the demand for a high data rate and a high reliability was still an issue. MIMO systems have been used to achieve the requirements of the contemporary communication system by increasing the channel capacity, high data rate and reliability of the communication channel. The channel

capacity can be defined as the amount of data that can be transmitted through the channel in a reliable manner. The channel capacity for simple environment modeling (Gaussian) can be calculated as [1]:

$$C = NB\log_2(1 + SNR) \quad (1.1)$$

Where C is the channel capacity in (bit/s/Hz), N is the number of antenna elements, B is the bandwidth in (Hz) and SNR is the signal to noise ratio. From (1.1), to increase the channel capacity this can be achieved by increasing the power to get high SNR , increase the bandwidth or increase the number of antenna elements. Increasing the power is not an option due to system constraints and regulations, thus the power should be limited. Also increasing the bandwidth is limited due to spectrum regulations [2]. The only parameter that we can play with is the number of antenna elements. In Fig 1.1 the relation between the channel capacity and the number of elements for a Rayleigh fast fading channel is shown. Also, from Fig 1.1 it is clear that the MIMO capacity increases linearly as the number of antenna elements increases also the capacity can be approximated by M times larger (where M is the number of antenna element used) than SISO capacity.

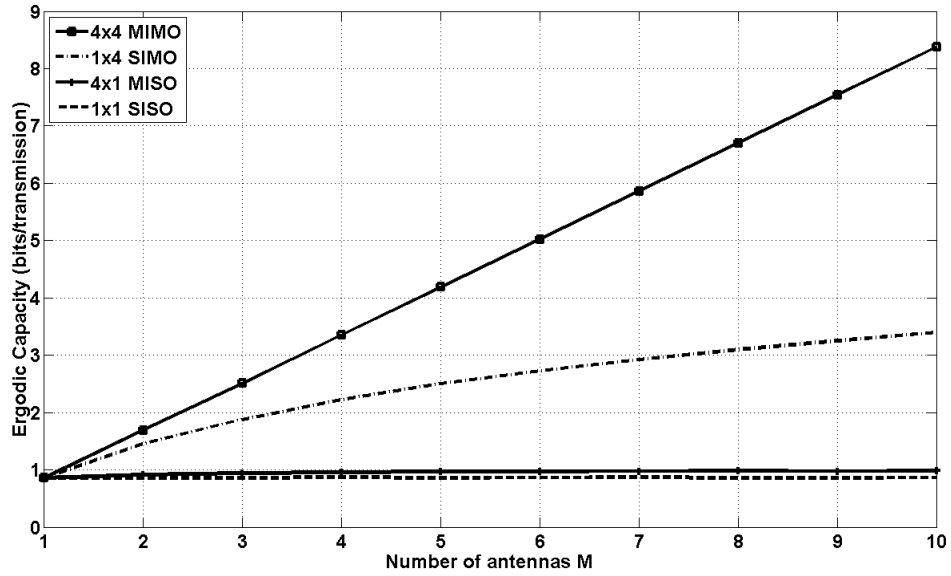


Figure 1.1 Capacity vs number of antennas for MIMO system, SIMO system, MISO system and SISO system. [1]

1.4 Work Motivation

MIMO systems were developed to enhance the performance of communication systems through increasing the channel capacity, data rate and reliability. However, to achieve these requirements the design and evaluation of different parts of the communication system needs careful attention. For example, modulation and signal conditioning part can play a major role thus enhancing the modulation technique as well as the modulation order to provide better links and higher data rates. Also, channel coding techniques are used for better error detection and correction. At the same time the RF part plays an important role especially the front end part (antenna). So to enhance the system performance the different parts of the communication system should be improved. In this work we are focusing on the front end part performance for MIMO systems and to be more specific we are focusing on the correlation coefficient metric. The front end of MIMO systems affects directly the

communication system performance through the antenna elements, such that good antenna design reflects good performance. One of the performance parameters in MIMO antenna systems is the correlation coefficient which indicates the isolation between the channels in air. For good design the correlation coefficient should be close to zero between different antenna elements which means their channels are independent.

The importance of the correlation coefficient also has direct effect on the channel capacity, therefore, the importance of calculating the exact values of the correlation coefficient help in estimating the channel capacity and power losses through calculating the multiplexing efficiency which gives an indication of a good design. Moreover, implementing an efficient and accurate method to calculate the value of the correlation coefficient such that it is close to the exact value by considering the antenna element losses has always been a challenge. Thus in this work, a comprehensive and comparative study of all available correlation coefficient methods is conducted and such a study will provide the antenna designer with good understanding of the various differences between the methods investigated and their applicability towards their designs.

1.5 Thesis Objectives

The thesis objectives as the follow:

1. To conduct a comprehensive study and implement different methods used for calculating the correlation coefficient of MIMO antenna systems.
2. To Design and fabricate two types of 4-element printed MIMO antenna systems for mobile handheld devices. The two types are a monopole and PIFA like ones. One

will cover the 1.8GHz cellular band while the other will cover the 2.45 GHz ISM band. Each will have at least 80 MHz of operating BW.

3. To apply the different methods of the correlation coefficient calculation on the four element antenna and compare between the obtained results.
4. To generalize the correlation coefficient method of [8] to include N-antennas instead of two.
5. To generalize the parallel equivalent circuit method in [10] to estimate the correlation coefficient to include N-antennas instead of two.

|

CHAPTER 2

BACKGROUND

In any wireless communication system, the antenna is an important element to enable the transmission of electromagnetic waves from the transmitter to the receiver, but this requires considering some factors during the design of the antenna. First, is the antenna radiates electromagnetic waves from different directions while the receiving antenna has a certain direction to receive that signal which affect the amount of power that should be transmitted between them in addition it will decay because of the path loss. This impact can be measured through antenna gain. Secondly, the amount of the power should be transmitted from the transmission line to the antenna ,this impact can be measured and optimized through the impedance matching between the antenna and the transmission line [1], however in case of MIMO systems there are other parameters that should be used to evaluate systems performance.

2.1 MIMO Parameters and Performance Metrics

In MIMO antenna systems, each antenna element gain and input impedance matching will be affected from the neighboring elements. For small MIMO terminals, because the antenna elements have to be closely spaced to each other, power will be coupled from one antenna to the others because of the mutual impedance thus the gain can be reduced which is not preferable. For MIMO systems there are many metrics to evaluate their performance in addition to the conventional antenna metrics such as gain, efficiency and resonance. The following section will discuss MIMO antenna metrics in details:

2.1.1 The Correlation Coefficient

In MIMO systems the communication channels should be independent. The correlation coefficient (ρ) is a parameter used to show how much these communication channels are isolated or correlated with each other in the far field. The envelop correlation coefficient (ECC) can be calculated based on the far field pattern data according to:

$$\rho_e = \frac{|\iint_{4\pi} [\overline{F_1}(\theta, \phi) * \overline{F_2}(\theta, \phi)] d\Omega|^2}{\iint_{4\pi} |\overline{F_1}(\theta, \phi)|^2 d\Omega \iint_{4\pi} |\overline{F_2}(\theta, \phi)|^2 d\Omega} \quad (2.1)$$

$$d\Omega = \sin \theta d\theta d\phi \quad (2.2)$$

Where $F_1(\theta, \phi)$ and $F_2(\theta, \phi)$ are the three-dimensional field radiation pattern of the antenna 1 and 2 when they are excited, and Ω is the solid angle. This method is complicated because it requires three-dimensional field radiation patterns of the antenna and numerical integration valid for a uniform distribution multipath radio environment [3].

2.1.2 Total Active Reflection Coefficient (TARC)

The scattering matrix is used to characterize the MIMO antennas efficiency and bandwidth (BW) of the antenna. But for MIMO antenna stable characterization, the total active reflection coefficient (TARC) which is more stable for MIMO antenna than the scattering matrix because its take into account the effect of multipath within the system. The total active reflection coefficient (TARC) is the metric for the effective bandwidth. For an N-element antenna, the TARC is given by [3].

$$\Gamma_a^t = \frac{\sqrt{\sum_{i=1}^N |b_i|^2}}{\sqrt{\sum_{i=1}^N |a_i|^2}} \quad (2.3)$$

Where a_i and b_i are the incident and reflected signals, respectively. TARC can be calculated using the S-parameters of the MIMO antenna as:

$$b = Sa \quad (2.4)$$

Where S is the S-parameter matrix. The TARC has a value between zero and one, which means either all the power is radiated or reflected. For more reliable performance evaluation the effect of the input excitation phase can be obtained from TARC for resonance frequency and impedance bandwidth of the whole antenna system. For a two-port MIMO antenna system TARC can be calculated using S parameters as follow [3]:

$$\Gamma_a^t = \frac{\sqrt{|S_{11} + S_{12}e^{j\theta}|^2 + |S_{21} + S_{22}e^{j\theta}|^2}}{\sqrt{2}} \quad (2.5)$$

Where θ is the input phase excitation, S_{xx} is the reflection coefficient of the port, and S_{xy} is the coupling between the two ports.

2.1.3 Mean Effective Gain (MEG)

Not only The antenna polarization is important to be considered for MIMO antenna systems design but also the radio environment polarization. Due to the objects the radiated or incident waves that propagate through the radio environment it is exposed to scattering and hence both $E_{i\theta}(\theta, \phi)$ and $E_{i\phi}(\theta, \phi)$ fields come at the receiving antenna will depend on what angles these scatterers are at from the antenna. Also, these two separated fields also have subsequent power densities which also mean that they have polarized antenna gains, G_θ and G_ϕ . The polarization of the antenna takes the electric fields radiated or received by an antenna, which contain A_θ and A_ϕ as the two polarization components in the far field.

When the antenna has A_θ components, it is considered as a vertically polarized antenna and horizontally polarized if the antenna has A_ϕ components [1].

For the radio environment, the vertical polarization of the environment $E_{i\theta}$, resulting in a vertical received power, P_V which represent the incident power density and can be calculated as:

$$P_v = \int_{-\pi}^{\pi} \int_0^{\pi} |E_{i\theta}(\theta, \phi)|^2 \sin\theta d\theta d\phi \quad (2.6)$$

On the other hand, For the radio environment, the horizontal polarization of the environment $E_{i\phi}$, resulting in a horizontal received power, P_H which represent the incident power density and can be calculated as:

$$P_H = \int_{-\pi}^{\pi} \int_0^{\pi} |E_{i\phi}(\theta, \phi)|^2 \sin\theta d\theta d\phi \quad (2.7)$$

The cross polarization ratio (XPR), is defined as the ratio of P_V to P_H as follows:

$$XPR = \frac{P_v}{P_H} \quad (2.8)$$

Objects and scatters around the antenna make multiple copies that appear at the receiving antenna and the gain value cannot be calculated as free space gain. Depending on the angles these scatters are from antenna it better to define the mean effective gain (MEG) instead of free space gain since the real environment contain objects and scatters. The mean effective gain can be defined as; at given environment the total power received to the total power that will be received by an isotropic antenna in that same environment. So that it should be

defined at a given angle according to statistical distribution the power received at angles θ and ϕ will be:

$$P_{\theta}(\theta, \phi) = P_V G_{\theta}(\theta, \phi) \quad (2.9)$$

$$P_{\phi}(\theta, \phi) = P_H G_{\phi}(\theta, \phi) \quad (2.10)$$

Mean effective gain (MEG) can be calculated as follow:

$$MEG = \frac{\int_{-\pi}^{\pi} \int_0^{\pi} (P_{\theta}(\theta, \phi) P_{\theta}(\theta, \phi) + P_{\phi}(\theta, \phi) P_{\phi}(\theta, \phi)) \sin\theta d\theta d\phi}{P_V + P_H} \quad (2.11)$$

Where $P_{\theta}(\theta, \phi)$ and $P_{\phi}(\theta, \phi)$ are the angle of arrival power density due to the incoming $E_{i\theta}$ and $E_{i\phi}$ fields at any given angle and they are related to the radio environment not the antenna. These power densities should satisfy:

$$\int_{-\pi}^{\pi} \int_0^{\pi} P_{\theta}(\theta, \phi) \sin\theta d\theta d\phi = 1 \quad (2.12)$$

$$\int_{-\pi}^{\pi} \int_0^{\pi} P_{\phi}(\theta, \phi) \sin\theta d\theta d\phi = 1 \quad (2.13)$$

Then the general MEG can be expressed as:

$$MEG = \int_{-\pi}^{\pi} \int_0^{\pi} \left(\frac{XPR}{1 + XPR} G_{\theta}(\theta, \phi) P_{\theta}(\theta, \phi) + \frac{1}{1 + XPR} G_{\phi}(\theta, \phi) P_{\phi}(\theta, \phi) \right) \sin\theta d\theta d\phi \quad (2.14)$$

Then to evaluate the MEG, it is necessary to have a model for the angle of arrival functions should be modeled according to specific statistic distribution, $P_\theta(\theta, \phi)$ and $P_\phi(\theta, \phi)$, which will depend on how scatters are positioned [1].

2.1.4 Diversity Gain (DG)

In a communication relying on diversity, multiple copies of the same signal are sent through multiple independent channels. The diversity gain is the number of independent channels carrying the same signal. In a MIMO channel, $M_T M_R$ links are available for communication where M_T and M_R the number of transmitter and receiver in MIMO channel respectively, so the maximal diversity gain is $M_T M_R$. The diversity gain can only be realized if the available SNR is sufficiently high the diversity gain and correlation coefficient are related. The lower the correlation coefficient, the higher is the diversity gain [1].

2.1.5 Branch Power Ratio

For closely spaced MIMO antenna system when the element receiving electromagnetic waves (receiving mode) a current will be induced however part of this current will be coupled into other elements this call as branch power ration (BPR). It is clearly that BPR is related to the coupling and isolation between the elements, also when part of the current will be coupled into other elements this lead to reduce the current in the driven element and therefore reduce the radiation efficiency. Moreover, due to the mutual coupling between antenna elements may radiate in different directions since there is current has been coupled and depends on the pattern that has been created from the coupling the channel capacity can be reduced. Generally BPR can be defined as the ratio of power in one antenna

to the other. This difference of power should be small value for optimum MIMO system [4].

2.1.6 System Capacity

The main advantage of MIMO systems is to provide reliability and increase the capacity of the transmission. Capacity is an important metric to characterize the performance of MIMO systems. The capacity of a communication system is the maximum transmission rate that can be transmitted with probability of error close to zero which can also be defined in term of reliability. A communication at rate R is said to be reliable if one can design a code at rate R that makes the error probability arbitrarily small. Capacity can be defined as the maximum transmission rate for which a reliable communication can be achieved [1].

The channel capacity of a MIMO antenna system depends on the channel matrix, which is a function of the radiation characteristics of the antenna elements and the channel environment. For N-element MIMO antenna with known channel matrix capacity can be calculated from (2.13) [1]. Where H is the channel coefficient matrix and includes the channel correlation coefficient and σ_n represent the signal to noise ratio.

$$C = \log_2 \det \left[I + \frac{HR_{XX}H^T}{\sigma_n^2} \right] \quad (2.15)$$

2.1.7 Multiplexing efficiency

For a single antenna element the losses come from reflection, conduction and dielectric losses, However for MIMO systems, antenna elements cannot be uncorrelated totally which means there is a part of the power that will be lost due to this correlation such that we need to define a new efficiency beside the total radiation efficiency.

The multiplexing efficiency was discussed in [5]. For N elements the multiplexing efficiency was derived for high signal to noise ratio (SNR) environment as follow [5]:

$$\tilde{\eta}_{\text{mux}} = \left(\prod_{k=1}^n \eta_k \right)^{\frac{1}{N}} \det(\underline{\mathbf{R}})^{\frac{1}{N}} \quad (2.16)$$

Where η_k is the total antenna efficiency for element k, and $\underline{\mathbf{R}}$ is the correlation matrix between the antenna elements such that it can be defined as:

$$\underline{\mathbf{R}} = \begin{pmatrix} \rho_{11} & \cdots & \rho_{1N} \\ \vdots & \ddots & \vdots \\ \rho_{N1} & \cdots & \rho_{NN} \end{pmatrix} \quad (2.17)$$

2.2 Some Field Based de-correlation techniques

In MIMO systems, the correlation between the antenna elements has an important contribution to enhance the performance. Therefore, before using the antenna elements in MIMO systems, these elements should be designed in such a way that they can communicate through de-correlated paths which means independent channels. This can be performed in different ways such as spatially separating the antenna elements, providing tilted beams or changing their polarization.

2.2.1 Spatial de-correlation

The correlation coefficient between elements can be calculated from the far field radiation pattern, for instance, the correlation between two elements i and j can be derived from the complex far field components which are $E_{\theta i}$, $E_{\phi i}$ and $E_{\theta j}$, $E_{\phi j}$ for element i and j respectively. These components have a magnitude as well as phase for any angle in the far field, by changing the spacing the element will have different radiated E-field pattern as

well as the phases will be different. Changing the spacing can be horizontally or vertically. For example, for two omnidirectional antennas the correlation between them for horizontal and vertical spacing is shown in Fig 2.1 which indicate that the horizontal spacing gives low correlation paths than vertical spacing. Also, the configuration using horizontal spacing is more compact compared with the vertical spacing.

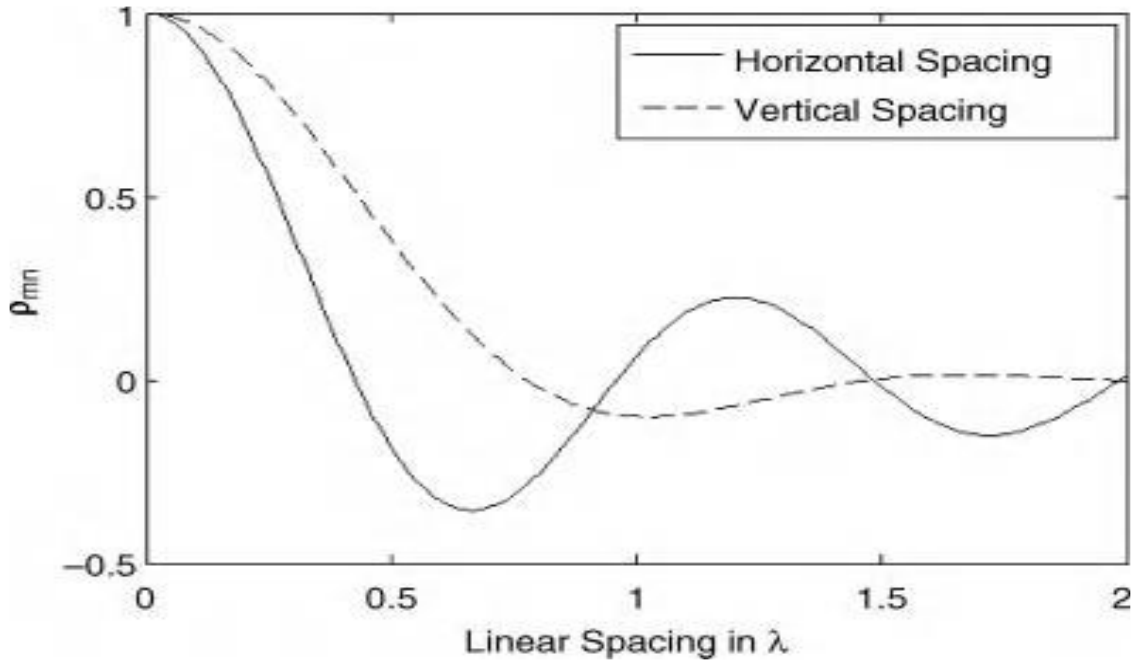


Figure 2.1 Two antenna elements when vertically and horizontally spaced correlation. [1]

2.2.2 Polarization De-correlation

Because of the limitation of the physical size of portable devices, polarized correlation can be suitable in all cases for MIMO antennas which are placed on mobile terminals, so the elements can be allocated close to each other with different polarizations to achieved de – correlated signals [1].

2.3 Summary

Increasing the number of elements to enhance the channel capacity is challenging and require good design and all this MIMO parameters should be evaluated and maintained at certain level to guarantee the required performance of the MIMO system. The main idea behind the MIMO system is to make each element transmit and receive in a channel that should be isolated from the other channels, therefore the correlation coefficient is vital parameter in MIMO system.

CHAPTER 3

LITERATURE REVIEW

MIMO systems were developed to increase the capacity of the communication system to meet the demand for high data rates. This needs good performance which means high accuracy to calculate MIMO system parameters. Here we are focusing on the correlation coefficient as well as the multiplexing efficiency which are related each other. There are many methods to calculate the correlation coefficient as will be discussed next.

3.1 Correlation coefficient calculations

Generally the correlation coefficient is a function of the magnitude and phase of E_θ and E_ϕ . However the distribution of the phase is random due to scattering and multipath and can be modeled through statistical distributions therefore the correlation coefficient can be calculated between element n and element m as follow:

$$\rho_{nm} = \frac{\int_{-\pi}^{\pi} \int_0^{\pi} (XPR A_{\theta m}(\theta, \phi) A_{\theta n}(\theta, \phi)^* P_\theta(\theta, \phi) + A_{\phi m}(\theta, \phi) A_{\phi n}(\theta, \phi)^* P_\phi(\theta, \phi)) \sin\theta d\theta d\phi}{\sqrt{\sigma_n^2 \sigma_m^2}} \quad (3.1)$$

Where:

$$\sigma_n^2 = \int_{-\pi}^{\pi} \int_0^{\pi} \left(XPR A_{\theta n}(\theta, \phi) A_{\theta n}^*(\theta, \phi) P_\theta(\theta, \phi) + A_{\phi n}(\theta, \phi) A_{\phi n}^*(\theta, \phi) \right) \sin\theta d\theta d\phi \quad (3.2)$$

$$\sigma_m^2 = \int_{-\pi}^{\pi} \int_0^{\pi} \left(XPR A_{\theta m}(\theta, \phi) A_{\theta m}^*(\theta, \phi) P_{\theta}(\theta, \phi) + A_{\phi m}(\theta, \phi) A_{\phi m}^*(\theta, \phi) \right) \sin\theta d\theta d\phi \quad (3.3)$$

It is clear to notice that, the correlation coefficient depends on the power distribution $P_{\theta}(\theta, \phi)$ and $P_{\phi}(\theta, \phi)$ which are due to the radio environment and have nothing to do with the antenna. For isotropic power distribution the correlation coefficient is just comparison between the radiated fields and incident fields which depend on the power distribution density of the radio channel [1]. The importance of modeling the radio environments as an isotropic is to have an idea about the correlation behavior in perfect environments the same when the antenna gain is compare with isotropic radiation pattern. Also, in rich scattering environments the probability of arrival and any angle becomes equal approximately hence antennas elements for indoor environment can be modeled as a uniform power distribution. The correlation coefficient can be calculated using different methods such as depending on 3D far field measurements or S-parameters or both by assuming a uniform angle of arrival (isotropic environment). Each of these methods has advantages and disadvantages the details of each are discussed next.

3.1.1 Correlation coefficient calculation using 3D far fields (method-I)

This method calculates the correlation coefficient from the complex far field radiation patterns covering the full spherical coordinates along the antenna elements such that the correlation coefficient can be given as follow [1]:

$$|\rho|^2 = \rho_e = \frac{|\iint_{4\pi} [\vec{F}_i(\theta, \phi) * \vec{F}_j(\theta, \phi)] d\Omega|^2}{\iint_{4\pi} |\vec{F}_i(\theta, \phi)|^2 d\Omega \iint_{4\pi} |\vec{F}_j(\theta, \phi)|^2 d\Omega} \quad (3.4)$$

Where ρ is the correlation coefficient, ρ_e is the envelope correlation coefficient and $F_i(\theta, \phi)$ and $F_j(\theta, \phi)$ are the three-dimensional complex field radiation patterns of the antenna when the i^{th} port and j^{th} port are excited and Ω is the solid angle. This method is complicated, time consuming and expensive to measure antenna patterns at different frequency point, due to the use of specialized equipment and facilities. However it gives accurate and exact value of the correlation coefficient. Also this method can be used for any number of antennas elements in MIMO system. This method will be denoted as method-I.

3.1.2 Correlation coefficient calculation using the S-parameters (method-II)

Due to the complexity of calculating the correlation coefficient using far field measurements, the calculation using others method like S-parameters become more attractive. In [6] a relation between the far filed and the S-parameters was demonstrated for highly efficient antennas. The correlation coefficient can be calculated using the S-parameters for N antennas elements as follows [7]:

$$\rho_{ij} = \frac{-\sum_{n=1}^N S_{ni}^* S_{nj}}{\sqrt{(1 - \sum_{n=1}^N |S_{ni}|^2)(1 - \sum_{n=1}^N |S_{nj}|^2)}} \quad (3.5)$$

Where ρ_{ij} is the correlation coefficient between elements i and j , the number of MIMO antenna elements is represented by N . This method has been used in most of the literature to calculate the correlation coefficient. The advantage of this method is fast and easy to calculate the correlation coefficient for high radiation efficiency antennas. On the other hand this method is unreliable when the radiation efficiency is moderate to low. This method will be denoted as method-II.

3.1.3 Correlation coefficient calculation using scattering S-parameters and Radiation Efficiencies (method- III)

This method gives more reliable calculations than using only the S-parameters (method-II) because it considers the effects of the radiation efficiency, but instead of giving the exact value, it gives the maximum value for the correlation coefficient such that the exact value within this range, as follow [8]:

$$\rho_{e12_{max,min}} = \frac{S_{11}^* S_{12} + S_{21}^* S_{22}}{\sqrt{(1 - |S_{11}|^2 - |S_{12}|^2)(1 - |S_{22}|^2 - |S_{21}|^2)} \eta_{rad,1} \eta_{rad,2}} \pm \sqrt{\left(\frac{1}{\eta_{rad,1}} - 1\right)} \sqrt{\left(\frac{1}{\eta_{rad,2}} - 1\right)} \quad (3.6)$$

Where $\eta_{rad,1}$, $\eta_{rad,2}$ are the radiation efficiencies of the two antenna elements, the second term in (3.6) represents the degree of uncertainty which will be high when the radiation efficiencies are low and the value of the correlation coefficient can be greater than one. So this method gives indication about the impact of the losses on the correlation coefficient computations using the S parameters. The upper and lower values of the correlation coefficient using (3.6) are valid for 2-element antenna systems. The solution for more than two elements has not been derived in the existing literature. In this present work we will generalize (3.6) to N-ports. This method will be denoted as method- III.

3.1.4 Correlation coefficient calculation based on the equivalent circuit in lossy MIMO antenna (method- IV)

The disadvantage of the calculation of the correlation coefficient using (3.5) is that it does not consider antenna conduction and dielectric losses thus the results are inaccurate and are not acceptable as a reliable indication of the MIMO antenna system. Recall that:

$$\eta_{rad,tot} = \eta_{ref} \eta_{cd} \quad (3.7)$$

Where $\eta_{rad,tot}$ is the total radiation efficiency, η_{ref} is the reflection efficiency and η_{cd} is the efficiency due to the conduction and dielectric losses, η_{cd} was considered as 100% in equation (3.5) therefore the results using (3.5) lack the accuracy when the antennas are lossy. In equation (3.6) the effect of the total radiation efficiency was considered to estimate the worst possible correlation performance and gave an indication for the impact in the correlation due to the antenna losses which can be shown in the degree of uncertainty, Although [8] considered the impact of losses in lossy antennas correlation behavior, the degree of uncertainty gets high and becomes difficult to have the exact value of the correlation coefficient. When the correlation coefficient is calculated using the far field as in (3.4) the effect of the radiation efficiency is canceled out because of normalization. In other words, if the antenna is loaded with lump elements, the radiation efficiency will change but the correlation coefficient will remain unchanged [9], So the exact value of the correlation coefficient using the S-parameters should be calculated from lossless antenna elements. Hence, we need to calculate the value of the loss component in the antenna to come up with the lossless antenna equivalent [10]. To illustrate the idea, the network approximation of two lossy antenna elements is shown in Fig.3.1. The loss components

(resistor connected in series or parallel) can be calculated using an equivalent circuit which depends on the antenna type, and then the transmission matrix can be calculated. The S-parameters of the lossy antenna can be measured using a VNA which represent the cascade S-parameters of the loss components plus lossless antenna elements [10].

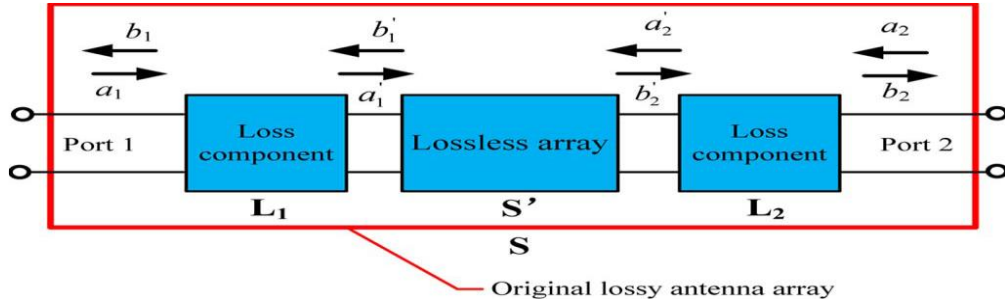


Figure 3.1 Equivalent lossy circuit module of two lossy elements [10]

In Fig.3.1, L_1 and L_2 are the transmission matrix or (ABCD) for the loss component and S' represent the transmission matrix of the S-parameters of the lossless element. S represents the complete matrix of the S-parameters of the lossy element [11].

$$[S]_{ABCD} = [L_1]_{ABCD} [S']_{ABCD} [L_2]_{ABCD} \quad (3.8)$$

$$[S]_T = [L_1]_T [S']_T [L_2]_T \quad (3.9)$$

Then the transmission matrix of the S-parameters of the lossless element can be calculated using (3.9) after that we can calculate the correlation coefficient using (3.5) after converting it back into S-parameter .ABCD matrix and S-parameters conversion can be used for two port systems, However, for $N > 2$, the conversion from S-parameters to transmission matrix and vice versa was discussed in [12].

$$[S']_{ABCD} = [L_1]_{ABCD}^{-1} [S]_{ABCD} [L_2]_{ABCD}^{-1} \quad (3.10)$$

$$[S']_T = [L_1]^{-1}_T [S]_T [L_2]^{-1}_T \quad (3.11)$$

To sum up, the procedure for calculating the correlation coefficient using the lossy equivalent circuit model is as follows:

1. Measure the S-parameters and antenna efficiencies.
2. Calculate the loss impedance components from the equivalent circuit.
3. Calculate the transmission matrix of each loss impedance component.
4. Extract the S-parameters of the lossless component.
5. Calculate the correlation coefficient of the lossless component from (3.5)

The challenge is how to get the loss components from the equivalent circuit because it is based on the equivalent circuit of the antennas. In [13] the equivalent circuit of the antennas was discussed such that for omnidirectional antennas such as dipoles, monopoles and slots it can be approximately represented by a series R-L-C circuit. On the other hand in [14] planar antenna types, like PIFA and patch antennas, their equivalent circuit can be expressed as a parallel R-L-C network, where R represents the radiation, conductor and dielectric losses. Because of limitation in the measurements (S-parameters and efficiency) [10], we design for the resistance only, also we are targeting the correlation coefficient at the central frequency (resonant frequency) where the imaginary part will be canceled out.

3.1.4.1 Series R-L-C equivalent circuits for two element antennas

For a series R-L-C, two elements with omnidirectional patterns such as dipole antennas can be represented as shown in Fig.3.2:

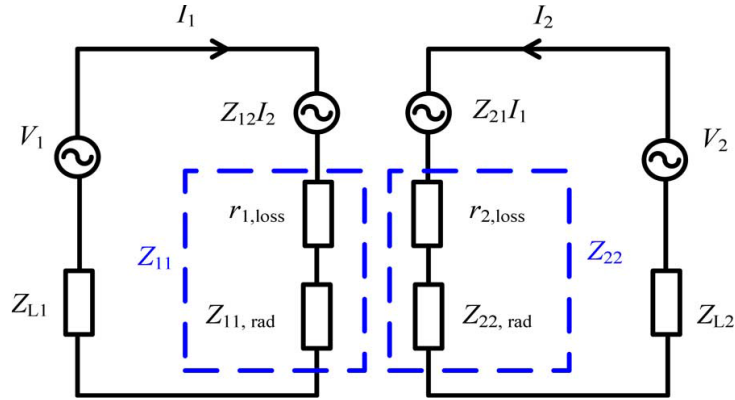


Figure 3.2 Equivalent circuit model for lossy dual antenna as a Series RLC [10].

In this circuit,

V_1 is element 1 excitation.

V_2 is element 2 excitation.

$r_{1,loss}$ is element 1 loss resistance.

$r_{2,loss}$ is element 2 loss resistance.

$Z_{11,rad}$ is element 1 radiation impedance which include $r_{1,rad}$ radiation resistance .

$Z_{22,rad}$ is element 2 radiation impedance which include $r_{2,rad}$ radiation resistance.

Z_{12} , Z_{21} are the mutual impedances between the antenna elements.

The magnitude of the mutual impedance depends on the spatial distance between the antenna elements [15], [16]. To start the analysis ,we assume that the two elements are identical such that $r_{1,loss} = r_{2,loss}$ and $r_{1,rad} = r_{2,rad}$ also $Z_{L1} = Z_{L2} = Z_L$ which are the load impedances.

Dual antenna elements can be defined in two ways, they can be defined as two networks with their inactive port connected to the load impedance, in this case if we assume that **port 1** is active and **port 2** is not, then the total efficiency can be calculated using equation (3.12):

$$\eta_{tot,1} = (1 - |S_{11}|^2 - |S_{21}|^2)\eta_{rad,1} \quad (3.12)$$

Where the radiation efficiency is calculated as:

$$\eta_{rad,1} = \frac{P_{rad}}{P_{rad} + P_{loss}} \quad (3.13)$$

$$= \frac{|I_1|^2 r_{rad} + |I_2|^2 r_{rad}}{|I_1|^2 r_{rad} + |I_2|^2 r_{rad} + |I_1|^2 r_{loss} + |I_2|^2 r_{loss}} \quad (3.14)$$

The relation between I_1 and I_2 can be calculated from non-excited port as:

$$I_2 = \frac{Z_{21} I_1}{Z_{22} + Z_L} \quad (3.15)$$

Then we can define the ratio k as follow:

$$k = \frac{|I_1|}{|I_2|} = \frac{Z_{22} + Z_L}{Z_{21} I_1} \quad (3.16)$$

Substitute (3.16) in (3.14):

$$\eta_{rad,1} = \frac{r_{rad}}{r_{rad} + r_{loss}} \quad (3.17)$$

The second way is to describe the dual antenna system by defining it as one active port and such that port two is lossy by considering a loss resistance, then the total efficiency can be describe as:

$$\eta_{tot,1} = (1 - |S_{11}|^2)\eta'_{rad,1} \quad (3.18)$$

Where the radiation efficiency is given as:

$$\eta'_{rad,1} = \frac{|I_1|^2 r_{rad} + |I_2|^2 r_{rad}}{|I_1|^2 r_{rad} + |I_2|^2 r_{rad} + |I_1|^2 r_{loss} + |I_2|^2 r_{loss} + |I_2|^2 Re(Z_L)} \quad (3.19)$$

$$\eta'_{rad,1} = \frac{(k^2 + 1)r_{rad}}{(k^2 + 1)r_{rad} + (k^2 + 1)r_{loss} + Re(Z_L)} \quad (3.20)$$

By solving (3.17) and (3.20), the loss resistance for the two similar elements ($r_{loss} = r_{1,loss} = r_{2,loss}$) is found using:

$$r_{loss} = \frac{\eta'_{rad,1}(1 - \eta_{rad,1})Re(Z_L)}{(\eta_{rad,1} - \eta'_{rad,1})(k^2 + 1)} \quad (3.21)$$

The cascade network can be represented as:

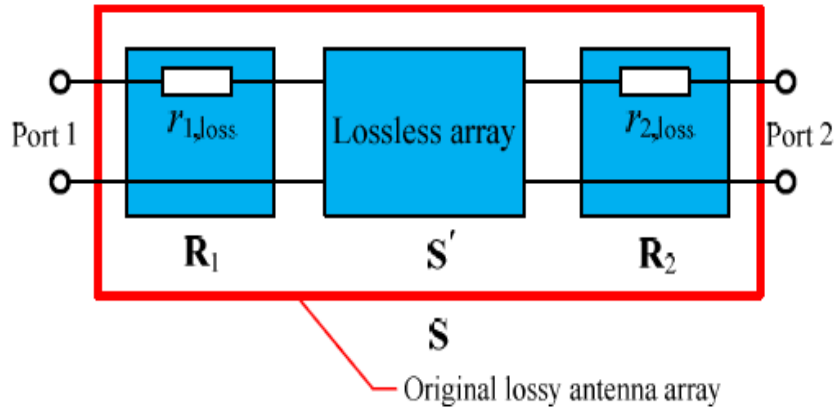


Figure 3.3 Series equivalent circuits model with lossy lumped components [17]

For N elements, we can use the same procedure mentioned assuming that the elements are identical. When voltage is applied to element i the other $(N-1)$ elements will not be excited.

The total efficiency for these N port antenna systems is:

$$\eta_{tot,i} = \left(1 - \sum_{j=1}^N |S_{ji}|^2 \right) \eta_{rad,i} \quad (3.22)$$

The relation between I_i and I_j can be calculated from non-excited elements assuming **port i** is excited as:

$$Z_{21}I_1 + (Z_{22} + Z_L)I_2 + Z_{23}I_3 + \dots + Z_{2N}I_N = 0 \quad (3.23)$$

$$Z_{31}I_1 + Z_{32}I_2 + (Z_{33} + Z_L)I_3 + \dots + Z_{3N}I_N = 0 \quad (3.24)$$

⋮

$$Z_{N1}I_1 + Z_{N2}I_2 + Z_{N3}I_3 + \dots + (Z_{NN} + Z_L)I_N = 0 \quad (3.25)$$

Dividing (3.23), (3.24) and (3.25) by I_1 and using matrix form as shown:

$$Z_{21} + (Z_{22} + Z_L)k_{12} + Z_{23}k_{13} + \dots + Z_{2N}k_{1N} = 0 \quad (3.26)$$

$$Z_{31} + Z_{32}k_{12} + (Z_{33} + Z_L)k_{13} + \dots + Z_{3N}k_{1N} = 0 \quad (3.27)$$

⋮

$$Z_{N1} + Z_{N2}k_{12} + Z_{N3}k_{13} + \dots + (Z_{NN} + Z_L)k_{1N} = 0 \quad (3.28)$$

$$\begin{pmatrix} k_{12} \\ k_{13} \\ \vdots \\ k_{1N} \end{pmatrix} = - \begin{pmatrix} (Z_{22} + Z_L) & \dots & Z_{2N} \\ Z_{32} & \ddots & Z_{3N} \\ \vdots & \ddots & \vdots \\ Z_{N2} & \dots & (Z_{NN} + Z_L) \end{pmatrix}^{-1} \begin{pmatrix} Z_{21} \\ Z_{31} \\ \vdots \\ Z_{N1} \end{pmatrix}$$

From (3.14) the radiation efficiency of element i can be described as:

$$\eta_{rad,i} = \frac{\sum_{j=1}^N k_{ij}^2 r_{j,rad}}{\sum_{j=1}^N k_{ij}^2 r_{j,rad} + \sum_{j=1}^N k_{ij}^2 r_{j,loss}} \quad (3.29)$$

The total efficiency when the system considered as one port network and other element loaded to lossy impedance is found as follow:

$$\eta_{tot,i} = (1 - |S_{ii}|^2) \eta'_{rad,i} \quad (3.30)$$

$$\eta'_{rad,i} = \frac{\sum_{j=1}^N k_{ij}^2 r_{j,rad}}{\sum_{j=1}^N k_{ij}^2 r_{j,rad} + \sum_{j=1}^N k_{ij}^2 r_{j,loss} + \sum_{j=1, j \neq i}^N k_{ij}^2 Re(Z_l)} \quad (3.31)$$

By solving for identical elements as well symmetric placement of the elements ($r_{loss} = r_{1,loss} = r_{2,loss} \dots \dots = r_{N,loss}$) using (3.29) and (3.31) the loss resistance can be calculated as:

$$r_{loss} = r_{i,loss} = \frac{\eta'_{rad,i} (1 - \eta_{rad,i}) \sum_{j=1}^N k_{ij}^2 Re(Z_l)}{(\eta_{rad,i} - \eta'_{rad,i}) \sum_{j=1}^N k_{ij}^2} \quad (3.32)$$

3.1.4.2 Parallel R-L-C equivalent circuit for two element antennas

For a parallel R-L-C, the two elements can be represented as follow:

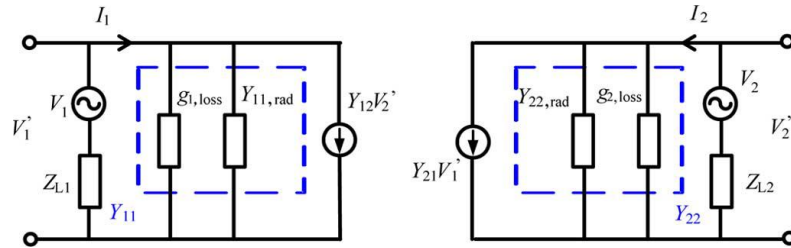


Figure 3.4 parallel equivalent circuits model for lossy dual antenna array [10].

In this circuit,

V_1 is element 1 excitation.

V_2 is element 2 excitation.

$g_{1,loss}$ is element 1 loss conductance.

$g_{2,loss}$ is element 2 loss conductance.

$Y_{11,rad}$ is element 1 radiation conductance .

$Y_{22,rad}$ is element 2 radiation conductance.

Y_{12} , Y_{21} are the mutual conductance between the two elements.

To start the analysis, we assume that the two elements are identical such that $g_{1,loss} = g_{2,loss}$ and $Y_{22,rad} = Y_{11,rad} = Y_{rad}$ also $Z_{L1} = Z_{L2} = Z_L$ which is the load impedance. Using the same analysis procedure we assume that **port 1** is active and **port 2** is not, then the total efficiency can be calculated using (3.17) where the radiation efficiency is calculated as:

$$\eta_{rad,1} = \frac{|V'_1|^2 Y_{rad} + |V'_2|^2 Y_{rad}}{|V'_1|^2 Y_{rad} + |V'_2|^2 Y_{rad} + |V'_1|^2 g_{loss} + |V'_2|^2 g_{loss}} \quad (3.33)$$

The relation between V'_1 and I_2 can be calculated from non-excited port as:

$$V'_1 = \frac{(1 + Z_L Y_{22}) I_2}{Y_{21}} \quad (3.34)$$

Then we can define the ratio m as follows:

$$m = \frac{|V_1|}{|I_2|} = \frac{(1 + Z_L Y_{22})}{Y_{21}} \quad (3.35)$$

From (3.33)

$$\eta_{rad,1} = \frac{Y_{rad}}{Y_{rad} + g_{loss}} \quad (3.36)$$

Using the second way to describe the dual antenna system by defining it as one port such that port two is lossy by considering the loss resistance. Then the total efficiency described in (3.31) becomes where the radiation efficiency is given as:

$$\eta'_{rad,1} = \frac{|V'_1|^2 Y_{rad} + |V'_2|^2 Y_{rad}}{|V'_1|^2 Y_{rad} + |V'_2|^2 Y_{rad} + |V'_1|^2 g_{loss} + |V'_2|^2 g_{loss} + |I_2|^2 Re(Z_L)} \quad (3.37)$$

Use (3.35)

$$\eta'_{rad,1} = \frac{(m^2 + Z_L) Y_{rad}}{(m^2 + Z_L) Y_{rad} + (m^2 + Z_L) g_{loss} + Re(Z_L)} \quad (3.38)$$

By solving for identical elements ($g_{loss} = g_{1,loss} = g_{2,loss}$) using (3.36) and (3.38) the shunt loss resistance can be calculated as:

$$g_{loss} = \frac{\eta'_{rad,1} (1 - \eta_{rad,1}) Re(Z_L)}{(\eta_{rad,1} - \eta'_{rad,1}) (m^2 + |Z_L|)} \quad (3.39)$$

The solution for more than two elements for parallel R-L-C has not been derived in the existing literature. Extending this method to N-elements is one of the contribution of this work. Generally, The drawback of this method(equivalent circuit model), is that when the number of the elements increases the complexity rise up through the calculation of the transmission matrixes, however, a good agreement will be maintained between the value

of the correlation coefficient using this method and the exact value. This method will be denoted as method-IV.

3.1.5 Correlation coefficient calculation for Lossy Compact Monopole Arrays with Decoupling Networks (method-V)

In [18] the power losses were more investigated by assuming the losses come from coupling and internal losses. The total power for two antenna elements can be expressed as:

$$p_{tot} = p_{rad} + p_{loss} + p_1 + p_2 \quad (3.40)$$

Where p_{rad} is the radiated power, p_{loss} is the dissipated power and p_1, p_2 are the reflection losses, as in [6] and [8]:

$$p_{tot} = \frac{1}{2} |a_1|^2 + \frac{1}{2} |a_2|^2 \quad (3.41)$$

$$p_{rad} = \int_{\Omega} |\sqrt{M(1 - |S_{11}|^2 - |S_{12}|^2)} a_1 \vec{F}_1(\theta, \phi) + \sqrt{M(1 - |S_{22}|^2 - |S_{12}|^2)} a_2 \vec{F}_2(\theta, \phi)|^2 d\Omega \quad (3.42)$$

$$p_{loss} = p_{loss}(|a_1|^2) + p_{loss}(|a_2|^2) + p_{loss}(a_1 a_2^*) + p_{loss}(a_2 a_1^*) \quad (3.43)$$

$$p_{ref,1} = \frac{1}{2} |a_1 S_{11} + a_2 S_{12}|^2 \quad (3.44)$$

$$p_{ref,2} = \frac{1}{2} |a_1 S_{12} + a_2 S_{22}|^2 \quad (3.45)$$

In (3.43), $p_{loss}(|a_1|^2)$, $p_{loss}(|a_2|^2)$ are the internal losses due to lumped components (resistors) in each element, and $p_{loss}(a_1 a_2^*)$, $p_{loss}(a_2 a_1^*)$ are the coupling losses, these

losses have been calculated as Ohmic Losses of Radiation Elements and Losses in the Feeding Network. In addition to the coupling losses in the network for two element monopoles in such way that the uncertainty of (3.4) to be determined [18]. For **port1** when **port2** is not active the power expression can be:

$$p_{tot,1} = \frac{1}{2}|a_1|^2 \quad (3.46)$$

$$p_{rad,1} = \int_{\Omega} |\sqrt{M(1 - |S_{11}|^2 - |S_{12}|^2)} a_1 \vec{F}_1(\theta, \phi)|^2 d\Omega \quad (3.47)$$

$$p_{loss,1} = p_{loss}(|a_1|^2) \quad (3.48)$$

$$p_{ref,1} = \frac{1}{2}|a_1 S_{11}|^2 \quad (3.49)$$

Then the total power for **port1** can be written as:

$$p_{tot,1} = p_{rad,1} + p_{loss,1} + p_{ref,1} \quad (3.50)$$

Solve for $|a_1 \vec{F}_1(\theta, \phi)|^2$ as:

$$|a_1 \vec{F}_1(\theta, \phi)|^2 = \frac{1 - |S_{11}|^2 - |S_{12}|^2 - \frac{p_{loss}(|a_1|^2)}{\frac{1}{2}|a_1|^2}}{M(1 - |S_{11}|^2 - |S_{12}|^2)} \quad (3.51)$$

The same procedure for port2 and solving for $|a_2 \vec{F}_2(\theta, \phi)|^2$ as:

$$|a_2 \vec{F}_2(\theta, \phi)|^2 = \frac{1 - |S_{22}|^2 - |S_{12}|^2 - \frac{p_{loss}(|a_2|^2)}{\frac{1}{2}|a_2|^2}}{M(1 - |S_{22}|^2 - |S_{12}|^2)} \quad (3.52)$$

For the coupling power $|a_1 \vec{F}_1(\theta, \phi) a_2 \vec{F}_2(\theta, \phi)|^2$ will be:

$$\begin{aligned}
& |a_1 \vec{F}_1(\theta, \phi) a_2 \vec{F}_2(\theta, \phi)|^2 \\
&= \frac{S_{11}^* S_{12} + S_{21}^* S_{22} - \frac{p_{loss,12}(a_1 a_2^*)}{\frac{1}{2}(a_1 a_2^*)}}{\sqrt{M(1 - |S_{11}|^2 - |S_{12}|^2)} \sqrt{M(1 - |S_{22}|^2 - |S_{12}|^2)}} \quad (3.53)
\end{aligned}$$

By using (3.1) the correlation coefficient can be calculated as:

$$\rho_{12} = \frac{S_{11}^* S_{12} + S_{21}^* S_{22} - \frac{p_{loss,12}(a_1 a_2^*)}{\frac{1}{2}(a_1 a_2^*)}}{\sqrt{(1 - |S_{11}|^2 - |S_{12}|^2 - \frac{p_{loss}(|a_1|^2)}{\frac{1}{2}|a_1|^2})(1 - |S_{22}|^2 - |S_{12}|^2 - \frac{p_{loss}(|a_2|^2)}{\frac{1}{2}|a_2|^2})}} \quad (3.54)$$

Now to calculate the correlation coefficient ρ_{12} should be calculated which depends on the current distribution along the elements. In [18] A sinusoid current distribution was assumed to calculate the correlation coefficient for two element monopoles. So the drawback of this method is requiring of the knowledge of the current distribution through the antenna elements which add a kind of complexity in the calculation of the correlation coefficient, however, a good agreement will be maintained between the value of the correlation coefficient using this method and the exact value. This method will be denoted as method-V *but due to its limited application it will not be investigated further.*

3.2 Related Works

Different designs and structures have been investigated for MIMO systems, and different methods have been used to evaluate the correlation coefficient. In [19]–[21], 2-element, 3-element and 4-element monopole antennas were employed to cover 2.4 GHz WLAN. The correlation coefficient was calculated used the 3D radiation field method in (3.1).

In [22]–[27], 2-elements monopole MIMO antennas were implemented to cover WLAN and WiMAX frequency ranges and the S-parameters method in (3.5) was used to calculate the correlation coefficient. The radiation efficiency was around 75%, so there will be a kind of disagreement from the exact value as (3.5) is only valid for 100% efficient antennas. In [28] a 2-element dipole antenna covering WLAN frequency range was introduced for MIMO systems and the correlation coefficient was calculated using the far field radiation pattern method. In addition, a 2-element monopole with slots was proposed and studied in [29] for TD-SCDMA (2.3-2.4 GHz)/LTE (2.5-2.7 GHz)/WLAN and 5.2 GHz industrial, scientific and medical band (ISM) and the correlation coefficient was calculated from S-parameters using (3.5). In [30], a 2-monopole based MIMO antenna with two inverted L-shape and rectangular slot with circular end was designed to cover five resonant frequencies (900 MHz, 1800 MHz, 2100 MHz, 3500 MHz, and 5400 MHz) was proposed. Both the radiation pattern and S-parameters methods were used for calculating the correlation coefficient. It is worth to notice that there was disagreement between the values using these two methods because of the low value of the radiation efficiency. In [31] four wideband Microstrip feedline printed monopole antennas loaded with ring shaped ground plane were presented to cover 2.4 GHz and 2.6 GHz with low correlation between the element which was calculated using the far field radiation pattern method.

There are also other work and designs for ISM band applications using PIFA elements. In [32] two, four and six element PIFA antenna and Minkowski monopole antenna were designed for MIMO systems to operate in the 5.2 GHz (ISM) band and the correlation coefficient metric was calculated from the far field radiation pattern using (3.4).

A 2-element PIFA antenna implemented for UMTS frequency range and a 3-elements PIFA antenna for covering LTE2500 frequency range were proposed in [33]. In [34] a 2-element PIFA antenna was introduced for LTE/WiMAX USB dongle operating in the 2.5-2.7 GHz, both of these configurations have used the s-parameters method to evaluate the correlation coefficients. Moreover there are some designs for slots antennas, In [35], four element slot antennas were presented to cover 1.84 GHz. Also, in [36] a two elements L-shape slot antenna was introduced for ultra-wide band (UWB) MIMO systems (3.1 - 10.6 GHz). Based on the S-parameters method the envelope correlation coefficient was calculated for each. A 4-elements F-shape slot antenna was introduced in [37] to cover ISM band as well as WLAN (2.4 GHz), Using the S-parameters the correlation coefficient was calculated.

In [38] three annular slot antenna elements were designed with resonant frequency at 2.45GHz and the S-parameters method was used to evaluate the correlation coefficient. In [39] a 4-element antenna was introduced for WLAN band, these 4-elements consist of 2-element patch antennas and 2-elements slot antennas and the 3D radiation far field was used to calculate the correlation coefficient. A patch antenna was also introduced for MIMO systems, In [40], [41] 4-elements and 2-elements were designed for 2.45 GHz and 3-11GHz respectively .The S-parameters method was used for correlation coefficient calculation. In [42] a 2-element patch antenna loaded with complementary split –ring resonator (CSRR) was designed for multi resonant frequencies (750 MHz, 1.18GHz, 1.7GHz and 2.26GHz) and the S-parameters method was used to calculate the correlation coefficient in spite of low radiation efficiency over the target bands. Also printed meander-line antennas have been developed for MIMO systems. In [43] two printed meander-line

monopole antennas were proposed with resonant at 710 MHz and the correlation coefficient was calculated using (3.5) with assumption that the elements are lossless. In [44], two printed meander-line monopole antennas covering 2.4 , 5.8 and 3.5 GHz (WLAN and WiMAX application) was proposed. The S-parameters method was used to calculate the correlation coefficient. In [45] two printed meandered loop antennas were presented to cover multiple communication bands such that the resonant frequencies are ($699\text{-}798\text{MHz}$), ($1.7\text{-}2\text{ GHz}$), 2.3 GHz , 3.5GHz , 2.4GHz and 5GHz . The correlation coefficient for these frequencies was calculated using S-parameters which assume that the elements are lossless. Also in [46] printed 3-element MIMO antenna systems was presented to cover WLAN band (2.4 GHz and 5GHz) and the correlation coefficient was calculated using the S-parameter method. In [33] three dual –loop antennas were demonstrated to cover UMTS/LTE2500 bands, the correlation coefficient was calculated using the S-parameters method.

Also in [47] a printed inverted-L antenna element was proposed to cover 2.5 GHz and 0.9GHz and the far field method was used to calculate the correlation coefficient . Moreover, in [48] two printed dual-band meander-line monopole antennas with resonant frequencies 870 MHz and 2.6GHz were presented. The effect of the radiation efficiency was considered for the correlation coefficient calculation through using (3.6). In [49] two folded monopole antennas were proposed to operate at the 2.4GHz WLAN band besides, in [50] two parallel folded monopole antenna elements were introduced to operate at 2.4 GHz , 5.2 GHz and 5.8GHz , and the correlation coefficient was calculated from the far field radiation pattern. In [51], two element 4-shaped monopole antennas were proposed to cover from $803\text{-}823\text{ MHz}$ and $2440\text{-}2900\text{ MHz}$ using (3.6).

3.3 Summary

From the literature review, Fig.3.5-3.7 shows the distribution of previous works in three categories. The first category illustrated in the tree, in Fig 3.5 the distribution was based on the number of elements illustrates that most of the previous works was for 2-element monopole antenna systems, on the other hand, few of research works for the other type of antennas with different number of elements is shown. The second category is shown in Fig 3.6 which classifies the work based on the correlation coefficient calculation method that was used. It is clear that most of works have used method- II method to calculate the correlation coefficient which is not accurate because it assumes lossless elements, and this is an impracticable case and all antennas elements are lossy. Fig 3.7 classifies the work based on the covered bands. From Fig 3.7 there is a lot of work targeting WLAN bands. This is because most devices are WLAN ready at that frequency such as routers and dongles and, it is worth to notice that most of the research work targeted 2-element MIMO systems. For devices that will support the next generation standard (5G), high data rates will be maintained through increasing the number of elements, so we are going to focus on 4-element antennas. Also the majority in the literature review shows that previous works used method- II method to calculate the correlation coefficient by assuming lossless antenna element which is not the real scenario and is not correct.

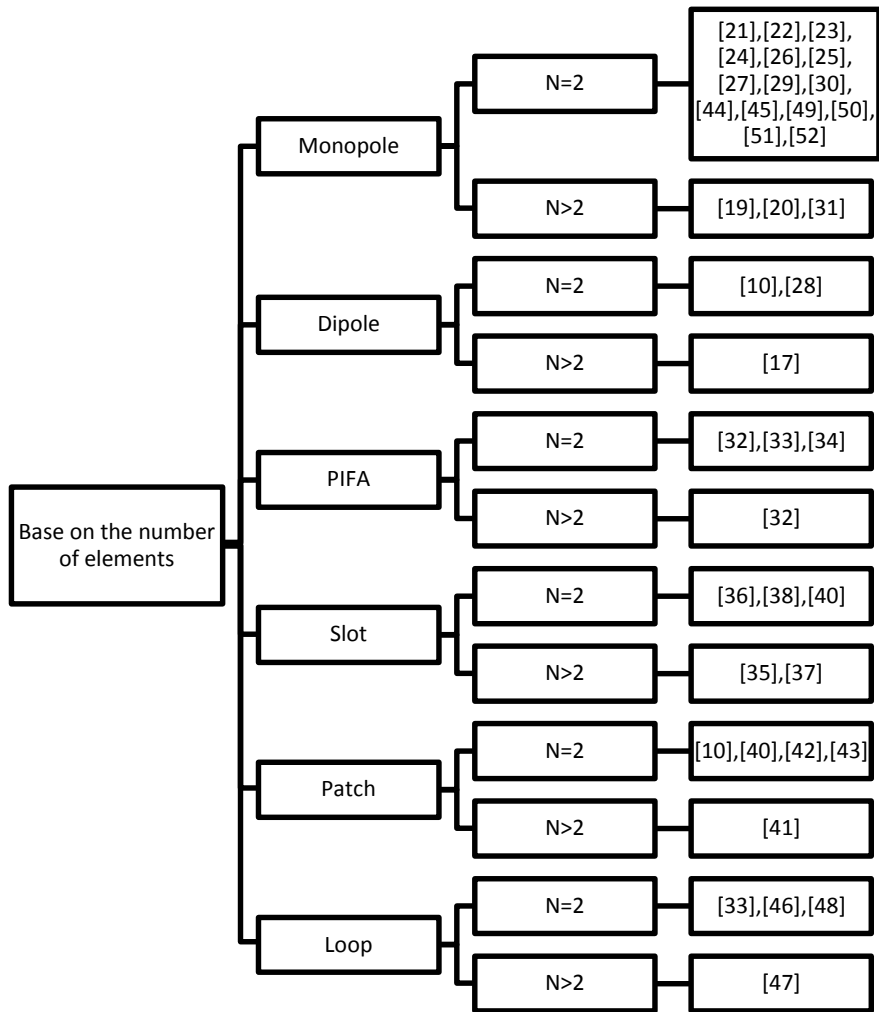


Figure 3.5 Classification based on the number of elements.

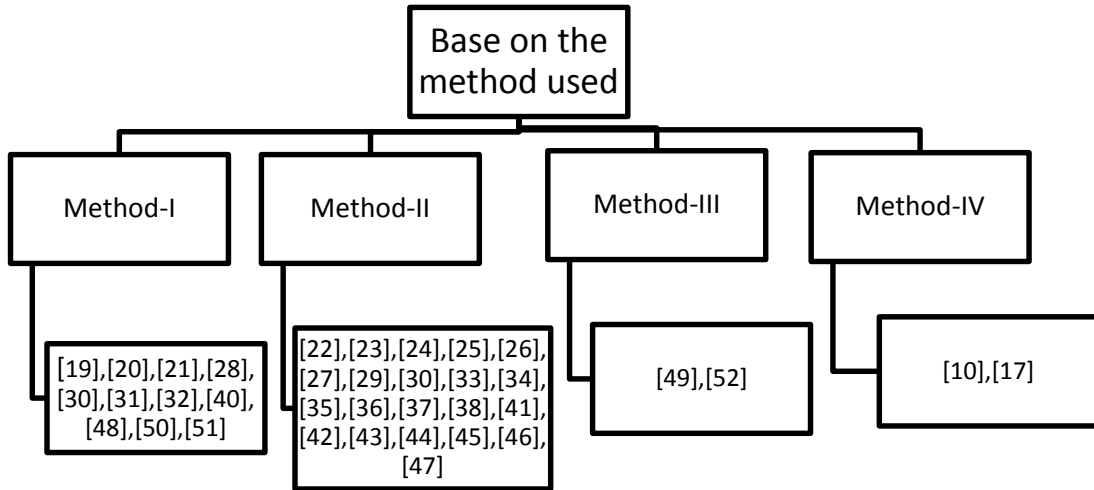


Figure 3.6 Classification based on the method used.

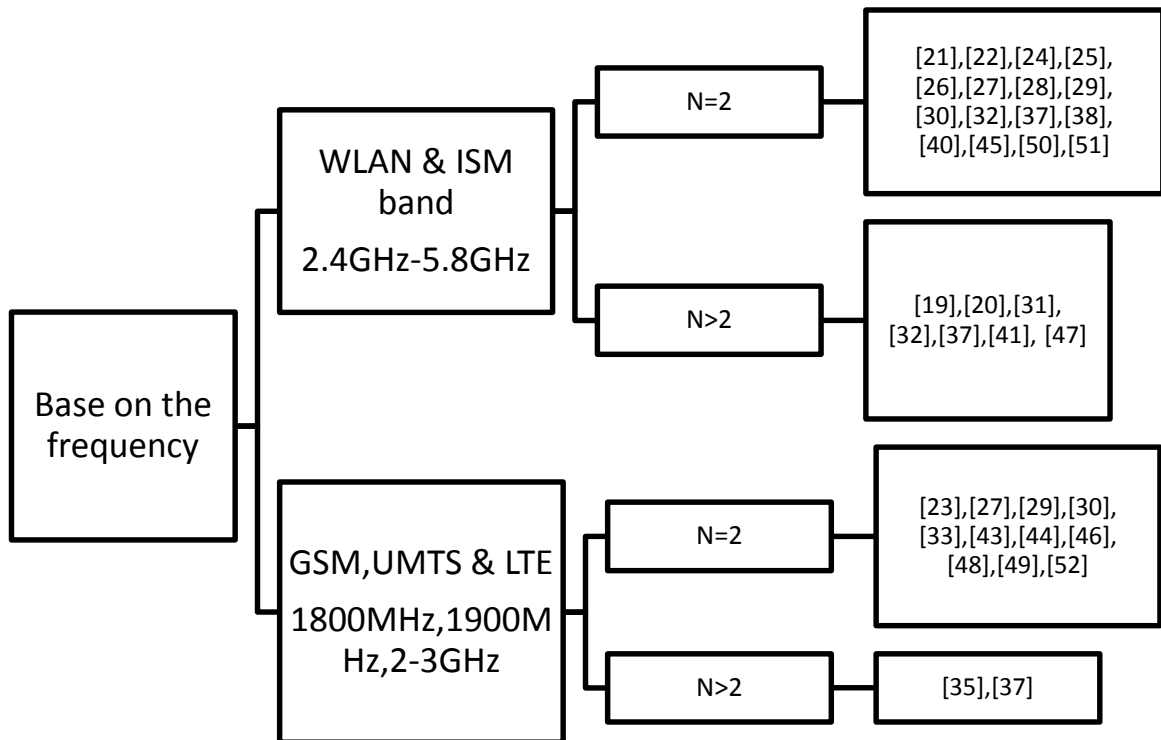


Figure 3.7 Classification based on the frequency.

CHAPTER 4

Analytical Extension of Method- III and IV to Cover N- Ports

The correlation coefficient calculation should be generalized to handle N-ports. Although the calculation of the correlation coefficient with the radiation efficiency (method- III) is unreliable for lossy antenna elements, but it provides more accurate values for antennas with high radiation efficient. The correlation coefficient equation for more than two elements has not been derived in the existing literature for Method-III. Moreover, the parallel equivalent circuit method- IV to estimate the correlation coefficient also has been derived only for two elements. Here we are derive the generalized formula for N elements such that the whole estimation method will be valid for N-elements.

4.1 Generalization of method- III to N-Port MIMO Systems

The upper and lower values of the correlation coefficient using (3.9) are valid for 2-element antenna systems [8]. The solution for more than two elements has not been derived in the existing literature. Here we are derive the solution for N elements. To make (3.9) valid for N elements we provide the steps to generalize it as part of this work contribution. As shown in Fig.4.1 either the antenna element is in receiving or transmitting mode the total radiated field in the far field can be the sum of each element contribution as follows [6]:

$$\bar{E} = \bar{E}_1 + \dots + \bar{E}_N \quad (4.1)$$

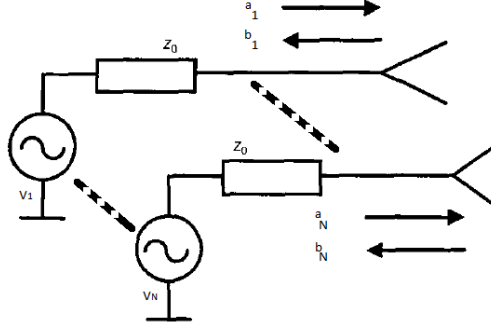


Figure 4.1 Representation of N- antenna elements

Where the radiated field of element j can be expressed in term of the incident wave \mathbf{a}_j , \mathbf{M} is constant which depends on the antenna dimensions and the directivity as well as the wave number k using the expression,

$$\bar{\mathbf{E}}_j = \mathbf{a}_j \cdot \mathbf{M} \cdot \bar{\mathbf{F}}_j(\theta, \phi) \cdot \frac{e^{-ikr}}{r} \quad (4.2)$$

For the isotropic power distribution, the correlation coefficient is just comparison between the radiated fields and incident fields which depends on the power distribution density of the radio channel. It can be represented in power form such that the total power can be written as:

$$\mathbf{p}_{tot} = \iint_{all\ space} |\bar{\mathbf{E}}|^2 d\mathbf{s} \quad (4.3)$$

The total power can be also expressed in S-parameter form as [6]:

$$\mathbf{p}_{tot} = \mathbf{a}^* (\mathbf{I} - \mathbf{S}^* \mathbf{S}) \mathbf{a} \quad (4.4)$$

Where \mathbf{a} is the incident wave vector of the N element, \mathbf{S} is $N \times N$ scattering matrix and \mathbf{I} is the identity vector. The total radiated power from element i can be calculated with the reflection losses consideration as follows [8]:

$$\mathbf{p}_{rad,i} = |\mathbf{a}_i|^2 \left(\mathbf{1} - \sum_{n=1}^N |\mathbf{S}_{ni}|^2 \right) \boldsymbol{\eta}_{rad,i} \quad (4.5)$$

However the conduction and dielectric loss should be included, hence the total radiated power for element i in term of the total power and internal losses can be as follow:

$$\mathbf{p}_{rad,i} = \mathbf{p}_{tot,i} - \mathbf{p}_{loss,i} \quad (4.6)$$

From (4.4) the total power from element i (input power) can be written as:

$$\mathbf{p}_{tot,i} = |\mathbf{a}_i|^2 \left(\mathbf{1} - \sum_{n=1}^N |\mathbf{S}_{ni}|^2 \right) \quad (4.7)$$

Then the internal losses power from element i from (4.4) , (4.5) can be written as:

$$\mathbf{p}_{loss,i} = |\mathbf{a}_i|^2 \left(\mathbf{1} - \sum_{n=1}^N |\mathbf{S}_{ni}|^2 \right) \left(\mathbf{1} - \boldsymbol{\eta}_{rad,i} \right) \quad (4.8)$$

From (4.3) the correlation coefficient can be related to the power such that if we calculate the correlation coefficient for different element i and j it becomes,

$$\begin{aligned} |\rho_{ij}| &= \frac{\left| \iint_{4\pi} [\overline{\mathbf{F}_i(\boldsymbol{\theta}, \boldsymbol{\phi})} \cdot \overline{\mathbf{F}_j(\boldsymbol{\theta}, \boldsymbol{\phi})}^*] d\Omega \right|}{\sqrt{\iint_{4\pi} |\overline{\mathbf{F}_i(\boldsymbol{\theta}, \boldsymbol{\phi})}|^2 d\Omega \iint_{4\pi} |\overline{\mathbf{F}_j(\boldsymbol{\theta}, \boldsymbol{\phi})}|^2 d\Omega}} \\ &= \frac{\left| \iint_{4\pi} [\overline{\mathbf{F}_i(\boldsymbol{\theta}, \boldsymbol{\phi})} \cdot \overline{\mathbf{F}_j(\boldsymbol{\theta}, \boldsymbol{\phi})}^*] d\Omega \right|}{\sqrt{\left(\mathbf{1} - \sum_{n=1}^N |\mathbf{S}_{ni}|^2 \right) \boldsymbol{\eta}_{radi} \left(\mathbf{1} - \sum_{n=1}^N |\mathbf{S}_{nj}|^2 \right) \boldsymbol{\eta}_{radj}}} \end{aligned} \quad (4.9)$$

Then the correlation coefficient can be expressed using orthogonality and power conservation law as [7]:

$$\begin{pmatrix} \rho_{11}(1 - \sum_{n=1}^N |S_{ni}|^2)\eta_{radi} & \cdots & \rho_{1N}\sqrt{(1 - \sum_{n=1}^N |S_{n1}|^2)\eta_{rad1} (1 - \sum_{n=1}^N |S_{nj}|^2)\eta_{radj}} \\ \vdots & \ddots & \vdots \\ \rho_{N1}\sqrt{(1 - \sum_{n=1}^N |S_{nN}|^2)\eta_{radN} (1 - \sum_{n=1}^N |S_{n1}|^2)\eta_{rad1}} & \cdots & \rho_{NN}(1 - \sum_{n=1}^N |S_{nN}|^2)\eta_{radN} \end{pmatrix} = (\mathbf{I} - \mathbf{S}^* \mathbf{S}) \quad (4.10)$$

however this equation is with no conduction and dielectric loss, thus for there is a missing term [7]. Now by considering internal losses, the S-parameters matrix can be divided into S-parameters matrix for the ports and another for the radiation function and losses [7]. The S-parameter for **Port i** = $(1 - \sum_{n=1}^N |S_{ni}|^2) (1 - \eta_{rad,i})$, however the reflection power losses and the power affects port **i** due to coupling from port **j** can be expressed as $\rho_{loss,ij}\sqrt{(1 - \sum_{n=1}^N |S_{ni}|^2)(1 - \eta_{radi}) (1 - \sum_{n=1}^N |S_{nj}|^2)(1 - \eta_{radj})}$ and this can be applied for all ports. Finally from power conservation low it is better to express in matrix form as:

$$\begin{aligned} \sum_{n=1}^N S_{ni}^* S_{nj} + \rho_{ij} \sqrt{(1 - \sum_{n=1}^N |S_{ni}|^2)\eta_{radi} (1 - \sum_{n=1}^N |S_{nj}|^2)\eta_{radj}} \\ + \rho_{ij,loss} \sqrt{(1 - \sum_{n=1}^N |S_{ni}|^2)(1 - \eta_{radi}) (1 - \sum_{n=1}^N |S_{nj}|^2)(1 - \eta_{radj})} \\ = 0 \end{aligned} \quad (4.11)$$

By substituting for (4.7) and (4.8) in (4.11), the correlation coefficient can be expressed as follow:

$$\begin{aligned} \rho_{i,j,max,min} &= \frac{\sum_{n=1}^N \mathbf{S}_{ni}^* \mathbf{S}_{nj}}{\sqrt{(\mathbf{1} - \sum_{n=1}^N |\mathbf{S}_{ni}|^2)(\mathbf{1} - \sum_{n=1}^N |\mathbf{S}_{nj}|^2) \eta_{rad,i} \eta_{rad,j}}} \\ &\pm \rho_{ij,loss} \sqrt{\left(\frac{\mathbf{1}}{\eta_{rad,i}} - \mathbf{1}\right)} \sqrt{\left(\frac{\mathbf{1}}{\eta_{rad,j}} - \mathbf{1}\right)} \end{aligned} \quad (4.12)$$

where, $\rho_{ij,loss}$ represent the losses in the correlation coefficient which can be considered as 1 for the worst case. Also the second term represent the uncertainly which depends on the efficiency, so that in case of low efficiency a high value of uncertainly is obtained .This comes from the difficulty of calculation of the exact value of the losses in the correlation coefficient .So, by taking the worst case, then the correlation coefficient can be expressed as:

$$\begin{aligned} \rho_{eij,max} &= \frac{\sum_{n=1}^N \mathbf{S}_{ni}^* \mathbf{S}_{nj}}{\sqrt{(\mathbf{1} - \sum_{n=1}^N |\mathbf{S}_{ni}|^2)(\mathbf{1} - \sum_{n=1}^N |\mathbf{S}_{nj}|^2) \eta_{rad,i} \eta_{rad,j}}} \\ &+ \sqrt{\left(\frac{\mathbf{1}}{\eta_{rad,i}} - \mathbf{1}\right)} \sqrt{\left(\frac{\mathbf{1}}{\eta_{rad,j}} - \mathbf{1}\right)} \end{aligned} \quad (4.13)$$

Equation (4.13) is valid for N elements MIMO antenna systems; in case of high radiation efficiency, the term of uncertainly can be negligible so that the equation (4.13) becomes similar to (3.4). The second term represent the uncertainly which leads to overestimate the value of the correlation coefficient to become more than unity for very lossy antenna elements.

4.2 Generalization of Parallel R-L-C equivalent circuit for method- IV to N-Ports MIMO

The solution for more than two elements for the parallel R-L-C equivalent circuit for method- IV has not been derived in the existing literature. For N elements, we use the same procedure for 2-element system however the equivalent circuit diagram should be modified as shown in Fig.4.2 for N-elements although 4 are only shown here for simplicity of visuality

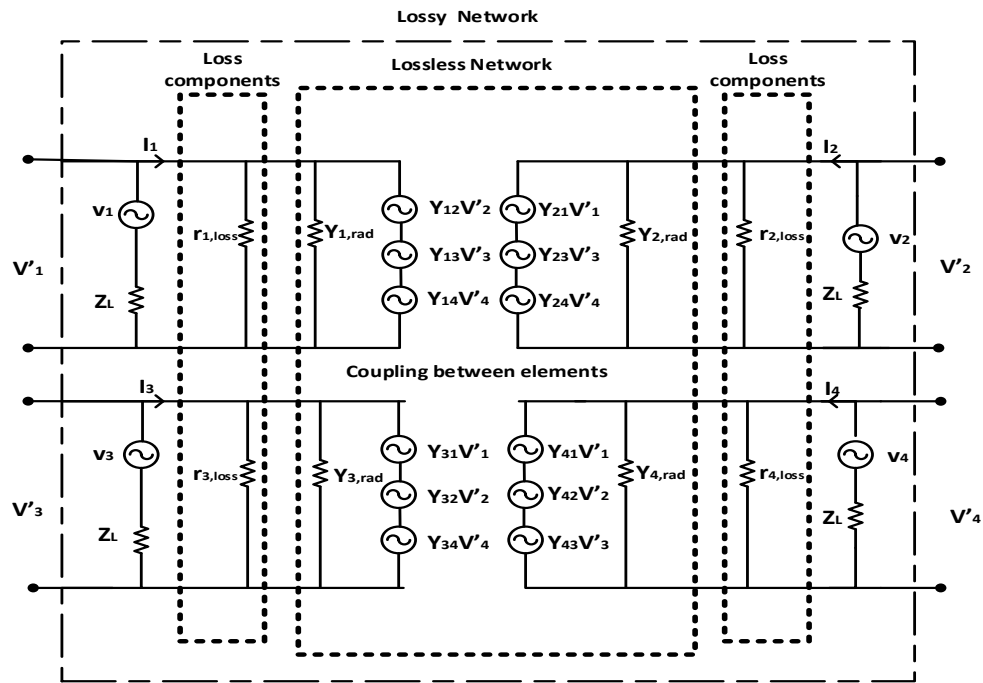


Figure 4.1 equivalent circuit diagram for 4-antenna elements

In Fig.4.2, v_i is element i excitation, r_{loss} is the loss conductance, Y_{rad} is the radiation impedance and Z_L is the antenna load which is the impedance of the feed cable. The S-parameters between the ports can be measured using a vector network analyzer (VNA) and the lossy part can be considered as network cascades with the lossless part as shown in Fig

4.2 then the S-parameters for the lossy part can be calculated by knowing the value of the conductance impedance as follows:

$$L_{13} = \begin{pmatrix} \frac{r_{loss,1}Z_0}{2+r_{loss,1}Z_0} & 0 & \frac{2}{2+r_{loss,1}Z_0} & 0 \\ 0 & \frac{r_{loss,2}Z_0}{2+r_{loss,2}Z_0} & 0 & \frac{2}{2+r_{loss,2}Z_0} \\ \frac{2}{2+r_{loss,1}Z_0} & 0 & \frac{r_{loss,1}Z_0}{2+r_{loss,1}Z_0} & 0 \\ 0 & \frac{2}{2+r_{loss,2}Z_0} & 0 & \frac{r_{loss,2}Z_0}{2+r_{loss,2}Z_0} \end{pmatrix} \quad (4.14)$$

$$L_{24} = \begin{pmatrix} \frac{r_{loss,3}Z_0}{2+r_{loss,3}Z_0} & 0 & \frac{2}{2+r_{loss,3}Z_0} & 0 \\ 0 & \frac{r_{loss,4}Z_0}{2+r_{loss,4}Z_0} & 0 & \frac{2}{2+r_{loss,4}Z_0} \\ \frac{2}{2+r_{loss,3}Z_0} & 0 & \frac{r_{loss,3}Z_0}{2+r_{loss,3}Z_0} & 0 \\ 0 & \frac{2}{2+r_{loss,4}Z_0} & 0 & \frac{r_{loss,4}Z_0}{2+r_{loss,4}Z_0} \end{pmatrix} \quad (4.15)$$

Where L_{13} is the S-parameter for lossy part in element 1 and 3, L_{24} is the S-parameter for lossy part in element 2 and 4. It worth to mention that in this configuration, identical elements and symmetric placement is considered such that ($r_{loss} = r_{1,loss} = r_{2,loss} = r_{3,loss} = r_{4,loss}$) and then obviously $L_{13} = L_{24}$. Then the transmission matrix for both S-parameters that are measured from the VNA and S-parameters of lossy part network can be calculated from [12] to extract lossless s-parameters as follow:

$$[S_{lossless}]_T = [L_i]_T [S_{lossless}]_T^{-1} [L_j]_T \quad (4.16)$$

Where $[S_{lossy}]_T$ is the transmission matrix for the S-parameters measured by the VNA, $[L_i]_T$ is the transmission matrix for the lossy part in element i and $[L_j]_T$ is the transmission matrix for lossy part in element j. The only missing parameter now is the value of the

conductance impedance. To calculate the value of the loss conductance r_{loss} , from Fig.4.2 antenna elements can be defined in two ways, first, It can be defined as four networks with its inactive port is connected to the load impedance, so that only port 1 is active, then the total efficiency can be calculated as :

$$\eta_{tot,1} = \left(\mathbf{1} - \sum_{j=1}^N |S_{j1}|^2 \right) \eta_{rad,1} \quad (4.17)$$

Where the radiation efficiency is calculated as:

$$\eta_{rad,1} = \frac{P_{rad}}{P_{rad} + P_{loss}} \quad (4.18)$$

$$\eta_{rad,1} = \frac{|V'_1|^2 Y_{rad} + \dots + |V'_N|^2 Y_{rad}}{|V'_1|^2 Y_{rad} + \dots + |V'_4|^2 Y_{rad} + |V'_1|^2 r_{loss} + \dots + |V'_N|^2 r_{loss}} \quad (4.19)$$

We assume that the elements are identical and when a voltage is applied to element i the other (N-1) elements will not be excited. The relation between V_i and V_j can be calculated from non-excited elements assuming port 1 is excited as:

$$Y_{21}V'_1 + (Y_{22}Z_L + \mathbf{1}) \frac{V'_2}{Z_L} + Y_{23}V'_3 + \dots + Y_{2N}V'_N = \mathbf{0} \quad (4.20)$$

$$Y_{31}V'_1 + Y_{32}V'_2 + (Y_{33}Z_L + \mathbf{1}) \frac{V'_3}{Z_L} + \dots + Y_{3N}V'_N = \mathbf{0} \quad (4.21)$$

⋮

$$Y_{N1}V'_1 + Y_{N2}V'_2 + Y_{N3}V'_3 + \dots + (Y_{NN}Z_L + \mathbf{1}) \frac{V'_N}{Z_L} = \mathbf{0} \quad (4.22)$$

Dividing (4.20), (4.21) and (4.22) by V_i and defining $\mathbf{k}_{ij} = \frac{|V_j|}{|V_i|}$, the using matrix form we

get:

$$Y_{21} + \frac{1}{Z_L}(Y_{22}Z_L + 1)\mathbf{k}_{12} + Y_{23}\mathbf{k}_{13} + \dots + Y_{2N}\mathbf{k}_{1N} = \mathbf{0} \quad (4.23)$$

$$Y_{31} + Y_{32}\mathbf{k}_{12} + \frac{1}{Z_L}(Y_{33}Z_L + 1)\mathbf{k}_{13} + \dots + Y_{3N}\mathbf{k}_{1N} = \mathbf{0} \quad (4.24)$$

⋮

$$Y_{N1} + Y_{N2}\mathbf{k}_{12} + Y_{N3}\mathbf{k}_{13} + \dots + \frac{1}{Z_L}(Y_{NN}Z_L + 1)\mathbf{k}_{1N} = \mathbf{0} \quad (4.25)$$

$$\begin{pmatrix} \mathbf{k}_{12} \\ \mathbf{k}_{13} \\ \vdots \\ \mathbf{k}_{1N} \end{pmatrix} = - \begin{pmatrix} \frac{1}{Z_L}(Y_{11}Z_L + 1) & \dots & Y_{2N} \\ Y_{32} & \dots & Y_{3N} \\ \vdots & \ddots & \vdots \\ Y_{N2} & \dots & \frac{1}{Z_L}(Y_{NN}Z_L + 1) \end{pmatrix}^{-1} \begin{pmatrix} Y_{21} \\ Y_{31} \\ \vdots \\ Y_{N1} \end{pmatrix} \quad (4.26)$$

The radiation efficiency of element i in term of \mathbf{k}_{ij} can be described as:

$$\eta_{rad,i} = \frac{\sum_{j=1}^N \mathbf{k}_{ij}^2 \mathbf{g}_{j,rad}}{\sum_{j=1}^N \mathbf{k}_{ij}^2 \mathbf{g}_{j,rad} + \sum_{j=1}^N \mathbf{k}_{ij}^2 \mathbf{g}_{j,loss}} \quad (4.27)$$

The second way is to describe the dual antenna system by defining it as one active port and such that other ports are lossy by considering a loss resistance, then the total efficiency is found as follow:

$$\eta_{tot,1} = (1 - |S_{11}|^2)\eta'_{rad,1} \quad (4.28)$$

$\eta'_{rad,1}$

$$= \frac{|V'_1|^2 Y_{rad} + \dots + |V'_N|^2 Y_{rad}}{|V'_1|^2 Y_{rad} + \dots + |V'_N|^2 Y_{rad} + |V'_1|^2 r_{loss} + \dots + |V'_N|^2 r + (|I_2|^2 + |I_3|^2 + \dots + |I_N|^2) Z_L} \quad (4.30)$$

$$\eta'_{rad,i} = \frac{\sum_{j=1}^N k_{ij}^2 g_{j,rad}}{\sum_{j=1}^N k_{ij}^2 g_{j,rad} + \sum_{j=1}^N k_{ij}^2 g_{j,loss} + \sum_{j=1, j \neq i}^N k_{ij}^2 (Z_L)} \quad (4.31)$$

The total efficiency when the system considered as one port network and other element loaded to lossy impedance as follow:

$$\eta'_{rad,i} = \frac{\sum_{j=1}^N k_{ij}^2 g_{j,rad}}{\sum_{j=1}^N k_{ij}^2 g_{j,rad} + \sum_{j=1}^N k_{ij}^2 g_{j,loss} + \sum_{j=1, j \neq i}^N k_{ij}^2 \text{Re}(Z_L)} \quad (4.32)$$

By solving for identical elements as well symmetric placement of the elements ($g_{loss} = g_{1,loss} = g_{2,loss} = \dots = g_{N,loss}$) then the loss resistance can be calculated as:

$$g_{loss} = g_{i,loss} = \frac{\eta'_{rad,i} (1 - \eta_{rad,i}) \sum_{j=1, j \neq i}^N k_{ij}^2}{(\eta_{rad,i} - \eta'_{rad,i}) \sum_{j=1}^N k_{ij}^2 \text{Re}(Z_L)} \quad (4.33)$$

Then the lossless S-parameter can be extracted using (4.16) and apply in (3.5) to estimate the value of the correlation coefficient.

CHAPTER 5

RESULTS & DISCUSSION

In this section we will reproduce some previous work to verify the code, then we will provide two new designs, fabricate, measure and apply the four methods to estimate the correlation coefficient and compare between them.

5.1 Correlation Coefficient for two elements

For two different antenna elements, the correlation coefficient was calculated using methods I-IV. A comparison is conducted between them. At the beginning, we wanted to verify our code by reproducing same of the results that already appeared in literature.

5.1.1 Two printed dipole elements

The two dipole elements in [10] were re-modeled in CST as shown in Fig.5.1 and the result for various methods of calculating the correlation coefficient were applied. Fig.5.2 shows the original result from [10] when the antenna efficiency was incorporated.

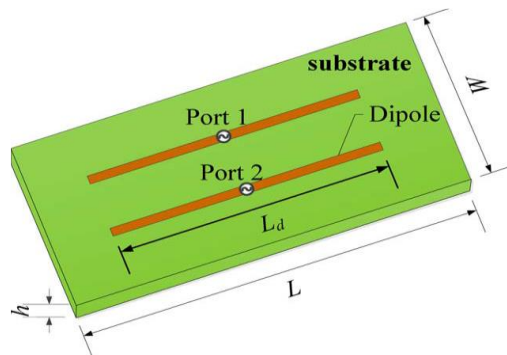


Figure 5.1 Geometries of the dual-dipole array [10]

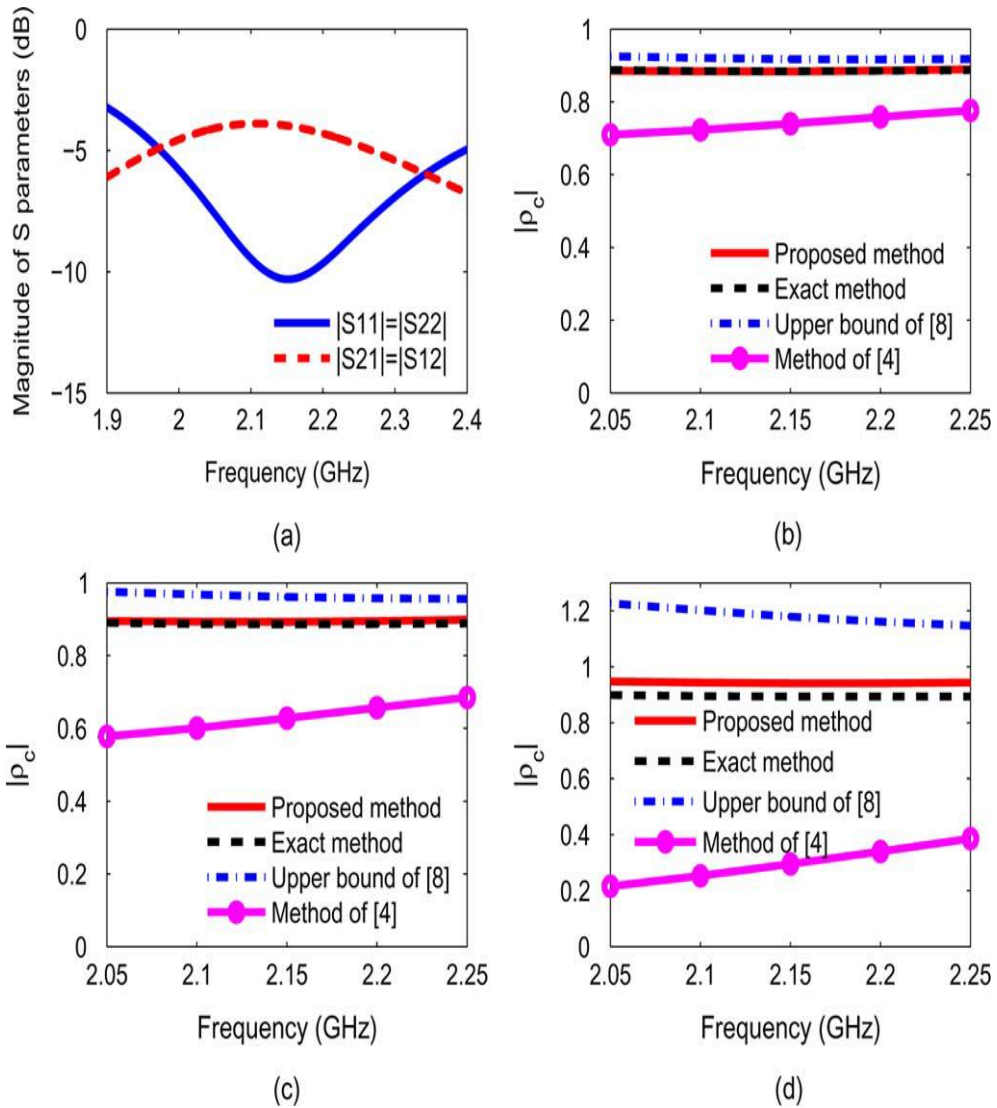


Figure 5.2 S-parameters and magnitude of correlation coefficients for different antenna

In Fig.5.2, the correlation coefficient was calculated as the pink color method-II, the black for method-I, the blue for method-III, and the red for method-IV. The result was reproduced using our CST modeled antenna with different loss tangents as shown in Figs.5.3, 5.4 and 5.5 for the efficiency of 88%, 79.9% and 73.2% respectively.

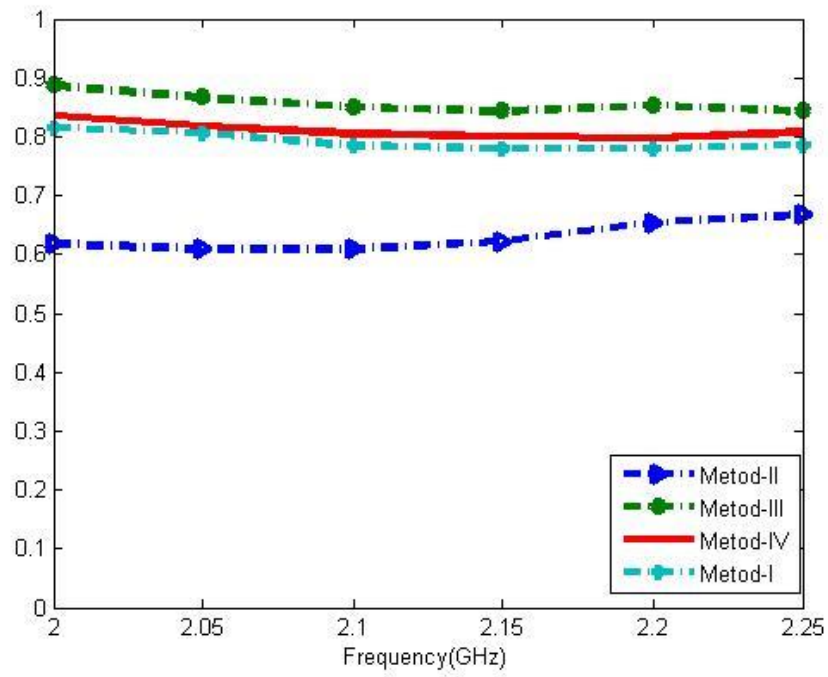


Figure 5.3 The correlation coefficients $\eta_{(rad.)}=88\%$.

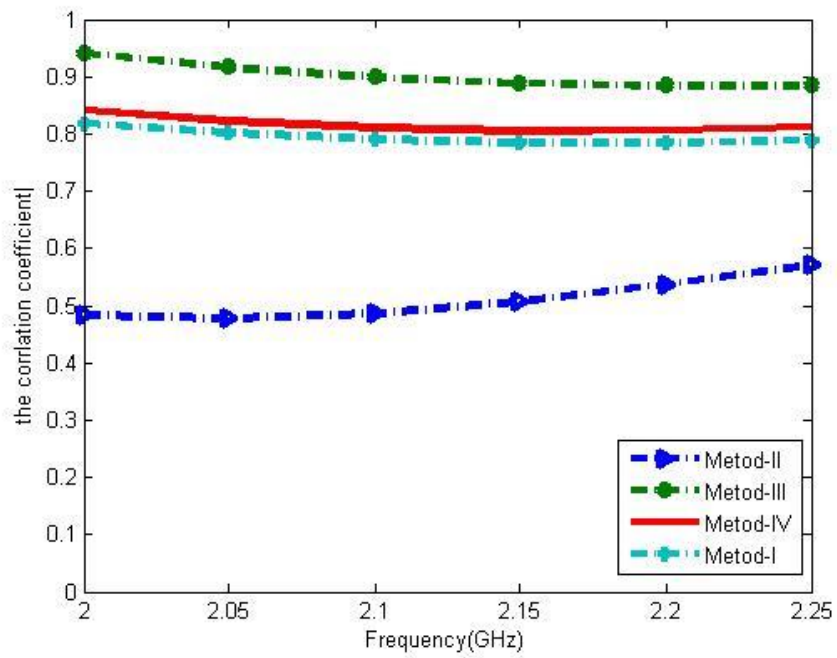


Figure 5.4 The correlation coefficients $\eta_{(rad.)}=79.9\%$.

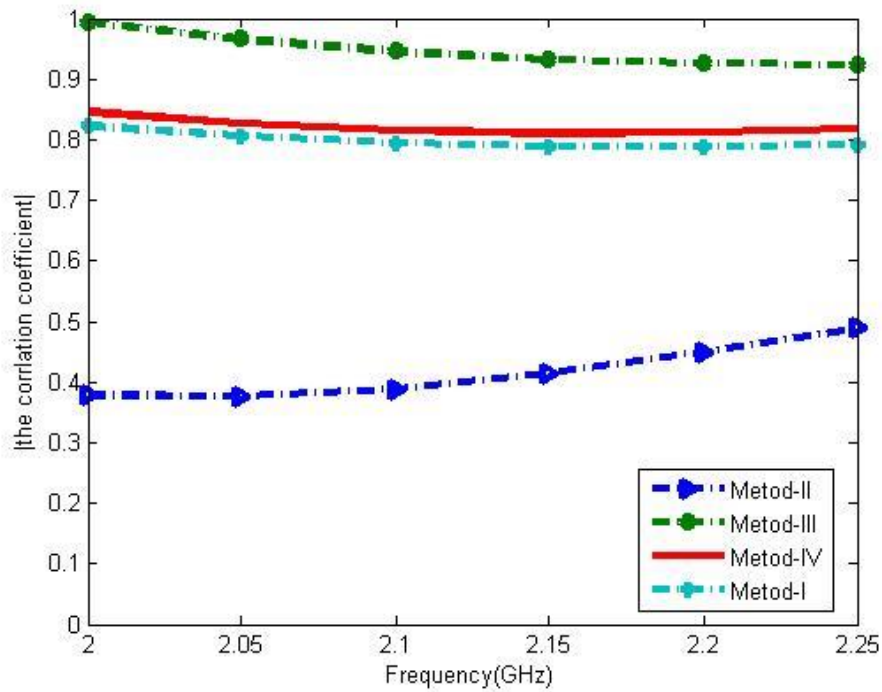


Figure 5.5 The correlation coefficient $\eta_{(rad.)}=73.2\%$.

We can notice that the correlation coefficient calculated using method-I does not depend on changing the radiation efficiency; however method-I and method-III are changing and show deviation from the exact method for high losses, also the method used in [10] method-IV is very close to the exact method and shows total independence from the radiation efficiency. The power losses due to antenna correlation have been calculated as shown in Fig.5.6, 5.7 and 5.8 using method-I, method-II, method-III and method-IV. The obtained results in Figs 5.3-5.5 are inline of those in Fig 5.2 indicating correct code/method implementation.

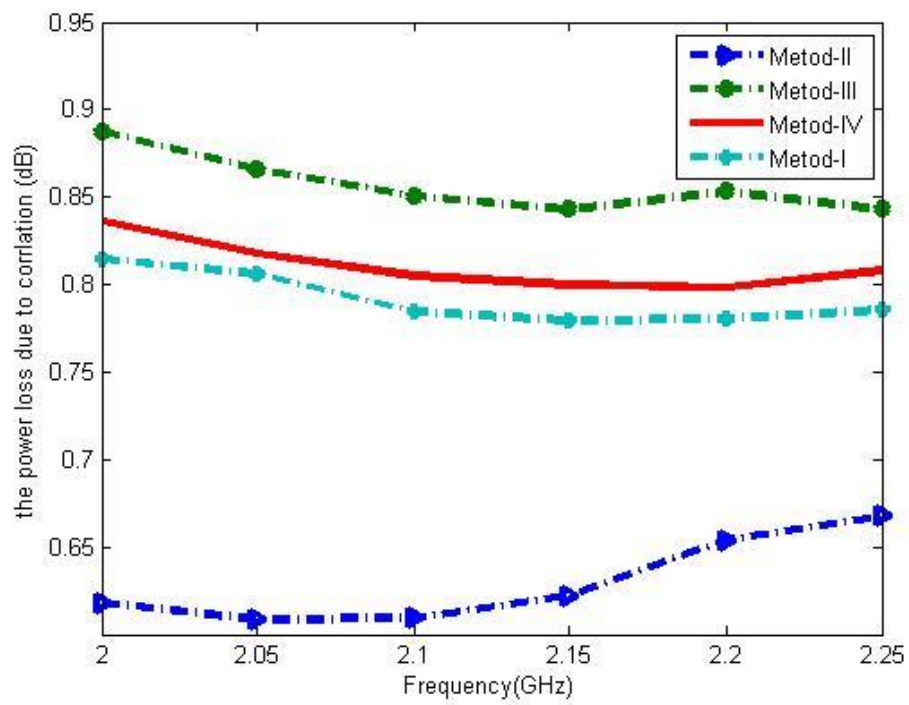


Figure 5.6 The power losses $\eta_{(rad.)}=88\%$.

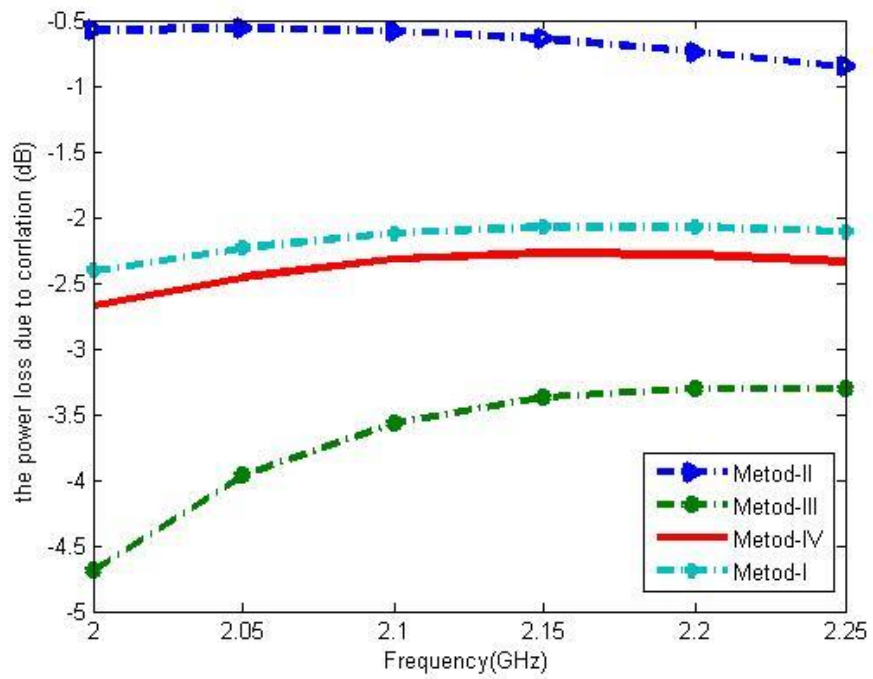


Figure 5.7 The power losses $\eta_{(rad.)}=79.9\%$.

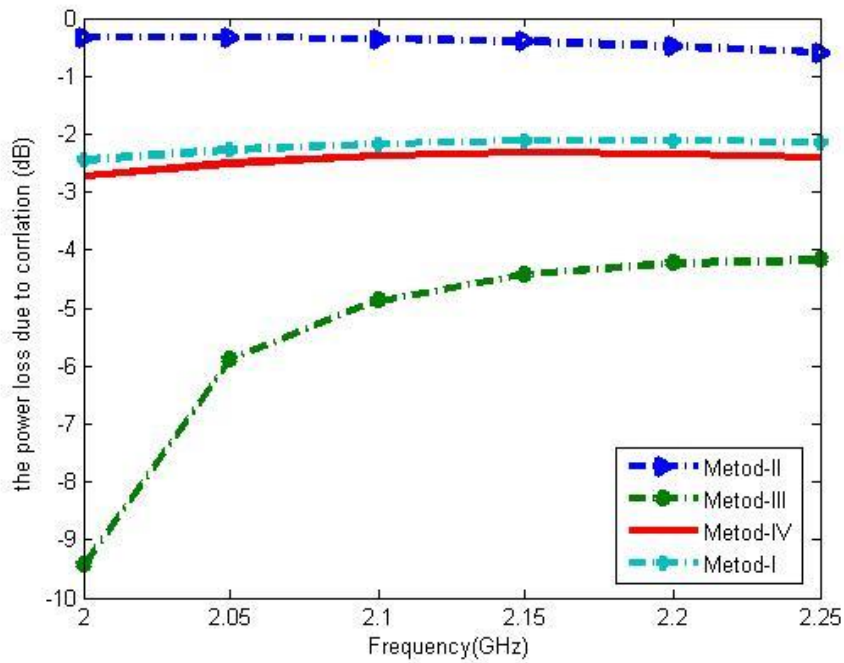


Figure 5.8 The power losses $\eta_{(rad.)}=73.2\%$.

We can notice that the power losses due to the correlation between the elements is 2.5 dB regardless the loss tangent value (radiation efficiency) for method-I and the method-IV, however for method-II the value is not reliable because of the assumption of using lossless elements ends up with unreliable values of correlation and power losses. For method-III the power loss due to the correlation between the elements is high because this method is based on the worst case which mean high uncertainly value and overestimate the value of the correlation coefficient.

5.1.2 Two folded monopole elements

A two folded monopole MIMO antenna was also investigated with a radiation efficiency of 85%. The geometries of the antennas are shown in Fig.5.9, following [14] and the results are presented in Fig.5.10 and 5.11.

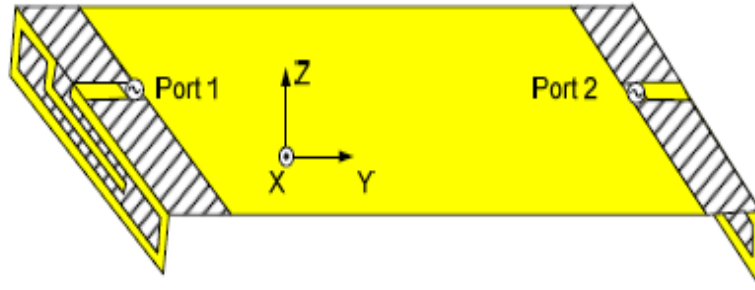


Figure 5.9 Geometries of the folded monopole antennas 2x2 [17]

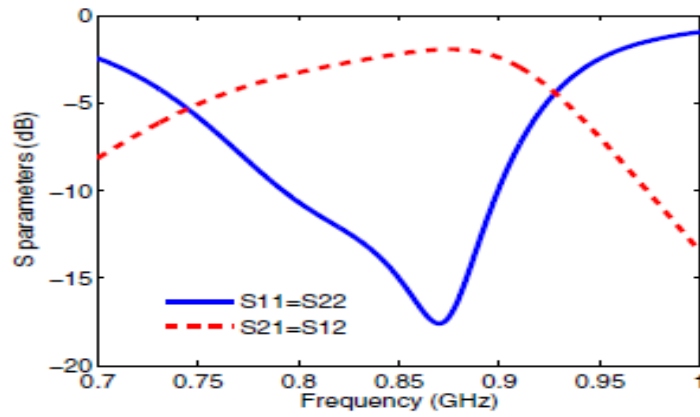


Figure 5.10 S-parameters and magnitude of correlation coefficients. [14]

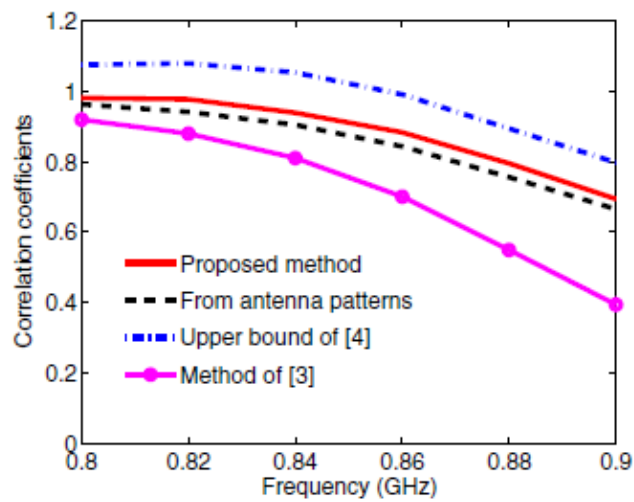


Figure 5.11 The correlation coefficients [14]

These results were reproduced as shown in Fig.5.12 where we calculated the correlation coefficient using the four methods, also the losses in power due to such correlation were calculated as Fig.5.13. We can see that the four methods are close to the exact value because of the high radiation efficiency for the folded monopoles.

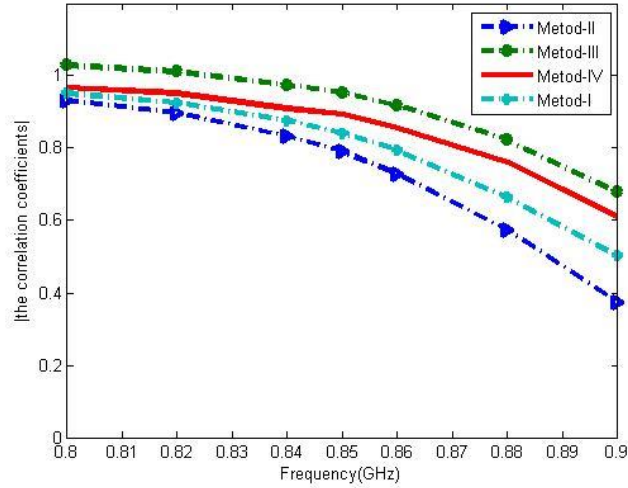


Figure 5.12 The correlation coefficients for the 2-elements folded monopole MIMO antenna

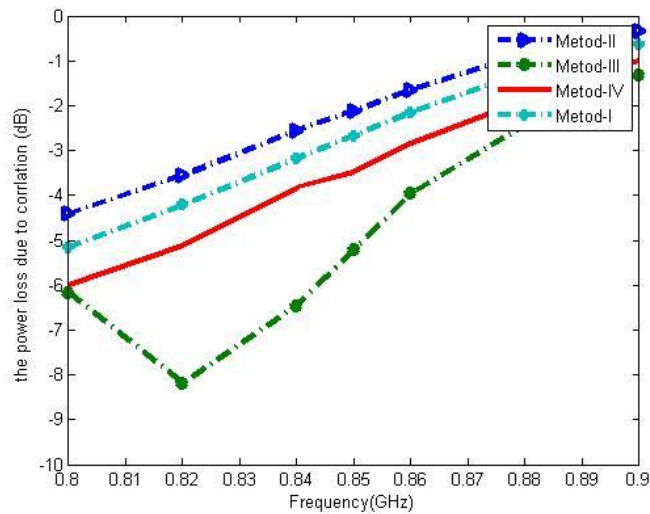


Figure 5.13 The power losses for the folded monopole

5.1.3 Two patch elements

A two patch MIMO antenna was also investigated. The geometry of the antenna is shown in Fig.5.14, following [11] and the results are presented in Fig.5.15- 5.22 with different efficiency to investigate the correlation coefficient calculation.

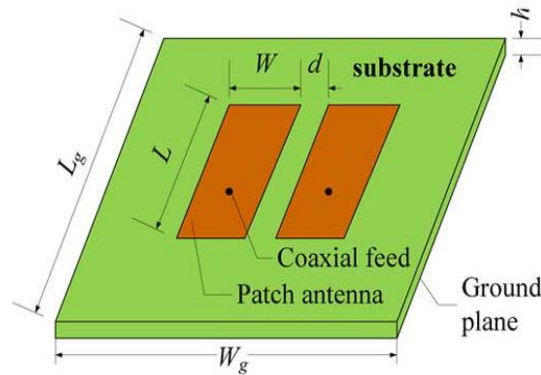


Figure 5.14 Geometries of the dual patch antenna system [11]

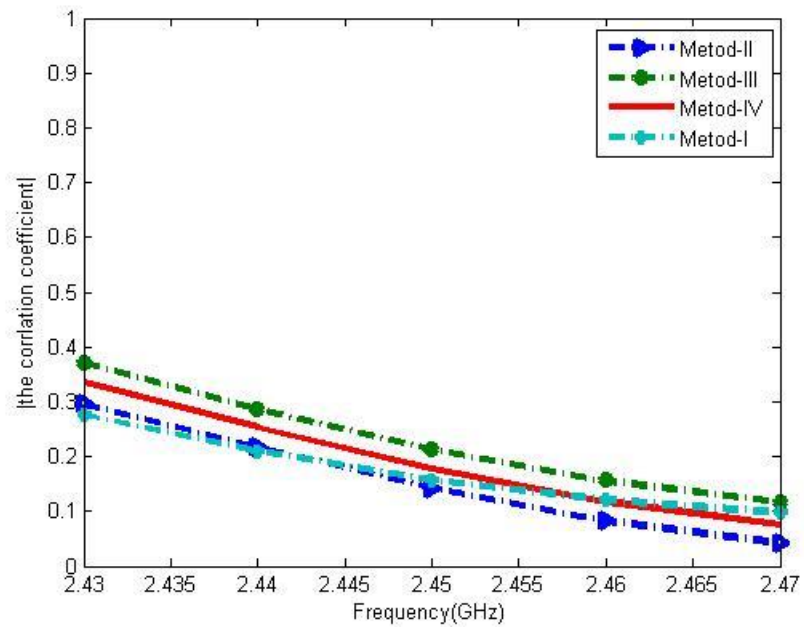


Figure 5.15 The correlation coefficient $\eta_{(rad)}=94.2\%$.

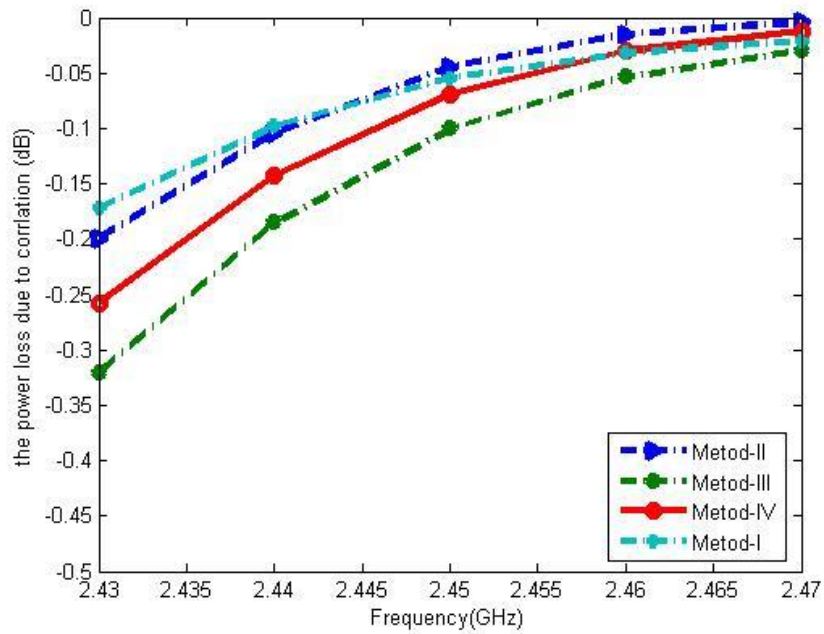


Figure 5.16 The power losses for the two patch antenna $\eta_{\text{rad}}=94.2\%$.

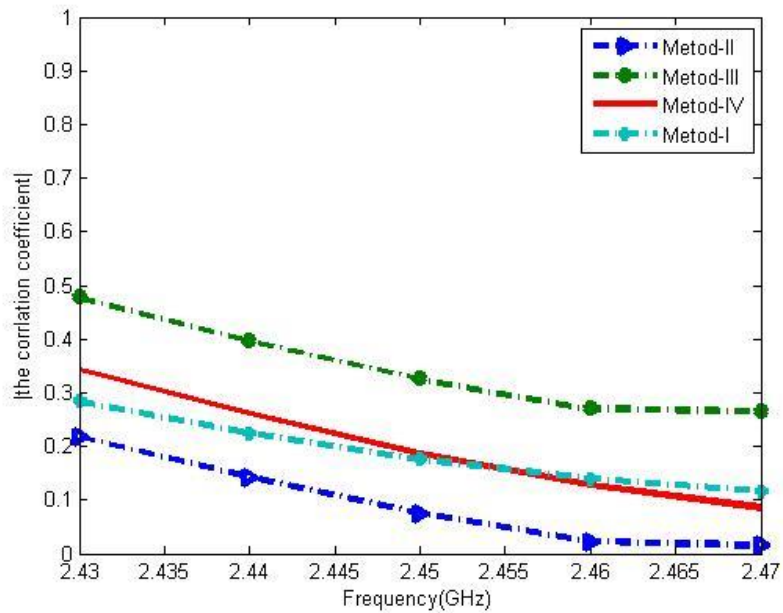


Figure 5.17 The correlation coefficients $\eta_{\text{rad}}=81.2\%$.

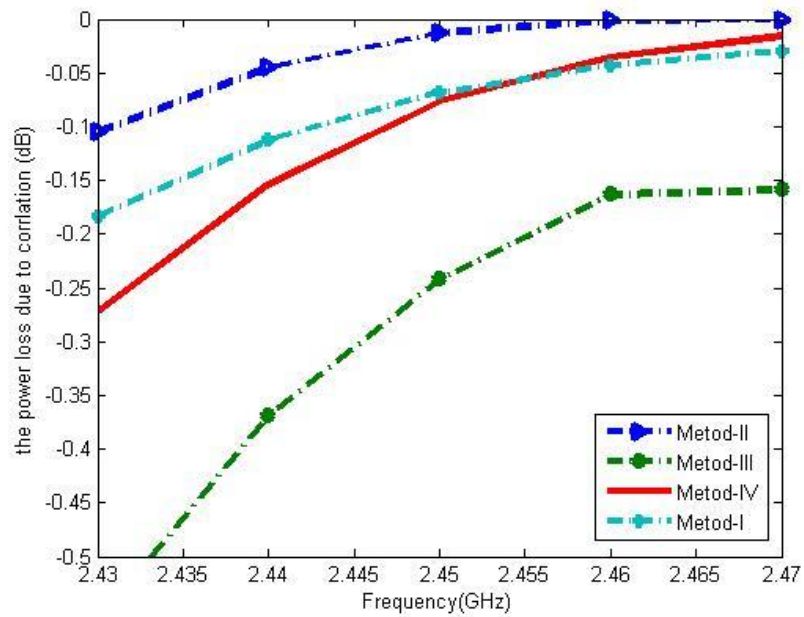


Figure 5.18 The power losses for the two patch antenna $\eta_{rad}=81.2\%$.

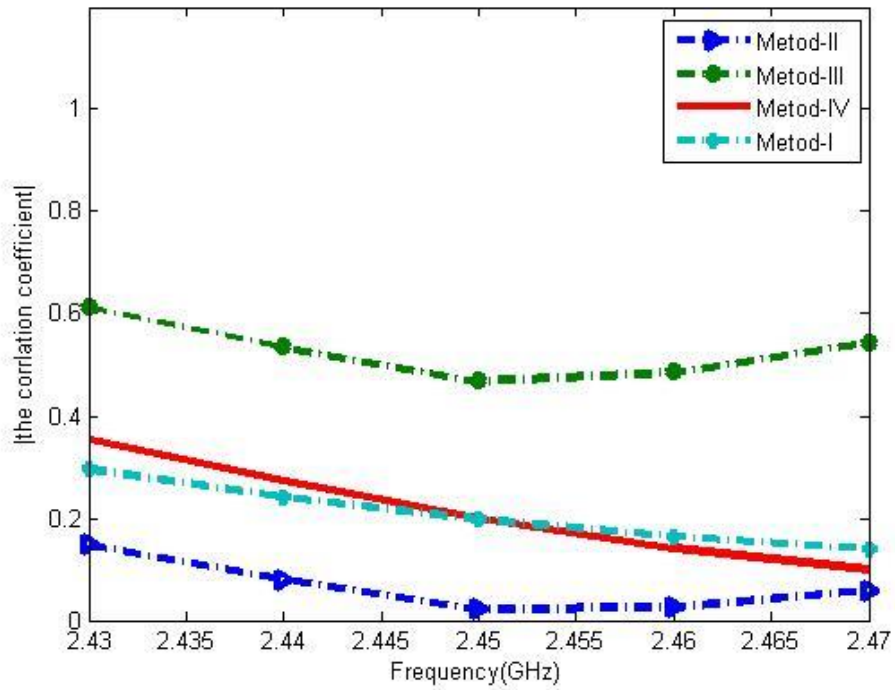


Figure 5.19 The correlation coefficients $\eta_{rad}=69.7\%$.

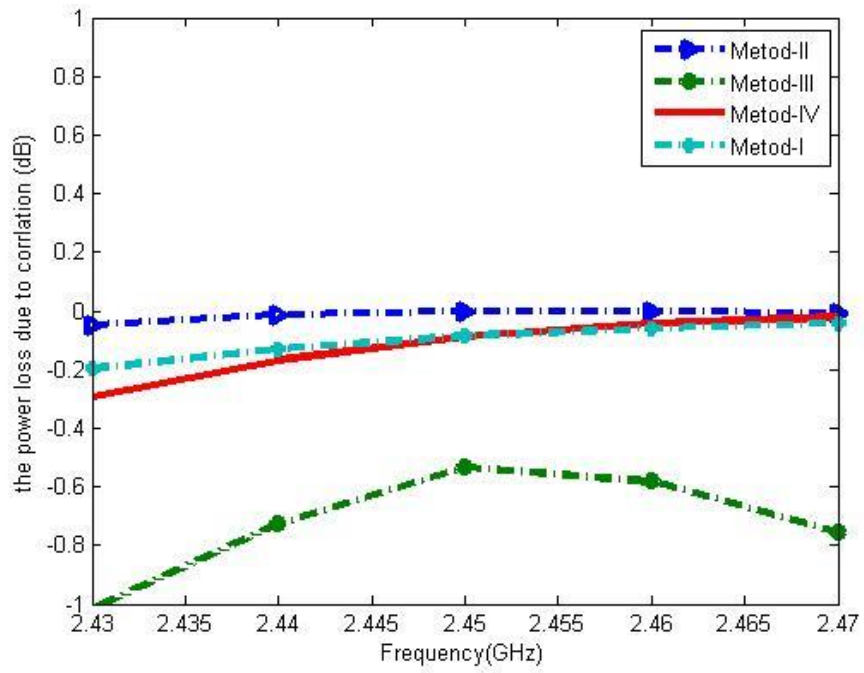


Figure 5.20 The power losses for the two patch antenna $\eta_{\text{(rad.)}}=69.7\%$.

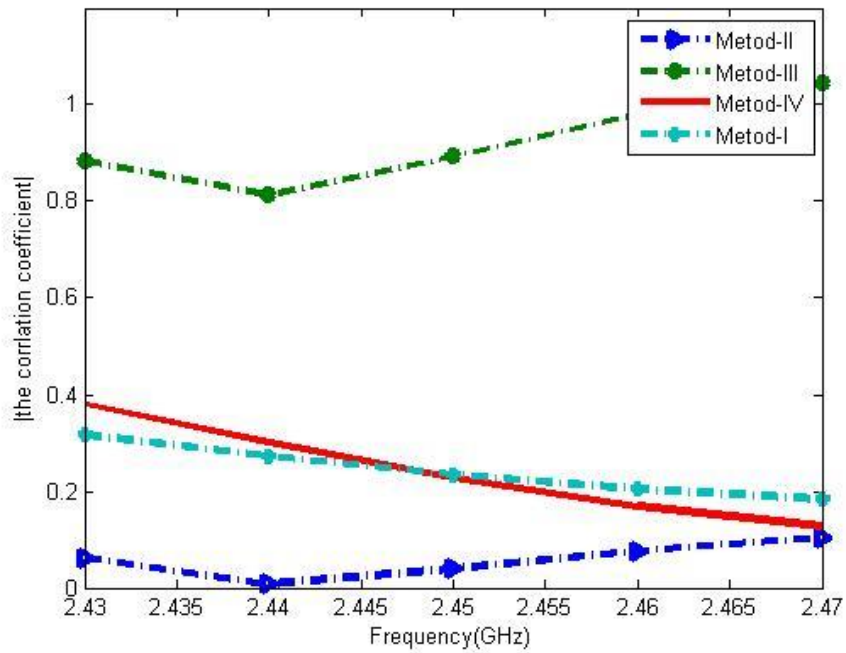


Figure 5.21 The correlation coefficients $\eta_{\text{(rad.)}}=54.9\%$.

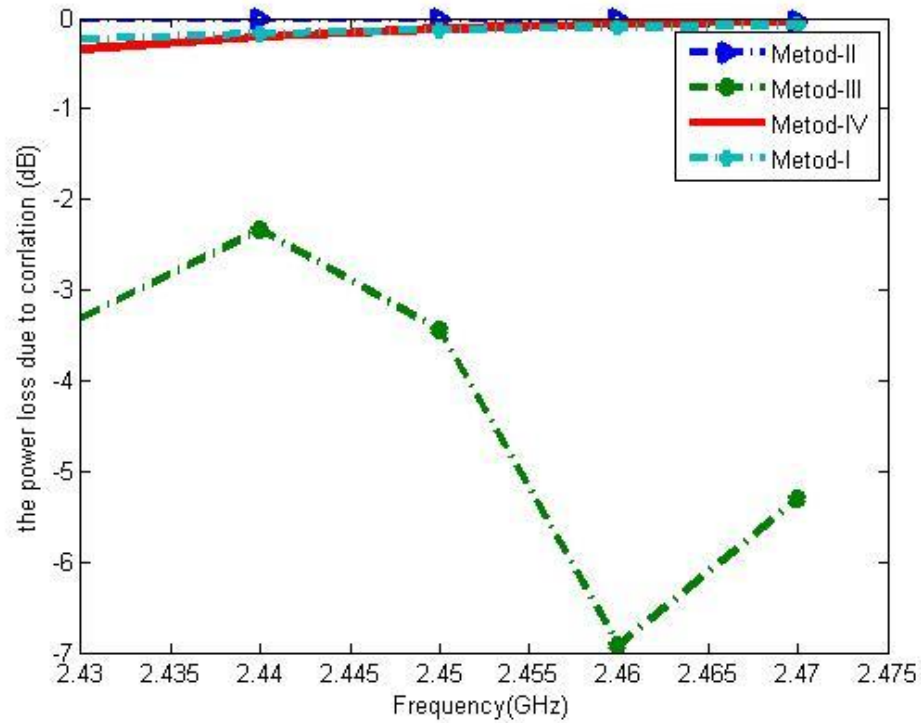


Figure 5.22 The power losses for the two patch antenna $\eta_{\text{rad}}=54.9\%$.

We can also notice that the correlation coefficient and the power losses due to the correlation between the elements calculated from method-I and method-IV are showing good agreement, however for method-II the value is not reliable because of the assumption of using lossless elements ends up with unreliable values of correlation coefficient and power loss. For method-III the power loss due to the correlation between the elements is high because this method is based on the worst case which mean high uncertainly value.

5.2 Correlation Coefficient Calculation for Four element MIMO antennas

In this section, the various methods of correlation coefficient calculation are applied to standard 4-element MIMO antennas have of different types. These elements cover a wide range of efficient to cover high and low, medium and low efficiency antenna system. Then

a two new 4-element MIMO antenna based on a monopole, patch and PIFA are designed and fabricated and their correlation coefficients are evaluated.

5.2.1 Four dipole elements

The four printed dipole element MIMO antennas system in [17] was reproduced and its geometry is shown in Fig.5.24. The correlation coefficients was calculated at the central frequency of 2.15 GHz and presented in Table 5.1. The exact value in this table from [17] was calculated using method-I and the second method (method of [3]) was calculated using method-II and the last method denoted as a proposed method in the table was calculated using method-IV. But for method-III the solution for more than two elements has not been derived in the existing literature and then was not shown in [17]. Table 5.2 shows the reproduced results for the four dipole elements using different methods including Method-III for $N=4$.

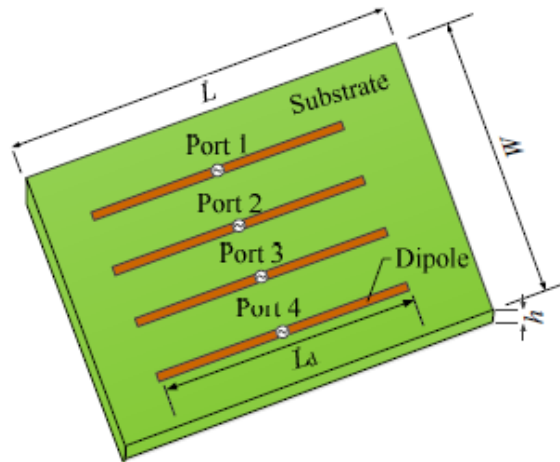


Figure 5.23 Geometries of the four dipole array, with $W=80\text{ mm}$ $L= 100\text{ mm}$ $h=2\text{ mm}$ $L_d=44\text{ mm}$ [17]

Table 5-1 The correlation coefficient of the four dipole array, [17]

	$ \rho_{c,12} ^2$	$ \rho_{c,13} ^2$	$ \rho_{c,14} ^2$	$ \rho_{c,23} ^2$
Exact value	0.688	0.063	0.096	0.452
Method of [3]	0.348	0.122	0.013	0.335
Proposed method	0.699	0.055	0.116	0.502

Table 5-2 correlation coefficients of four-dipole array

Method Used	ρ_{e12}	ρ_{e13}	ρ_{e14}	ρ_{e23}
Method-I	0.668	0.067	0.101	0.443
Method- IV	0.670	0.069	0.099	0.501
Method- II	0.331	0.125	0.012	0.343
Method- III	1.001	0.213	0.310	0.912

5.2.2 Half Circle Shape 4-Elements monopole elements

This is the first design contribution of this work with 4-element MIMO antennas system covering 2.4 GHz. The four curved monopoles were designed using FR4 substrate with thickness 0.8mm and dielectric constant 4.3. These four elements were targeting to cover 2.4 GHz. A microstrip transmission-line is used to feed the antenna elements. The feeding point on the transmission line is optimized so that the part of transmission-line opposite to antenna from feeding point acts as a shunt capacitor in the operating band whose loading matches the input impedance to 50Ω as shown in Figs 5.24. the antenna was modeled and optimized using CST. The -10 dB bandwidth was 200 MHz and isolation of 11 dB is obtained. Then the design was fabricated. Fig. 5.25 shows the top and bottom side of the

fabricated antenna. Because of the symmetrical arrangement between the four antenna elements, the simulated and measured reflection coefficients and the coupling of one antenna elements are shown in Fig.5.26 and Fig.5.27, respectively. Due to fabrication tolerances there is a small shift between the simulated and the measured results, however a good agreement is maintained. Each antenna element resonates at 2.4 GHz with simulated impedance bandwidth of 250 MHz. the measured bandwidth was 230 GHz. The minimum measured isolation between the antenna elements is 11 dB.

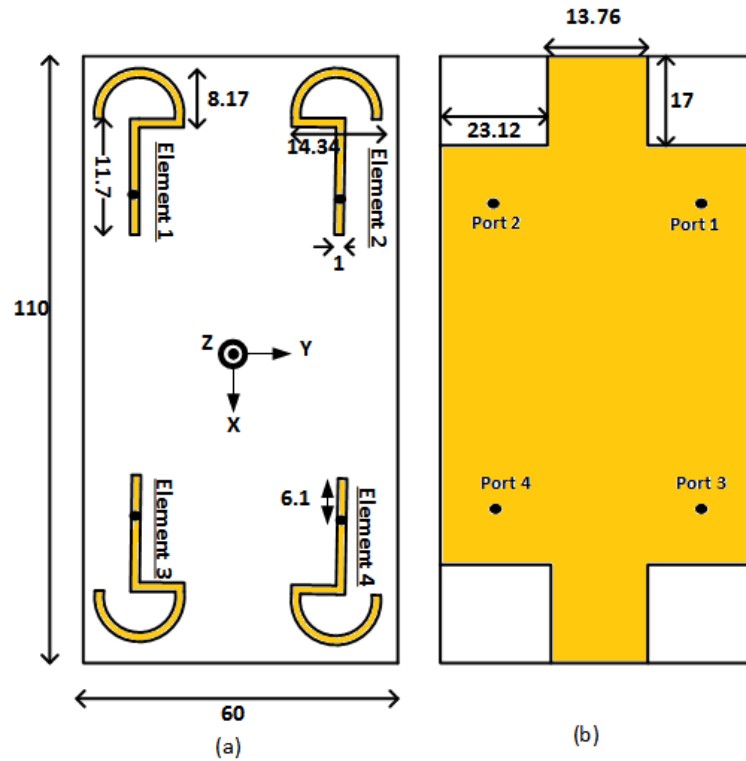


Figure 5.24 Geometry of the proposed antenna. (a) Top side, (b) Bottom side. (All dimensions are in mm)

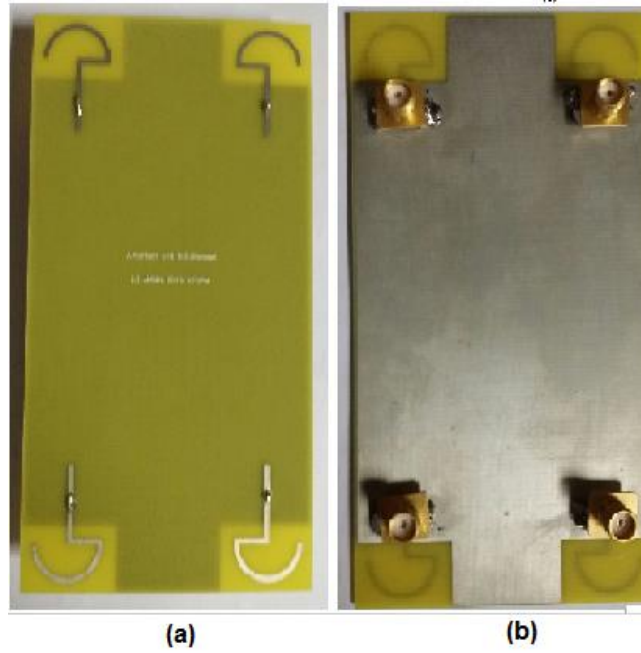


Figure 5.25 Geometry of the Fabricated antenna. (a) bottom side, (b) top side

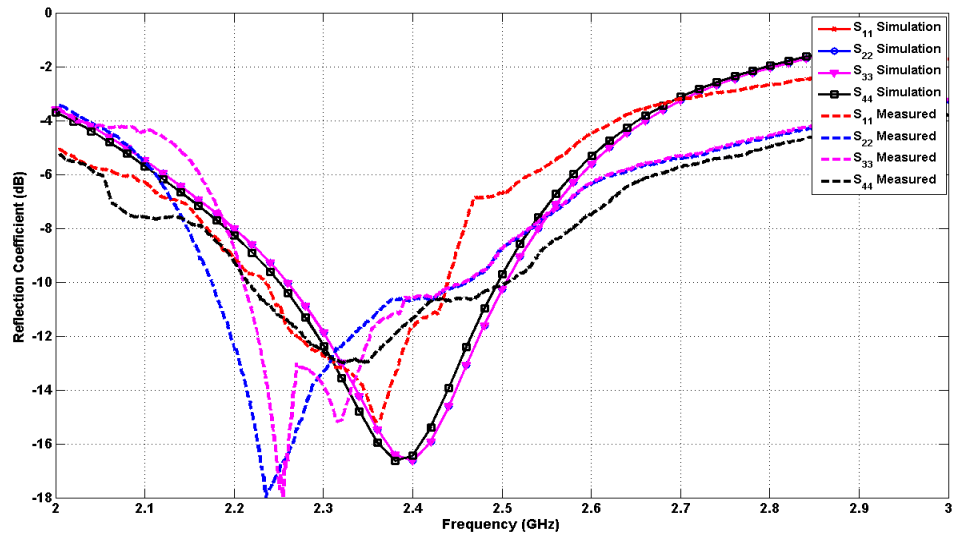


Figure 5.26 Four monopole elements S-parameter with FR4

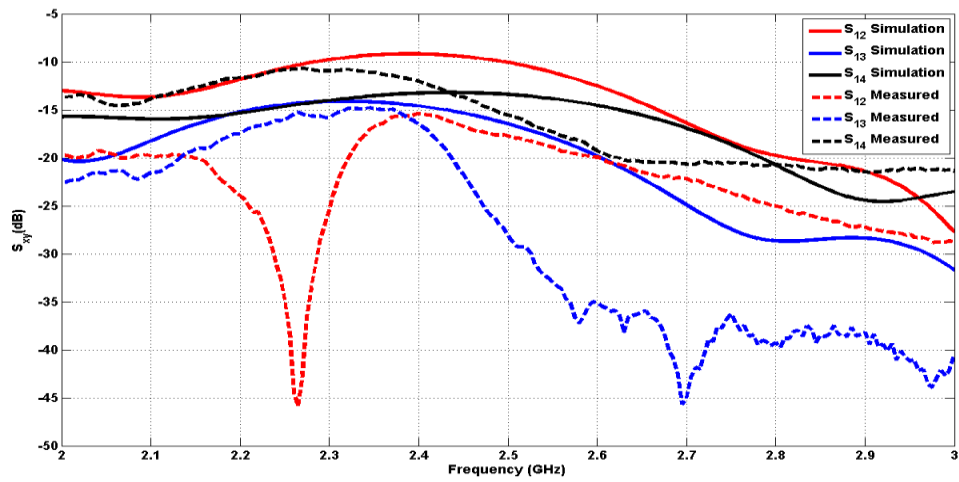


Figure 5.27 Simulated and measured isolation

The realized gain was 3.95dB and the total efficiency was -1.344 dB as shown in Figs 5.28-5.31.

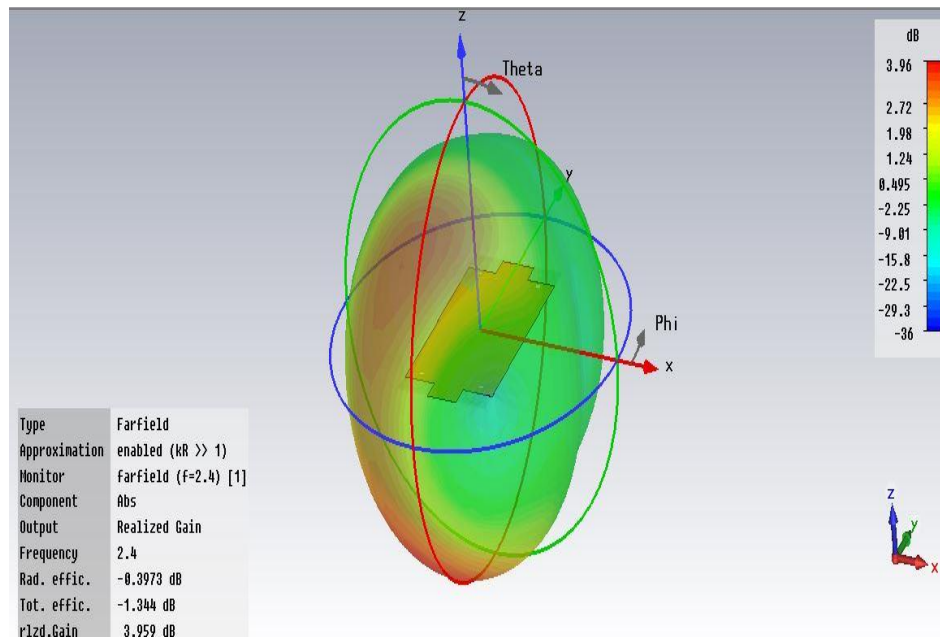


Figure 5.28 Element 1 realized gain

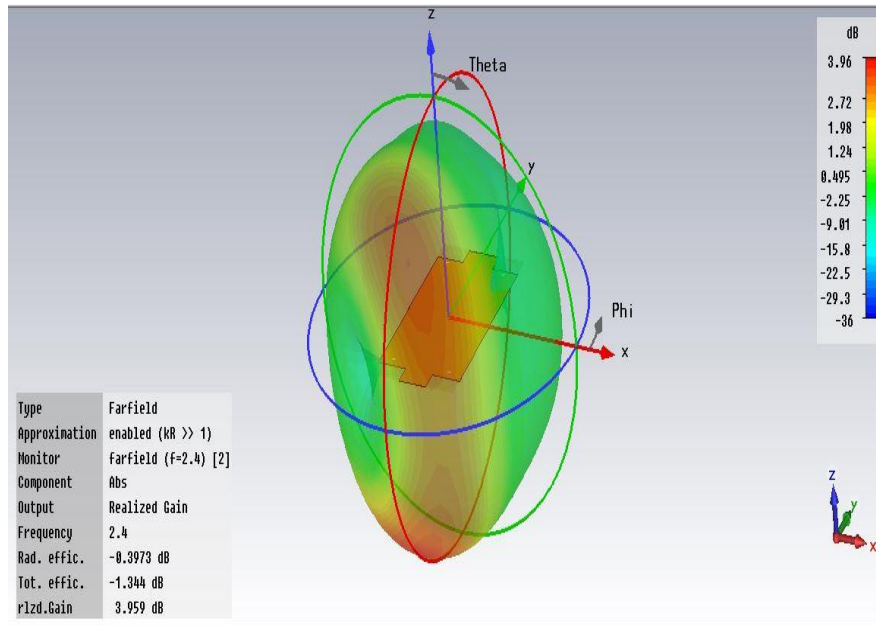


Figure 5.29 Element 2 realized gain

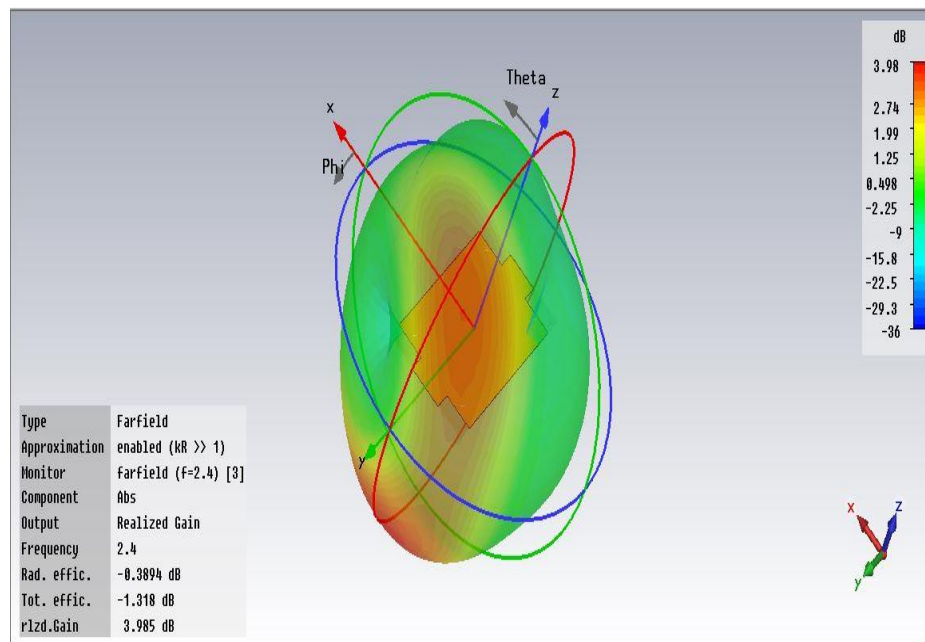


Figure 5.30 Element 3 realized gain

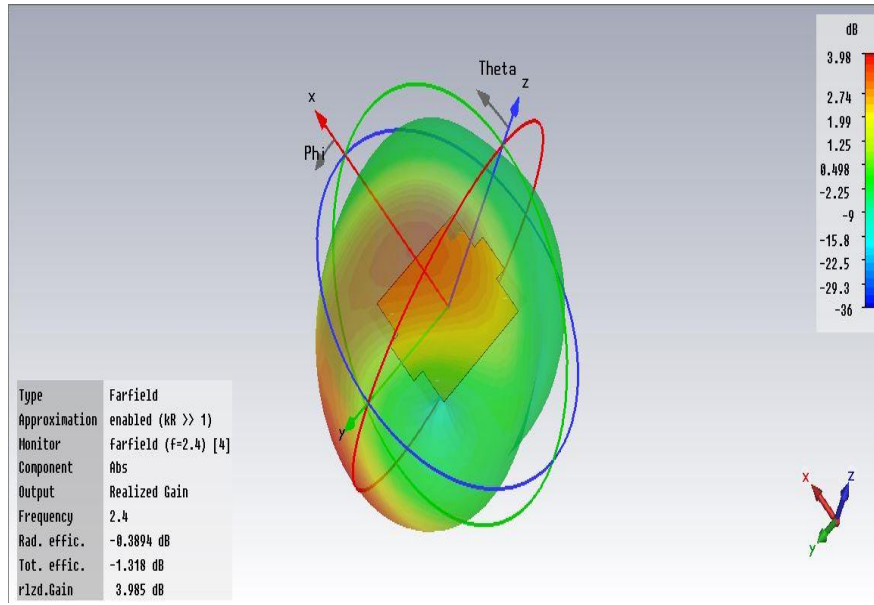


Figure 5.31 Element 4 realized gain

The measured far-field characteristics of the proposed antenna are also analyzed. The measured radiation patterns were conducted at MVG-Italy, in a Satimo star-Lab chamber as shown in Fig 5.32 for the measurement setup. Fig. 5.33 shows the 2-D radiation patterns of the antenna at 2.4 GHz for the four elements obtained from measurement and simulations as well at $\theta = 90^\circ$ Along XY axis and $\phi = 0^\circ$ along YZ . Good agreement is observed, note that the tilts in the radiation patterns that will provide good MIMO channel isolation. At the resonant frequency, the measured maximum gain of each element was 3.12 dBi while the radiation efficiency was 81.5%.

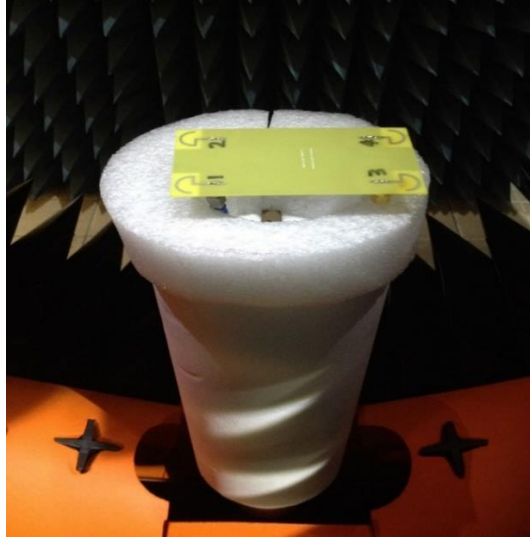


Figure 5.32 Measurement setup in a Satimo star-Lab

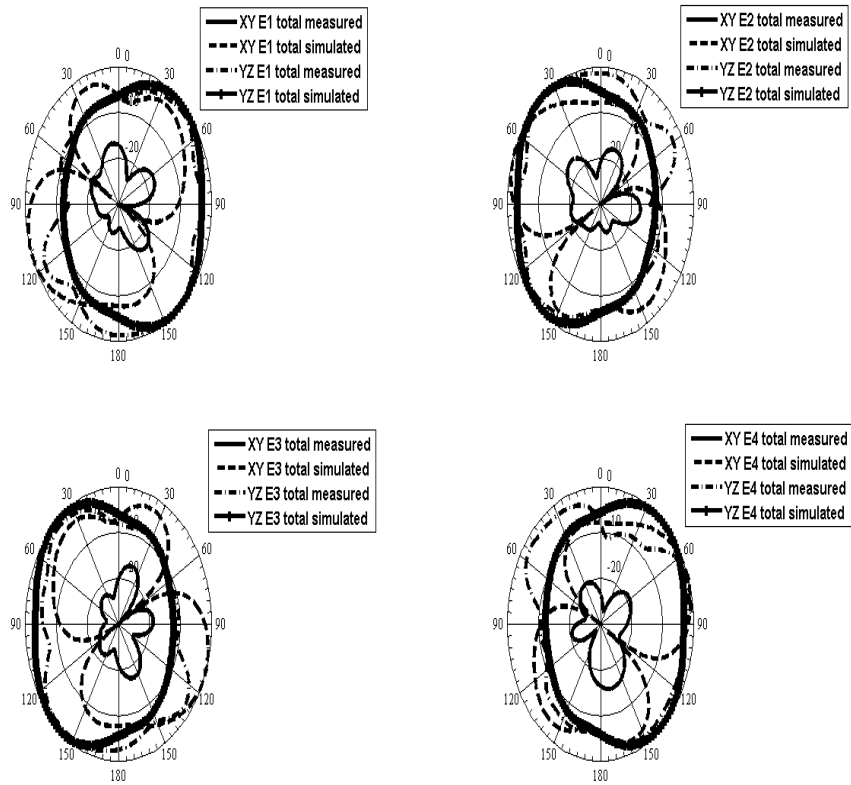


Figure 5.33 The measured and simulated of E_{Total} for each element at $\theta = 90^\circ$ Along XY axis and $\phi = 0^\circ$ along YZ

By applying method I-IV the correlation coefficient was calculated .The results are represented in Table 5.3 shows a good agreement among the different methods in addition to the calculation from the measured 3D far fields, this comes from the true that at high radiation efficiency these different methods become close and more accurate.

Table 5-3 correlation coefficients of four curved array with fr4 and reflector at 2.4GHz

Method Used	ρ_{e12}	ρ_{e13}	ρ_{e14}
method-I	0.1869	0.2094	0.2742
method-II	0.1122	0.1342	0.2353
method-III	0.0454	0.2196	0.3283
method-IV	0.1409	0.1642	0.2586
Measured Far field	0.2186	0.2029	0.2685

5.2.3 Annular Slot Based Printed MIMO Antenna System Design

A four annular slot based MIMO antenna was designed using an FR4 substrate with thickness *0.8mm* and dielectric constant *4.3*. These four elements were targeting to cover WLAN band. The structure is shown in Fig 5.34 and the detailed geometry is provided in [38]. This design was chosen to cover the case of medium radiation efficiency MIMO antenna. The S-parameters are shown in Fig 5.35 and the -10 dB bandwidth was 200 MHz and isolation of 11 dB is obtained. The realized gain was 2.88 dB and the total efficiently

was 65.7% and the 3D radiation patterns shown in Fig. 5.36. This design was reproduced and thus was not fabricated.

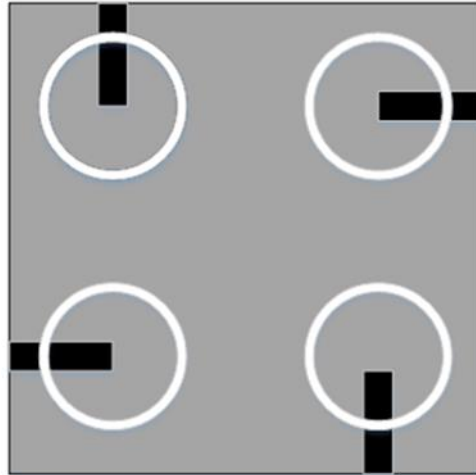


Figure 5.34 Annular Slot Based Printed MIMO Antenna

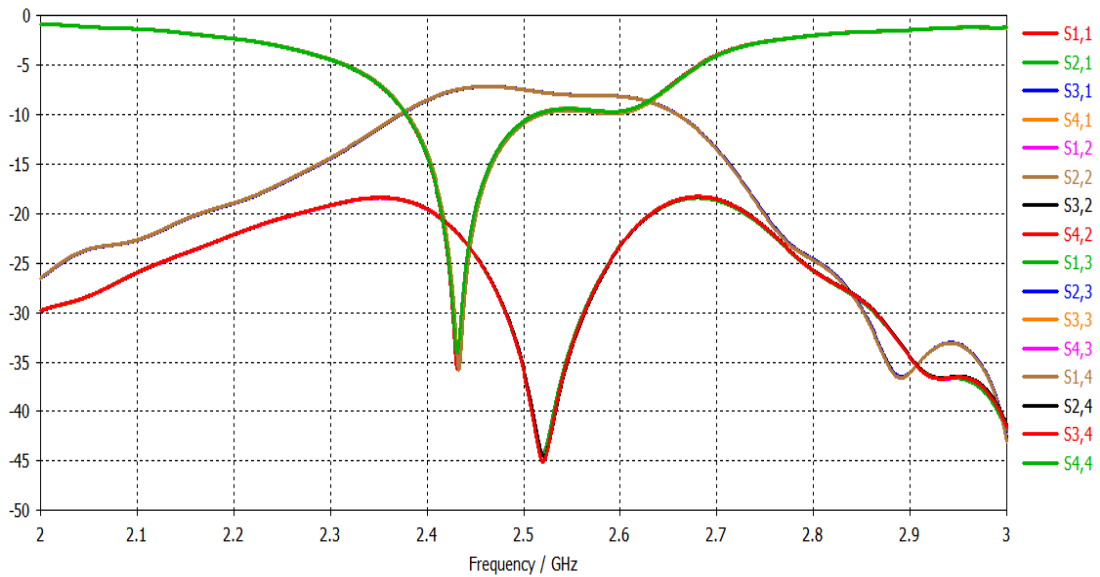


Figure 5.35 The four annular slot S-parameter with FR4

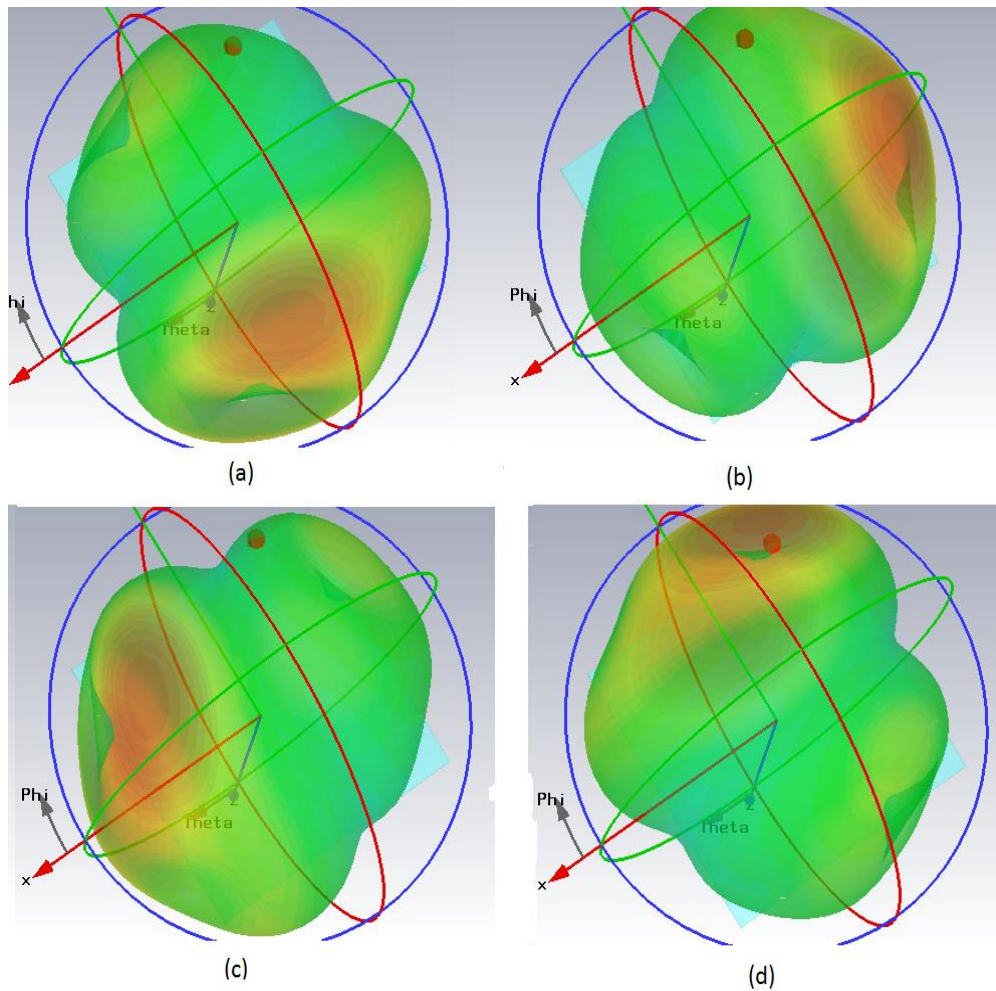


Figure 5.36 3D radiation patterns the four annular slot

By applying method I-IV the correlation coefficient was calculated for the four annular slot MIMO antenna. The results are given in Table 5.4 and show a good agreement among between method-I and method-IV. Here a moderate value of radiation efficiency is obtained to validate the accuracy for these methods, and clearly this illustrates the disadvantages of method-II and method-III which are radiation efficiency dependent.

Table 5-4 correlation coefficients of the four annular slot with FR4 at 2.4 GHz

Method Used	ρ_{e12}	ρ_{e13}	ρ_{e14}
method-I	0.0998	0.0992	0.4736
method-II	0.0241	0.0258	0.0084
method-III	0.5580	0.5616	0.5357
method-IV	0.0518	0.0489	0.3386

5.2.4 Four PIFA Elements

This design is the second distribution of this work for a 4-element MIMO antenna covering 1.8 GHz. Some antenna element should be represented by a parallel RLC equivalent circuit such as PIFA and patch antenna, in order for the estimation of the correlation coefficient to be accurate. The 4-element PIFA antenna was designed using FR4 substrate with thickness 0.8mm and dielectric constant 4.3 as shown in Fig 5.37 also the design was fabricated as shown in Fig 5.38. CST was used for modeling and optimization. The simulated and measured reflection coefficients are shown in Fig 5.39 and the -10 dB bandwidth was 100 MHz and an isolation of 10 dB is obtained from simulation and more than 15 dB for the measurement as shown in Fig 5.40. The slight shift in the resonance is due to the different dielectric constant of the modeled and fabricated designs. Since we do not have a concrete idea about the exact value of the dielectric constant of the FR-4 which has been used for fabrication, we tuned the dielectric constant of the FR-4 into 4 for the simulation environment such that the measurement and simulation are match as shown in

fig 5.41. The realized gain was 2.957 dB and the total efficiency was -1.68 dB for the four elements as shown in Figs 5.42-5.45.

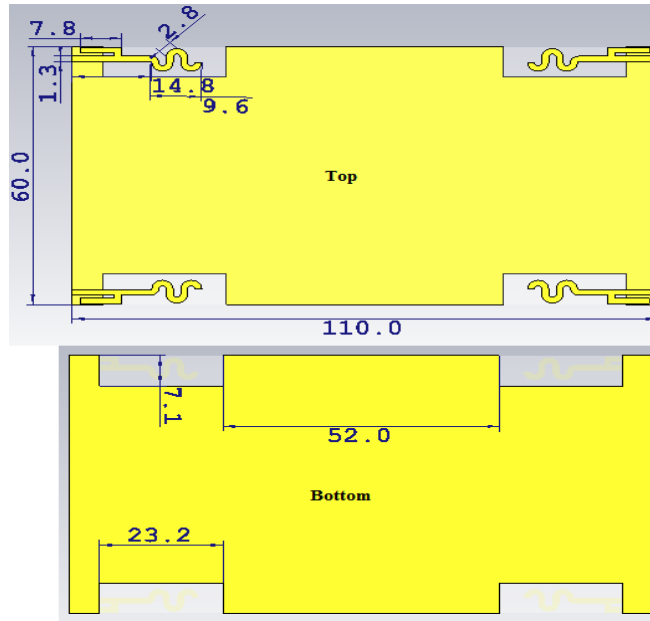


Figure 5.37 PIFA MIMO Antenna geometry. (All dimension are in mm)

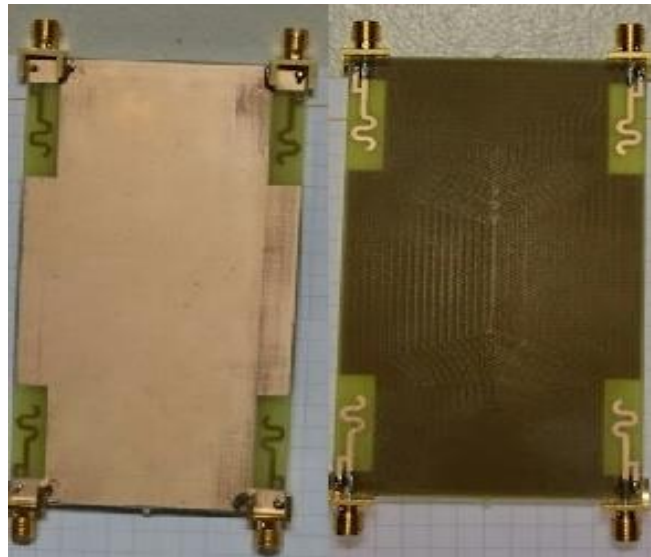


Figure 5.38 Geometry of the Fabricated antenna bottom side and top side

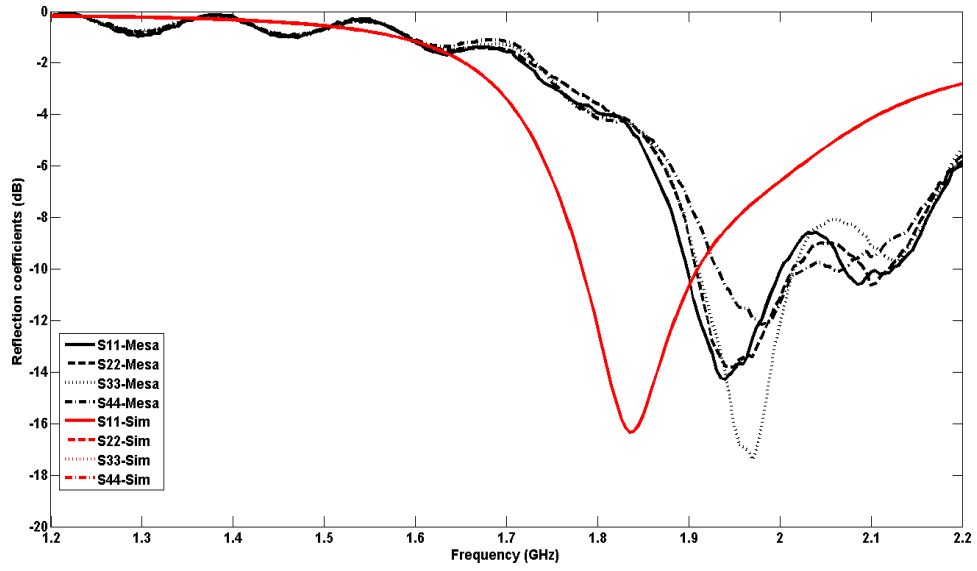


Figure 5.39 PIFA Simulated and measured S-parameter with FR4

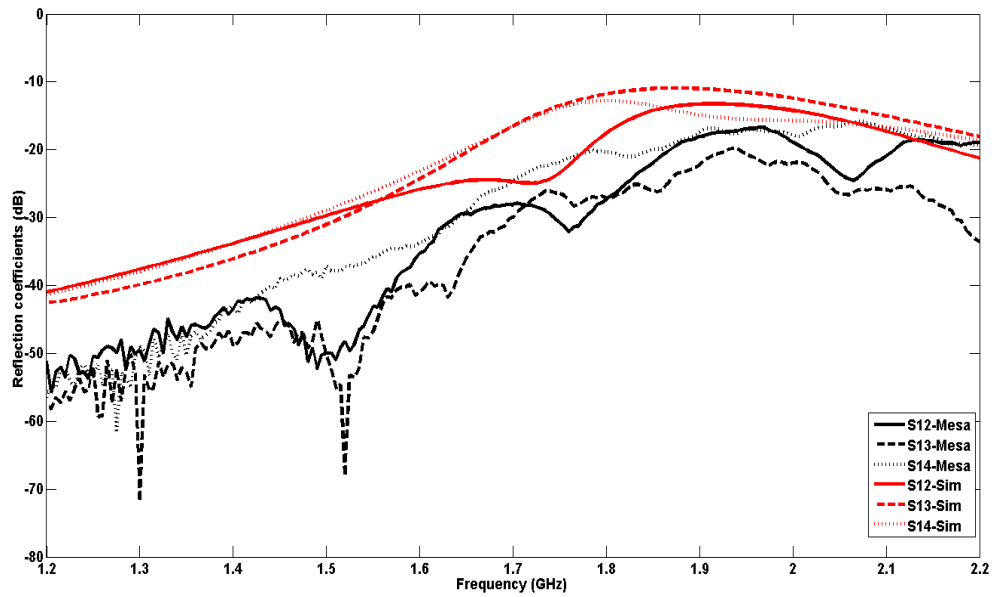


Figure 5.40 PIFA Simulated and measured isolation

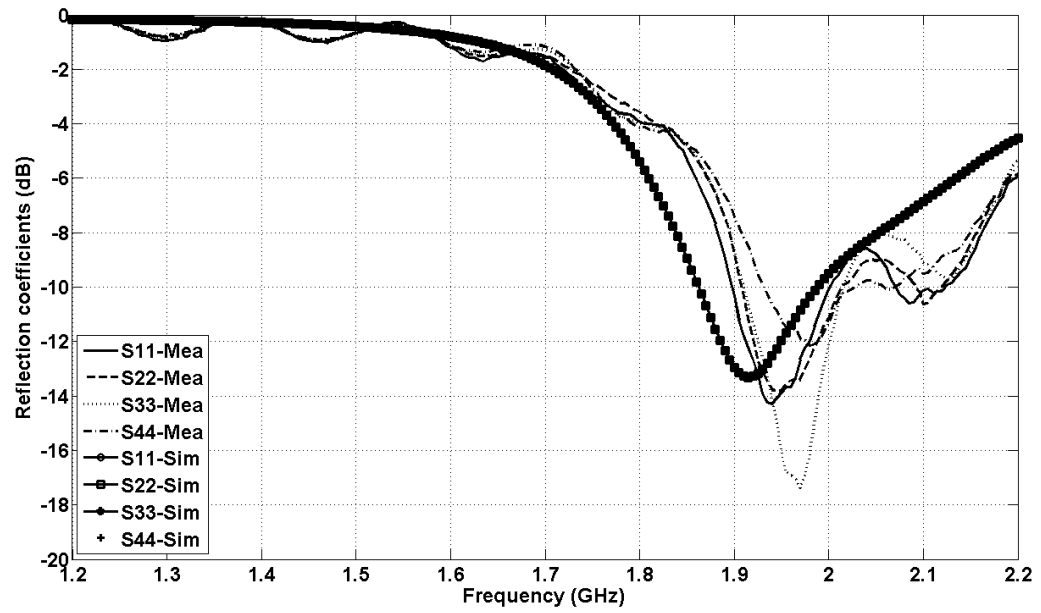


Figure 5.41 PIFA Simulated and measured S-parameter with the dielectric constant of 4

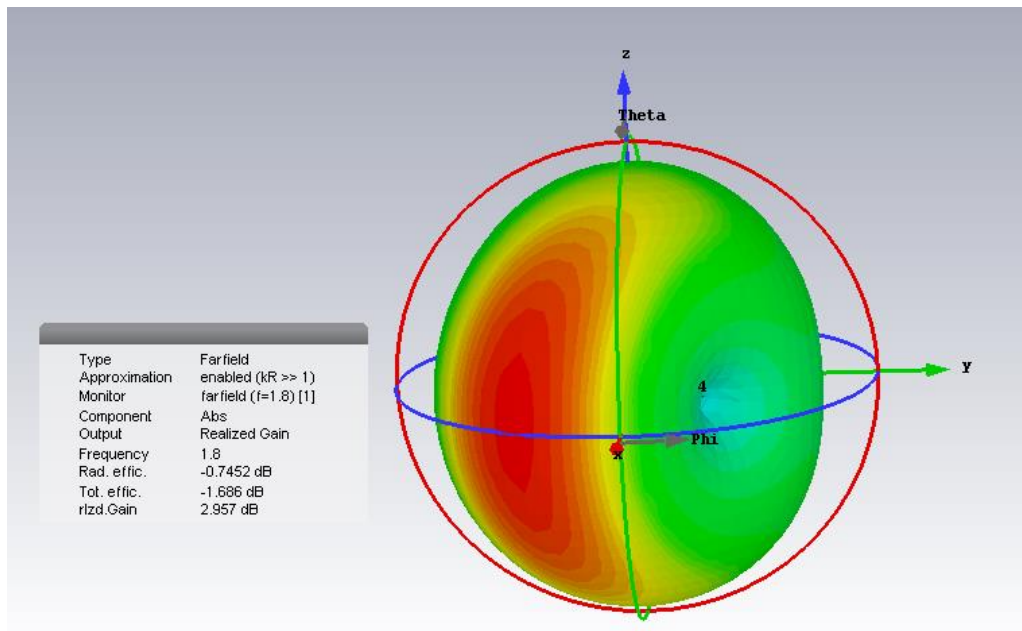


Figure 5.42 Element 1-3D radiation patterns

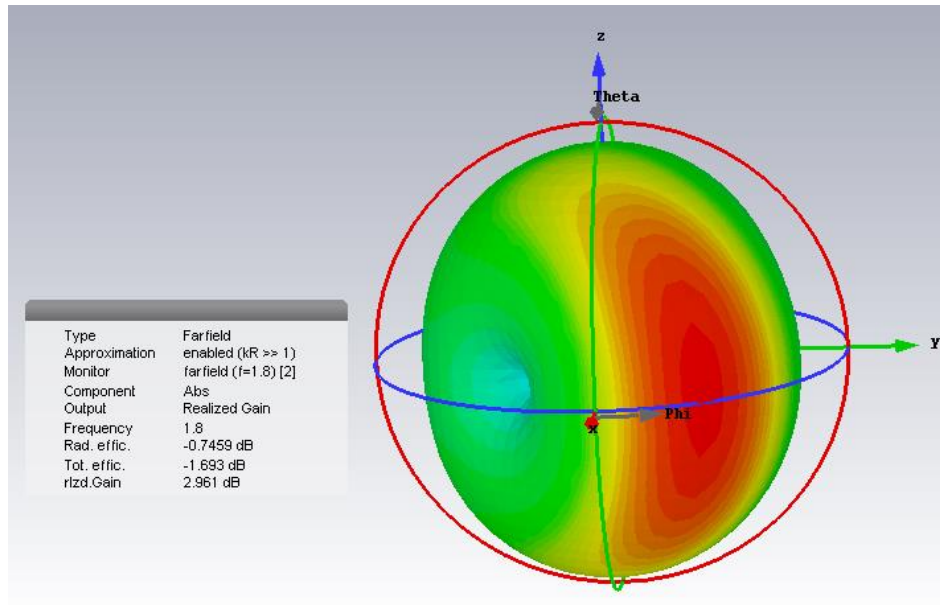


Figure 5.43 Element 2-3D radiation patterns

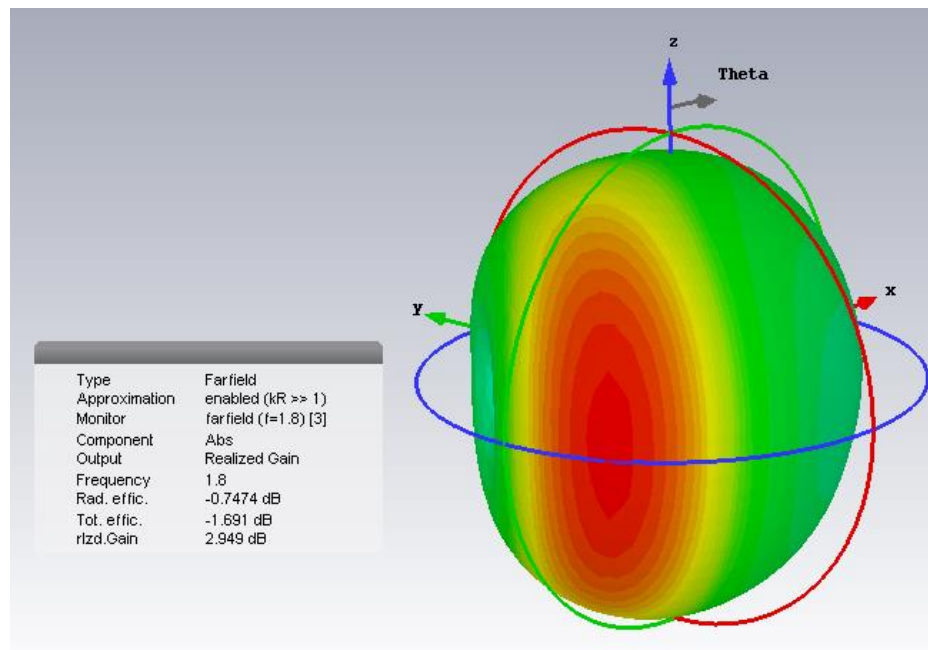


Figure 5.44 Element 3-3D radiation patterns

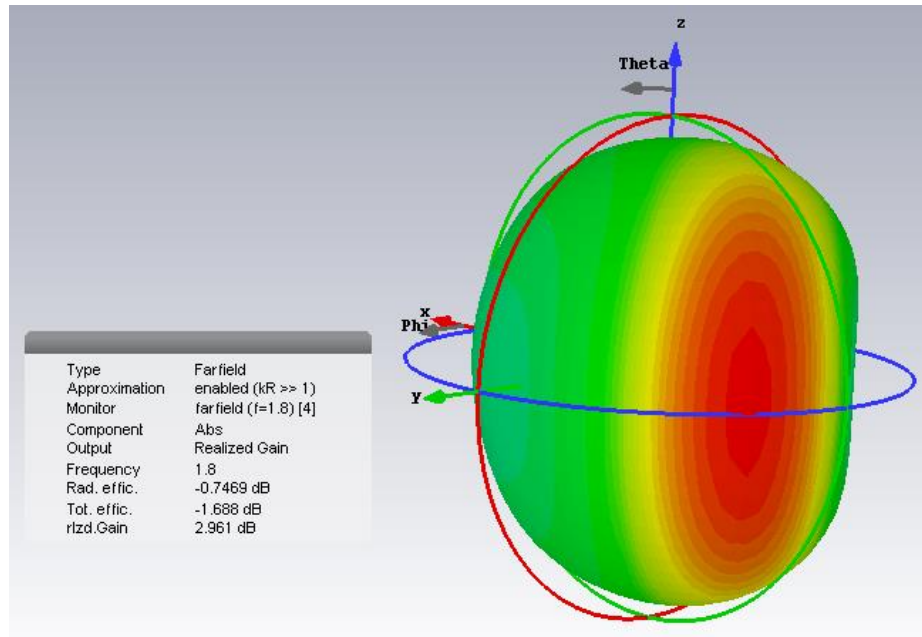


Figure 5.45 Element 4-3D radiation patterns

By applying method I -IV the correlation coefficient was calculated .The results are presented in Table 5.5 and show good agreement between the different methods, this comes from the high radiation efficiency of the antenna, thus the different methods become close and more accurate. However method-III shows high value of the correlation comparing with the other method and this because of uncertainty term.

Table 5-5 correlation coefficients of the four PIFA with FR4 at 1.8 GHz

Method Used	ρ_{e12}	ρ_{e13}	ρ_{e14}
Method I	0.0614	0.0550	0.1135
Method II	0.0402	0.0403	0.1066
Method III	0.1688	0.1689	0.2434
Method IV	0.0680	0.0881	0.1284

5.2.5 The Four Patch Elements

The 4-element patch antenna was designed using FR4 substrate with thickness 0.8mm and dielectric constant 4.3 as shown in Fig 5.45. This design represent a low radiation efficiency. These four elements were targeting to cover 2.4 GHz . The S-parameters are shown in Fig 5.46 and the -10 dB bandwidth was 50 MHz and isolation of 9 dB is obtained. The realized gain was 0.264 dB and the total efficiency was -6.4 dB for the four elements as shown in Figs 5.47-5.50.

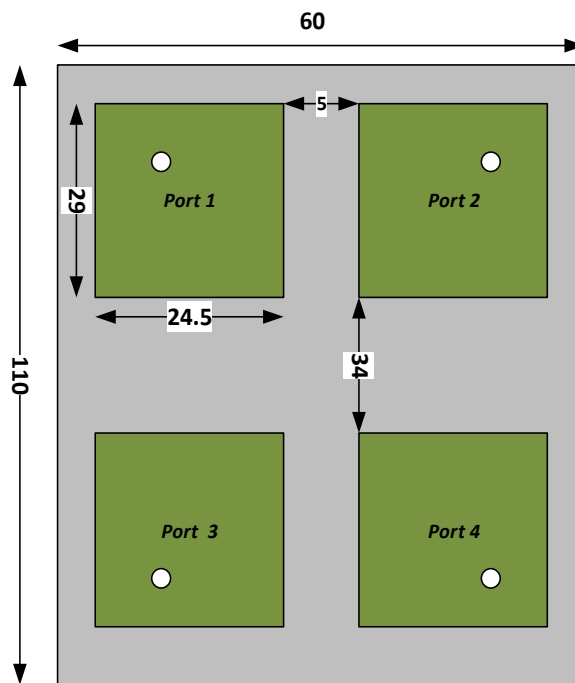


Figure 5.46 Four patch geometric (All dimensions are in mm)

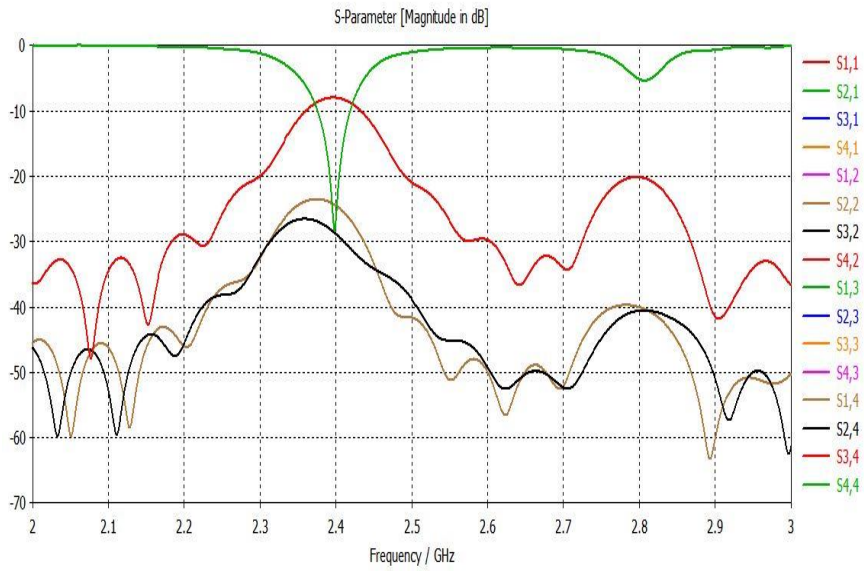


Figure 5.47 Four patch elements S-parameter with FR4

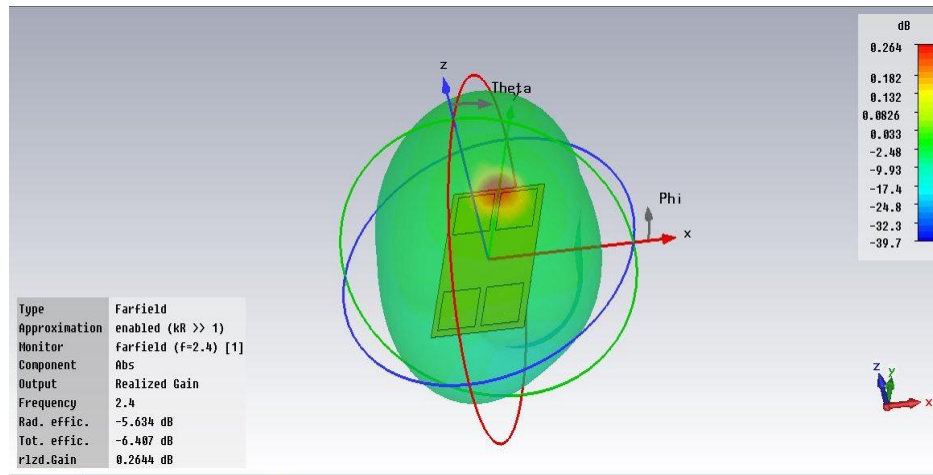


Figure 5.48 Element 1 realized gain

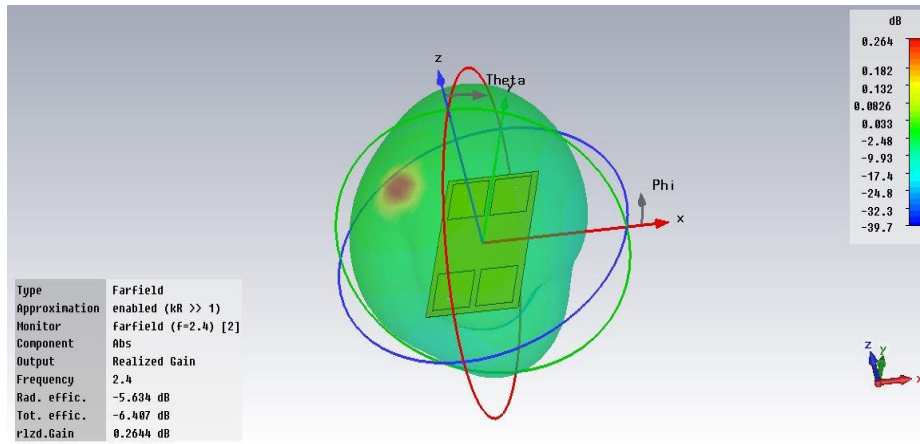


Figure 5.49 Element 2 realized gain

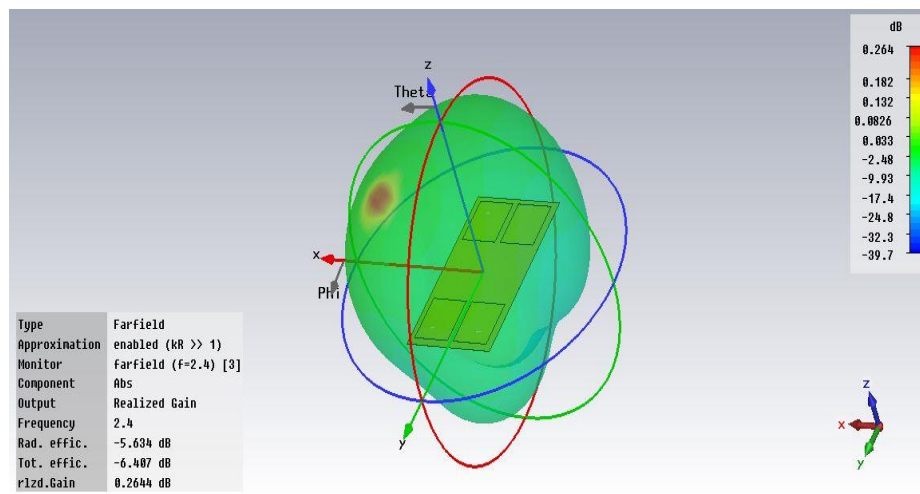


Figure 5.50 Element 3 realized gain

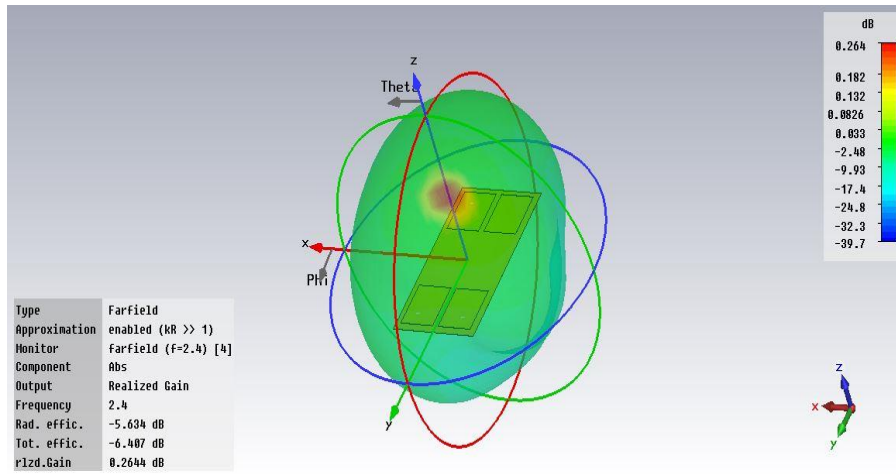


Figure 5.51 Element 4 realized gain

By applying method I-IV the correlation coefficient was calculated. From Table 5.6 we can notice that the correlation coefficient for method-III is greater than 1 this comes from the high uncertainty term in because of low radiation efficiency. Also in method-II gives wrong values for the correlation coefficient because of the drawback of this method which assume lossless.

Table 5-6 correlation coefficients of four patch array with FR-4 at 2.4 GHz

Method Used	ρ_{e12}	ρ_{e13}	ρ_{e14}
method-I	0.7005	0.1215	0.2898
method-II	0.0541	0.0032	0.0162
method-III	2.5032	2.691	2.6437
method-IV	0.7678	0.1046	0.1842

5.2.6 The Four Patch Elements with high radiation efficiency

The 4-element patch antenna was designed using FR4 substrate with thickness 0.8mm and dielectric constant 4.3 and loss tangents 0.002 as shown in Fig 5.51. This design represent a high radiation efficiency. These four elements were targeting to cover 5.35 GHz . The S-parameters are shown in Fig 5.52 and the -10 dB bandwidth was 60 MHz and isolation of 21 dB is obtained. The realized gain was 5.84 dB and the total efficiency was -0.66 dB for the four elements as shown in Figs 5.53-5.56.

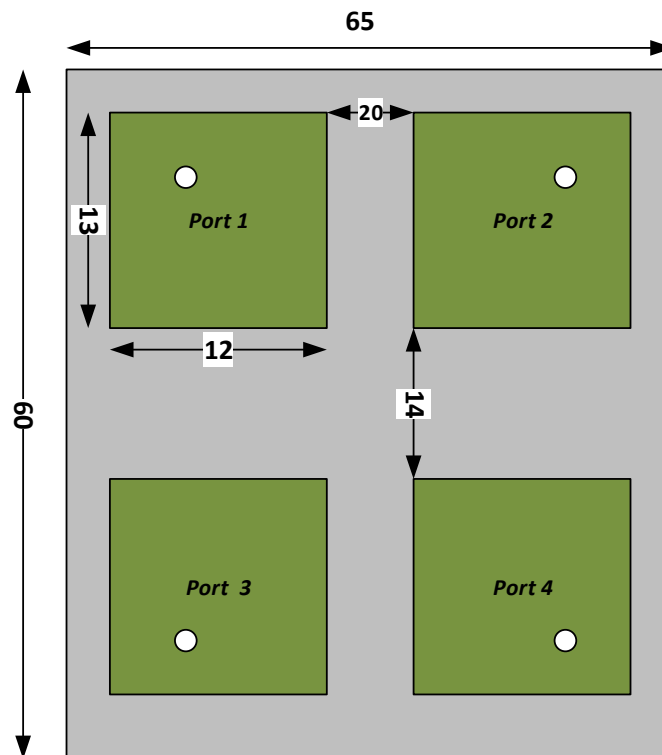


Figure 5.52 Four patch geometric (All dimensions are in mm)

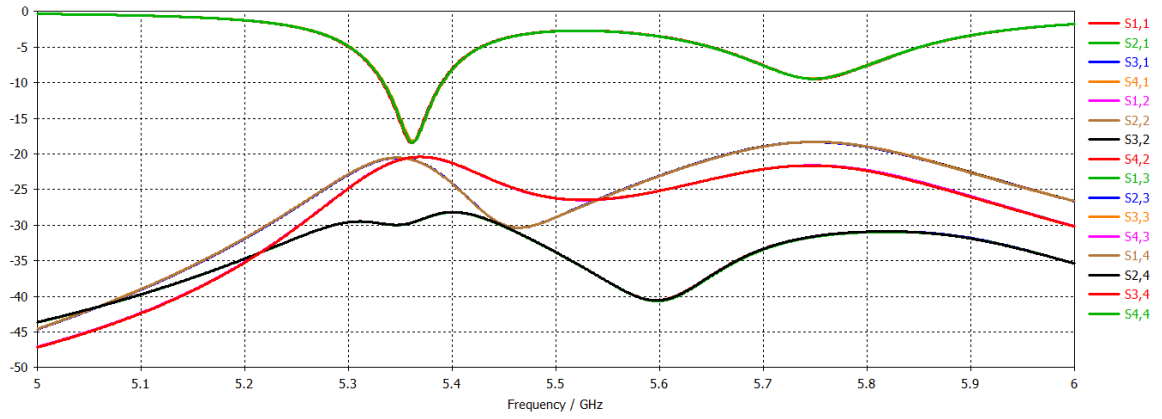


Figure 5.53 Four patch elements S-parameter with FR4

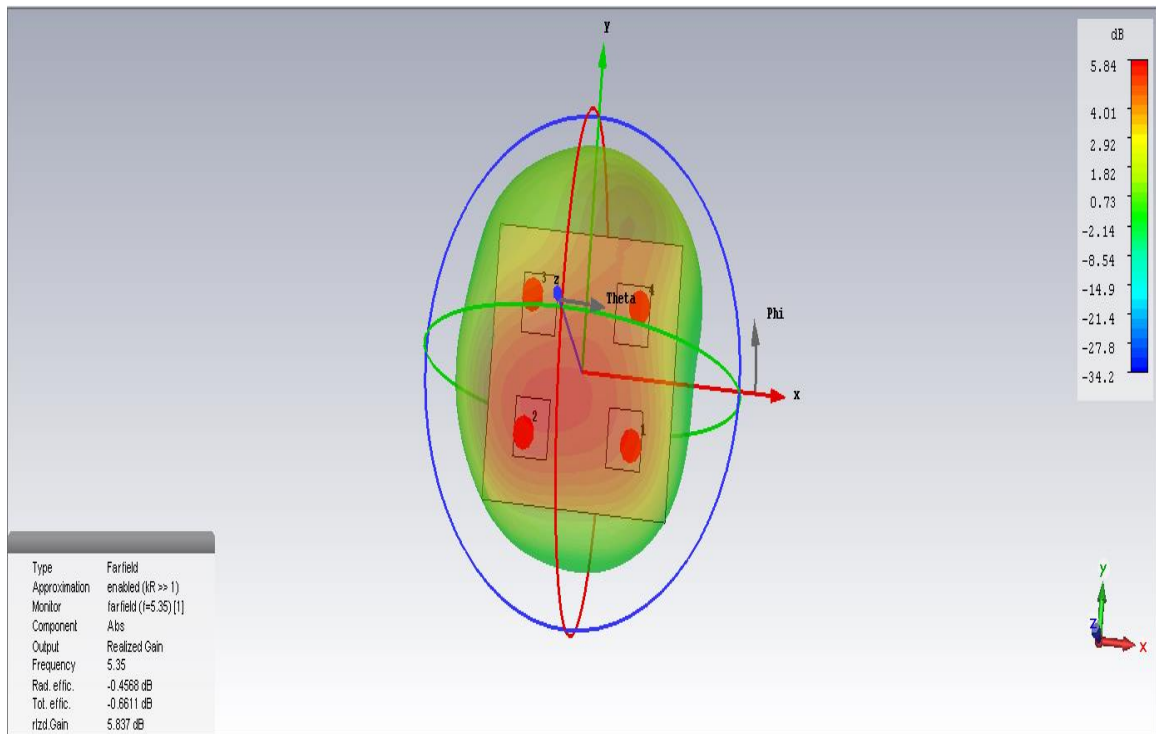


Figure 5.54 Element 1 realized gain

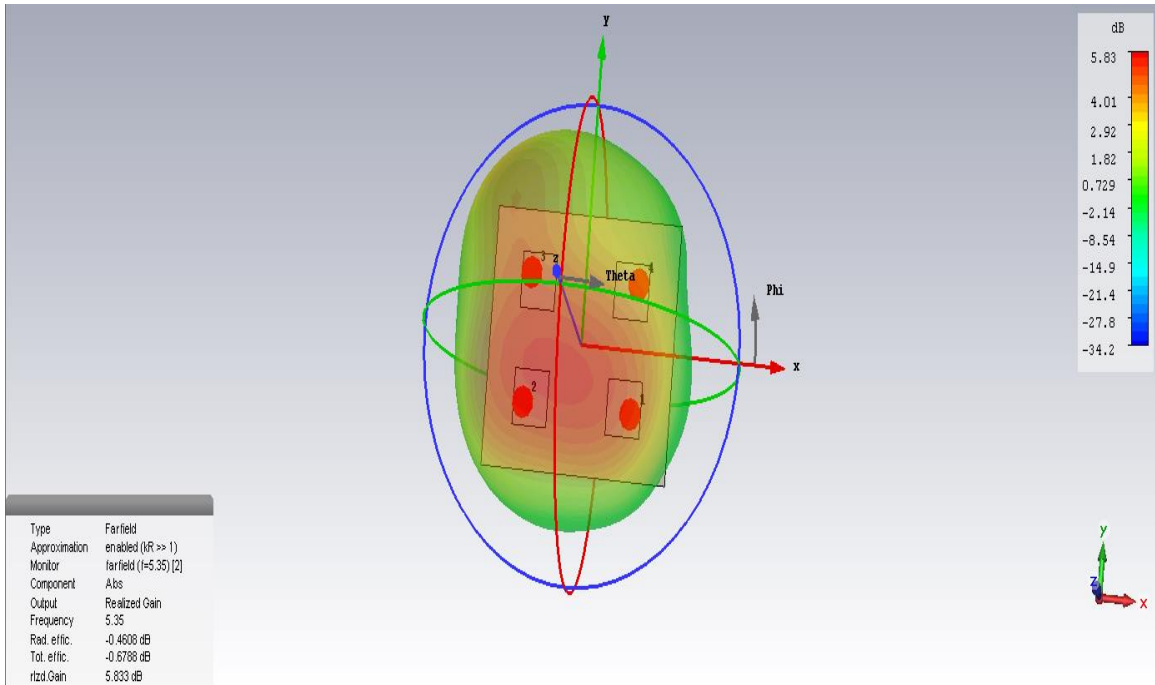


Figure 5.55 Element 2 realized gain

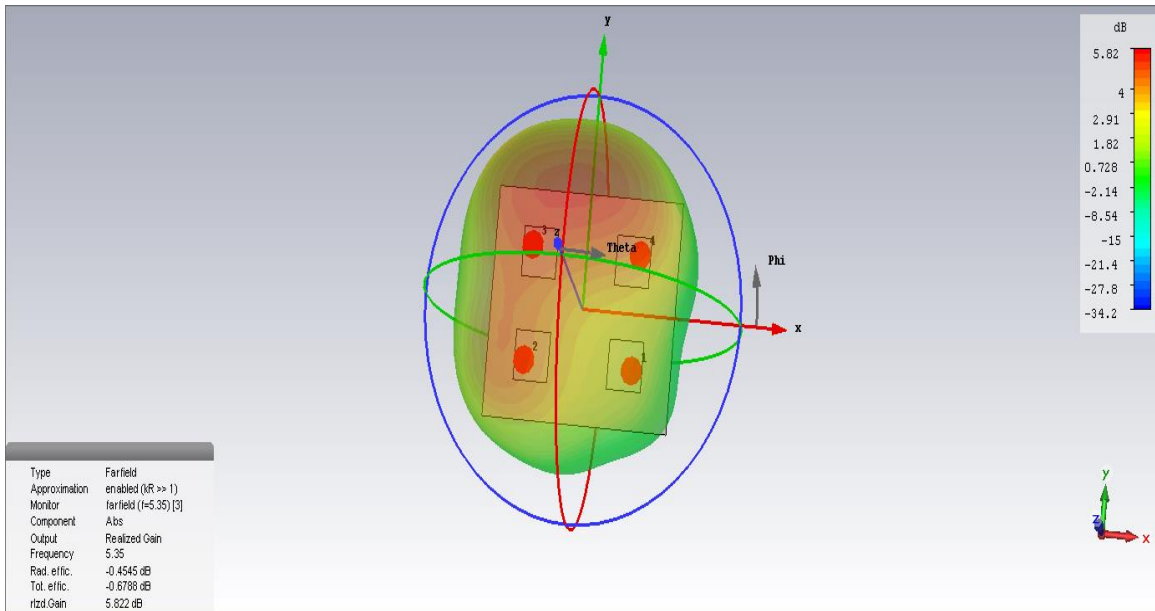


Figure 5.56 Element 3 realized gain

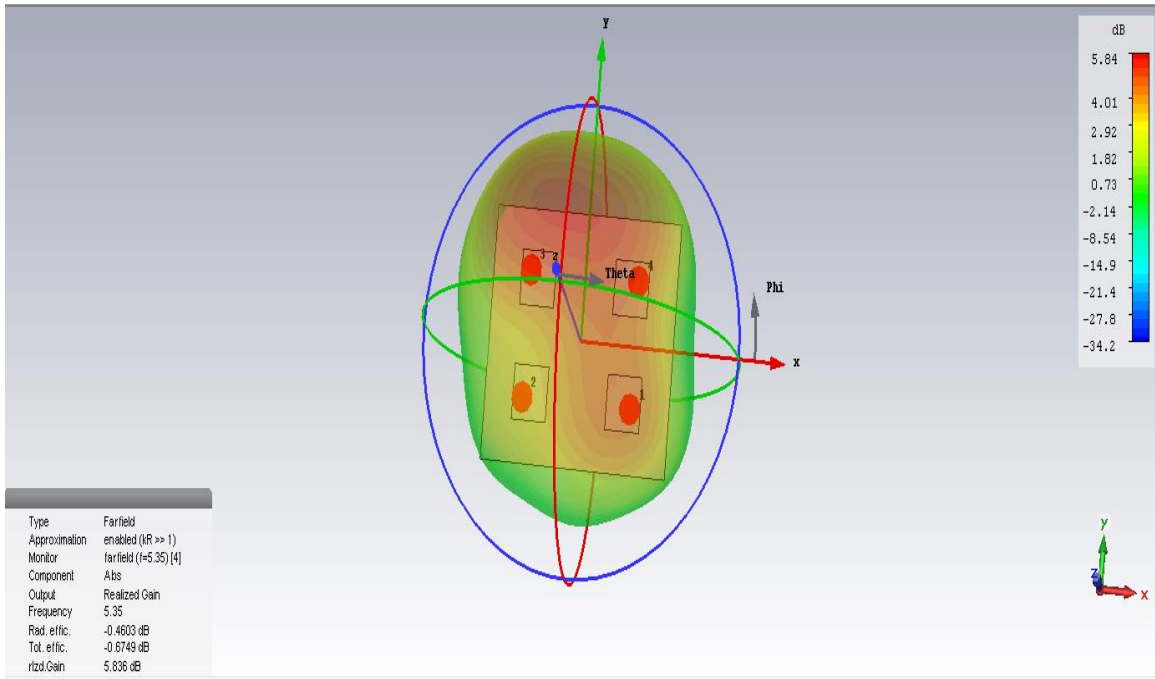


Figure 5.57 Element 4 realized gain

By applying method I-IV the correlation coefficient was calculated. From Table 5.7 we can notice that the correlation coefficient for the all methods show good agreement because of high radiation efficiency.

Table 5-7 correlation coefficients of high radiation efficiency four patch array with FR-4 at 5.35 GHz

Method Used	ρ_{e12}	ρ_{e13}	ρ_{e14}
method-I	0.2597	0.4163	0.2776
method-II	0.2115	0.4213	0.2125
method-III	0.1608	0.4275	0.1613
method-IV	0.2264	0.4448	0.2461

5.3 Summary

The correlation coefficient is a far field parameters which means it is independent of the radiation efficiency. Method-I and IV calculate the correlation coefficient by excluding the effect of the radiation efficiency, however method-II and III evaluate the correlation coefficient by taking into account the effect of the antenna radiation efficiency therefore inaccurate estimation is obtained at low radiation efficiency. To demonstrate this, a different antenna types and radiation efficiency have been used.

CHAPTER 6

THESIS CONCLUSIONS

6.1 Conclusions

The performance of MIMO antenna systems is evaluated through several parameters which are directly related to the antenna design. The benefits of MIMO systems can be fully utilized when the wireless channels are isolated; hence the calculation of the correlation coefficient is critical because most of the MIMO systems performance metrics rely on the value of the correlation coefficient such metrics are the multiplexing efficient and the diversity gain therefor the correlation coefficient is indispensable metric to evaluate the performance of the communication system. There are five method to evaluate the correlation coefficient, in this work a comprehensive study is conducted to compare their characterizations when applied to different antenna types. This comparison can be classified in term of accuracy and complexity that is needed to deploy these methods. Also, two methods were extended to cover N-element MIMO. Also, in this work two designs of 4-element MIMO antennas systems for current 4G handsets were proposed. One was the monopole based and the other was PIFA. The PIFA covered the 1.8GHz cellular band while the monopole covered the 2.45 GHz ISM band and both have a more than 80 MHz of operating BW. Also to validate the proposed methods a different antennas based MIMO with different radiation efficiency have been investigated. It was found that the result obtained from method-IV were close to method-I which is the exact method, however

method II-III were only be reliable for high radiation efficiency and cannot be used for low radiation efficiency.

6.2 Future work

This work is focused on studying and implementation of several algorithms to calculate the correlation coefficient for N antenna elements. Future work can include:

1. Investigate and analyze the other parameters that are used to evaluate MIMO system performance using the values obtained from these different method such as diversity gain and multiplexing efficiency.
2. Come up with simple and reliable methods to evaluate the correlation coefficient for different power distributions for the radio environment which can be applied for MIMO systems that are used in outdoor.
3. Test and apply the compatibility of the all method on dielectric resonator based MIMO antennas.

APPENDIX – SOFTWARE TOOL

In this work, the electromagnetic simulation software CST STUDIO SUITE® (CST) software tool was used to simulate the results for the designs. Computational Electromagnetics have several numerical techniques that can be applied to acquire solutions with certain tolerance.

CST is one of the commercial industrial tools used to solve the structures for the 3D full wave electromagnetic properties. Its solver is based on a numerical technique that will divide the required structures into small parts and finds the incremental electric and magnetic field components and then sums them geometrically for the whole structure to find to total fields. There are many techniques are used currently such as Finite Integration Technique, Finite Element Method, Method of Moments, Transmission-line matrix method.

CST provided several domains for solving Maxwell equations for instance, Time Domain solver and the Frequency Domain solver, besides, offers further solver modules for specific applications.

References

- [1] T. Brown, E. De Carvalho, and P. Kyritsi, *Practical Guide to the MIMO Radio Channel with MATLAB examples*. Chichester, West Sussex, U.K. ; Hoboken, N.J: Wiley, 2012.
- [2] Y. S. Cho, Ed., *MIMO-OFDM wireless communications with MATLAB*, Reprinted. Singapore: Wiley, 2011.
- [3] M. S. Sharawi, "Printed Multi-Band MIMO Antenna Systems and Their Performance Metrics [Wireless Corner]," *IEEE Antennas Propag. Mag.*, vol. 55, no. 5, pp. 218–232, 2013.
- [4] M. S. Sharawi, "Printed MIMO antenna systems: Performance metrics, implementations and challenges," in *Forum for Electromagnetic Research Methods and Application Technologies (FERMAT)*, 2014, vol. 1.
- [5] Ruiyuan Tian, Buon Kiong Lau, and Zhinong Ying, "Multiplexing Efficiency of MIMO Antennas," *IEEE Antennas Wirel. Propag. Lett.*, vol. 10, pp. 183–186, 2011.
- [6] S. Blanch, "Exact representation of antenna system diversity performance from input parameter description," vol. 39, no. 52, pp. 705–707, 2003.
- [7] A. Stjernman, "Relationship between radiation pattern correlation and scattering matrix of lossless and lossy antennas," *Electron. Lett.*, vol. 41, no. 12, pp. 678–680, 2005.
- [8] P. Hallbjorner, "The significance of radiation efficiencies when using S-parameters to calculate the received signal correlation from two antennas," *Antennas Wirel. Propag. Lett.*, vol. 4, pp. 97–99, 2005.
- [9] R. Vaughan and J. B. Andersen, *Channels, Propagation and Antennas for Mobile Communications*, ser. IEE Electromagnetic Waves. London, U.K.: Inst. Elect. Eng., 2003, vol. 50, pp. 569–576.
- [10] H. Li, X. Lin, B. K. Lau, and S. He, "Equivalent Circuit Based Calculation of Signal Correlation in Lossy MIMO Antennas," *Antennas Propagation, IEEE Trans.*, vol. 61, no. 10, pp. 5214–5222, 2013.
- [11] D. M. Pozar, *Microwave Engineering*, 3rd ed. Hoboken, NJ, USA: Wiley, 2005.

- [12] J. Frei, X. Cai, and S. Muller, "Multiport S -Parameter and T -Parameter Conversion With Symmetry Extension," *IEEE Trans. Microw. Theory Tech.*, vol. 56, no. 11, pp. 2493–2504, 2008.
- [13] L. J. Chu, "Physical limitations of omni-directional antennas," *J. Appl. Phys.*, vol. 19, no. 12, pp. 1163–1175, 1948.
- [14] R. Garg, P. Bhartia, I. Bahl, and A. Ittipiboon, *Microstrip Antenna Design Handbook*. Norwood, MA, USA: Artech House, 2001.
- [15] R. S. Elliott, *Antenna Theory and Design*, Revised ed. Hoboken, NJ, USA: Wiley, 2003.
- [16] C. A. Balanis, *Antenna Theory: Analysis and Design*, 3rd ed. Hoboken, NJ, USA: Wiley, 2005, pp. 468–490.
- [17] H. Li, X. Lin, B. K. Lau, and S. He, "Calculating Signal Correlation in Lossy Dipole Arrays Using Scattering Parameters and Efficiencies," no. 2009, pp. 511–515, 2013.
- [18] K. Wang, L. Li, and T. F. Eibert, "Estimation of Signal Correlation of Lossy Compact Monopole Arrays With Decoupling Networks," vol. 63, no. 1, pp. 357–363, 2015.
- [19] M. Karaboikis, C. Soras, G. Tsachtsiris, and V. Makios, "Four-element printed monopole antenna systems for diversity and MIMO terminal devices," in *Applied Electromagnetics and Communications*, 2003. ICECom 2003. 17th International Conference on, 2003, pp. 193–196.
- [20] A. Ando, N. Kita, and W. Yamada, "2.4 / 5 GHz Dual-Band Planar Antennas mounted on WLAN Card for 3-MIMO-OFDM Systems," *Iraq*, 2006.
- [21] S. W. Su, C. T. Lee, and F. S. Chang, "Printed MIMO-antenna system using neutralization-line technique for wireless USB-dongle applications," *IEEE Trans. Antennas Propag.*, vol. 60, no. 2, pp. 456–463, 2012.
- [22] a R. Mallahzadeh, S. F. Seyyedrezaei, N. Ghahvehchian, S. Mohammad, and S. Mallahzadeh, "Tri-Band Printed Monopole Antenna for WLAN and WiMAX MIMO Systems," pp. 548–551, 2011.
- [23] S. M. Ali and J. Warden, "Controlling coupling between two transmitting antennas for MIMO handset applications," *2011 IEEE 22nd Int. Symp. Pers. Indoor Mob. Radio Commun.*, pp. 2060–2064, 2011.

- [24] C. H. See, R. a Abd-alhameed, Z. Z. Abidin, N. J. Mcewan, P. S. Excell, and S. Member, "Wideband Printed MIMO / Diversity Monopole Antenna for WiFi / WiMAX Applications," *IEEE Trans. Antennas Propag.*, vol. 60, no. 4, pp. 2028–2035, 2012.
- [25] A. Ghasemi, N. Ghahvehchian, A. Mallahzadeh, and S. Sheikholvaezin, "A reconfigurable printed monopole antenna for MIMO application," *Proc. 6th Eur. Conf. Antennas Propagation, EuCAP 2012*, pp. 1–4, 2012.
- [26] Z.-J. Jin, J.-H. Lim, and T.-Y. Yun, "Frequency reconfigurable multiple-input multiple-output antenna with high isolation," *IET Microwaves, Antennas Propag.*, vol. 6, no. 10, p. 1095, 2012.
- [27] J. M. Lee, K. B. Kim, H. K. Ryu, and J. M. Woo, "A compact ultrawideband MIMO antenna with WLAN band-rejected operation for mobile devices," *IEEE Antennas Wirel. Propag. Lett.*, vol. 11, pp. 990–993, 2012.
- [28] D. Piazza, N. J. Kirsch, A. Forenza, R. W. Heath, and K. R. Dandekar, "Design and Evaluation of a Reconfigurable Antenna Array for MIMO Systems," *IEEE Trans. Antennas Propag.*, vol. 56, no. 3, pp. 869–881, Mar. 2008
- [29] W. Li, Y. Yao, and J. Yu, "A Dual Broad-band Antenna for WLAN Application with High Isolation," pp. 37–41, 2011.
- [30] S. Shoaib, I. Shoaib, N. Shoaib, X. Chen, and C. G. Parini, "Design and Performance Study of a Dual-Element Multiband Printed Monopole Antenna Array for MIMO Terminals," *IEEE Antennas Wirel. Propag. Lett.*, vol. 13, no. c, pp. 329–332, 2014.
- [31] A. Moradikordalivand, T. A. Rahman, and M. Khalily, "Common elements wideband MIMO antenna system for WiFi / LTE access-point applications," *IEEE Antennas Wirel. Propag. Lett.*, vol. 13, pp. 1601–1604, 2014.
- [32] M. P. Karaboikis, V. C. Papamichael, G. F. Tsachtsiris, C. F. Soras, and V. T. Makios, "Integrating compact printed antennas onto small diversity/MIMO terminals," *IEEE Trans. Antennas Propag.*, vol. 56, no. 7, pp. 2067–2078, 2008.
- [33] W.-Y. Li and W.-J. Chen, "Concurrent 2-port/3-port MIMO antenna system for UMTS/LTE2500 operation in the mobile phone," pp. 1918–1921, 2011.
- [34] V. Ssorin, a Artemenko, a Sevastyanov, and R. Maslennikov, "Compact Planar Inverted-F Antenna System for MIMO USB Dongle Operating in 2 . 5-2 . 7 GHz Band," vol. 0, pp. 408–411, 2012.

- [35] S. Zhang, P. Zetterberg, and S. He, "Printed MIMO Antenna System of Four Closely-Spaced Elements with Large Bandwidth and High Isolation," *Electron. Lett*, vol. 46, no. 15, pp. 1052–1053, 2010.
- [36] J. Ren, W. Hu, Y. Yin, and R. Fan, "Compact Printed MIMO Antenna for UWB Applications," vol. 13, pp. 1517–1520, 2014.
- [37] R. Karimian, H. Oraizi, S. Fakhte, and M. Farahani, "Novel F-shaped quad-band printed slot antenna for WLAN and WiMAX MIMO systems," *IEEE Antennas Wirel. Propag. Lett*, vol. 12, pp. 405–408, 2013.
- [38] M. U. Khan and M. S. Sharawi, "Annular Slot Based Printed MIMO Antenna System Design," pp. 675–676, 2014.
- [39] H. Li, S. Member, J. Xiong, S. Member, S. He, and S. Member, "A Compact Planar MIMO Antenna System of Four Elements with Similar Radiation Characteristics and Isolation Structure," vol. 8, pp. 1107–1110, 2009.
- [40] M. U. Khan, W. A. A. Al-saud, and M. S. Sharawi, "Channel Capacity Measurement of a 4-Element Printed MIMO Antenna System," pp. 10–13, 2014.
- [41] P. Gao, S. He, L. Xiong, and Y. Zheng, "A compact dual polarized UWB diversity wide-slot antenna," *2013 Int. Work. Microw. Millim. Wave Circuits Syst. Technol.*, pp. 131–133, 2013.
- [42] M. U. Khan, M. S. Sharawi, and D. N. Aloï, "A multi-band MIMO antenna system consisting of CSRR loaded patch elements," *IEEE Antennas Propag. Soc. AP-S Int. Symp*, pp. 2239–2240, 2013.
- [43] R. A. Bhatti, S. Yi, and S. O. Park, "Compact antenna array with port decoupling for LTE-standardized mobile phones," *IEEE Antennas Wirel. Propag. Lett*, vol. 8, no. in mm, pp. 1430–1433, 2009.
- [44] A. Mallahzadeh, A. Sedghara, and S. Mohammad, "A Tunable Multi-band Meander Line Printed Monopole Antenna for MIMO Systems," pp. 315–318.
- [45] S. C. Fernandez and S. K. Sharma, "Multiband printed meandered loop antennas with MIMO implementations for wireless routers," *IEEE Antennas Propag. Mag.*, vol. 12, pp. 96–99, 2013.
- [46] S. W. Su and C. T. Lee, "Low-cost dual-loop-antenna system for dual-WLAN-band access points," *IEEE Trans. Antennas Propag.*, vol. 59, no. 5, pp. 1652–1659, 2011.

- [47] X. Zhao and J. Choi, "Multiband MIMO antenna for 4G mobile terminal," *2013 Asia-Pacific Microw. Conf. Proc.*, no. c, pp. 49–51, 2013.
- [48] A. B. Numan and M. S. Sharawi, "A printed dual-band meander-line MIMO antenna system," *2013 IEEE Antennas Propag. Soc. Int. Symp.*, vol. 1, no. c, pp. 188–189, 2013.
- [49] S.-M. Wang, L.-T. Hwang, F.-S. Chang, C.-F. Liu, and S.-T. Yen, "A compact printed MIMO antenna integrated into a 2.4 GHz WLAN access point applications," *2013 Asia-Pacific Microw. Conf. Proc.*, pp. 639–641, 2013.
- [50] C.-J. Lee, L.-T. Hwang, T.-S. J. Horng, S.-M. Wang, Y.-C. Lin, and K.-H. Lin, "A MIMO antenna with built-in isolation for WLAN USB dongle applications," *2013 Asia-Pacific Microw. Conf. Proc.*, pp. 1055–1057, 2013.
- [51] M. S. Sharawi, A. B. Numan, M. U. Khan, and D. N. Aloi, "A dual-element dual-band MIMO antenna system with enhanced isolation for mobile terminals," *IEEE Antennas Wirel. Propag. Lett.*, vol. 11, pp. 1006–1009, 2012.

Vitae

Name :[ABDELMONIEM TAJELSIRMAHMOUD HASSAN]

Nationality :[SUDAN]

Date of Birth :[11/24/1991]

Email :[ABDOSIR99@GMAIL.COM]

Address :[OMDURMAN, KHARTOUM, SUDAN]

Academic Background :[September 2012] Bachelor of Science (B.Sc.) Honors degree: University of Khartoum- Faculty of Engineering – Electrical and Electronics Engineering Dept. - Communications Engineering (first class).]

Publications

1. **Abdelmoniem T. Hassan**, Muhammad U. Khan, Mohammad S. Sharawi, “Parallel RLC Equivalent Circuit Based Correlation Coefficient Calculation for MIMO Antennas,” **Accepted**, in 2016 IEEE International Symposium on Antennas and Propagation (AP-S/URSI), 2016.
2. **Abdelmoniem T. Hassan**, Muhammad U. Khan, Mohammad S. Sharawi, “Half Circle Shape Monopole Based 4-Element MIMO Antenna,” **Accepted**, in 2016 IEEE International Symposium on Antennas and Propagation (AP-S/URSI), 2016.

3. Syed Jehangir, **Abdelmoniem Hassan**, Mohammad Sharawi, "A 4-Element Dual Wideband Circular Yagi MIMO Antenna System with Loop Excitation," **Accepted**, in 2016 IEEE International Symposium on Antennas and Propagation (AP-S/URSI), 2016.
4. **Abdelmoniem T. Hassan** and Mohammad S. Sharawi, "Four element half circle shape printed MIMO antenna," **Submitted**, *Microwaves and Optical Technology Letters*, Wiley, April 2016.
5. **Abdelmoniem T. Hassan**, Muhammad U. Khan, Mohammad S. Sharawi, "revisiting the correlation coefficient calculations for MIMO antenna system," **to be Submitted**, *IET Microwaves, Antennas and Propagation (MAP)*, May 2016.